UNCLASSIFIED

ARGONNE NATIONAL LABORATORY
P. O. Box 5207
Chicago 80, Illinois

ANL-4000(Del.)
Progress Report

AEC RESEARCH AND DEVELOPMENT REPORT

SUMMARY REPORT FOR JULY, AUGUST AND SEPTEMBER, 1946

Chemistry Division, Section C-II

W. M. Manning, Division Director

O. C. Simpson, Associate Division Director

June 2, 1947.

Photostat Price $ 19.80
Microfilm Price $ 6.30

Available from the
Office of Technical Services
Department of Commerce
Washington 25, D. C.

Report Received: July 11, 1947

Figures Received: August 6, 1947

Issued: August 22, 1947

4000-1

Operated by the University of Chicago

under

Contract W-31-109-eng-38

4000-1

4000

UNCLASSIFIED

TABLE OF CONTENTS

LIST OF FIGURES

LIST OF TABLES

SUMMARY REPORT FOR JULY, AUGUST AND SEPTEMBER, 1946

Chemistry Division, Section C-II
under the supervision of O. C. Simpson

Group	Group Leader
Solid State	Theodore Neubert
Radiochemistry	Melvin S. Freedman
Analytical Chemistry	Frank S. Tomkins
High Temperature Pile	C. A. Boyd
Special Problems	O. C. Simpson
Theoretical Physics	R. G. Sachs

(The Theoretical Physics Group became a Division separate from the Chemistry Division August, 1946)

The greater part of the material covered in this report has appeared in the Weekly Abstracts of this section, but is repeated here for several reasons: (1) the abstracts were issued as memos from the division office and did not have wide circulation; (2) the weekly memos could not carry complete descriptions of apparatus and methods used; (3) as work progressed some methods were of course abandoned and it is therefore difficult to get an overall picture of results; (4) in some cases the interpretation of results was different after reviewing the work in perspective.

Several entirely new subjects not reported in the weekly memos have been included in this summary. The individual sections have in some cases been written by the scientists working on the problems herein presented. When this is the case, the underlined name in the listing under each problem indicates the author. The remaining parts of the report were written and the whole assembled and edited by J. R. Gilbreath, Katharine Jones, and O. C. Simpson. The able assistance of Beatrice Stein in preparing the manuscript is acknowledged.

1 POWER PILE PROBLEMS

1.1 Structural Properties of Beryllia (P. Boykin, T. Drugas, L. W. Fromm, S. R. Gaarder, J. R. Gilbreath, J. Karp, R. Phillips, D. H. Rich, J. L. Weeks)

1.1.1 Effect of Prolonged Heating on the Density of Hot-Pressed Beryllia Bricks

Previous investigations (CT-3528, J. R. Gilbreath and S. R. Gaarder, 5/20/46) have indicated that, in almost all cases, small beryllia pieces (density 2.7 - 2.95 g cm^{-3}) made by the hot-pressing technique expand on prolonged heating at 1400°C - 1500°C in either air or nitrogen, although the expansion in many cases is very slight. These changes in density were the same for small pieces cut from the same fabricated shape. In general the density change was much more gradual on prolonged heating in nitrogen than in air although the trend was still downward. The maximum density decrease observed was 6% for a sample which had been heated 500 hours in air at 1450°C - 1500°C.

A full size ($4\frac{1}{2}$") hexagonal beryllia brick* (Brush S.P. BeO powder; density of brick = 2.768 g cm^{-3}) has now been heated at 1250°C - 1300°C for approximately 1000 hours in a stream of oxygen-free helium. This treatment caused no significant change in weight, density, or linear dimensions nor did any cracks develop. The fact that no density change was observed in this one isolated experiment could be due either to the low temperature which was employed or to the possibility that the expansion previously noticed on small pieces was due merely to surface effects.

1.1.2 Resistance of Beryllia Bricks to Thermal Stresses

A number of experiments were performed in an effort to determine whether hexagonal beryllia bricks ($4\frac{1}{2}$" high) which had been annealed for several hours at temperatures greater than 1300°C were superior to unannealed bricks in their resistance to thermal stress. The apparatus used consisted of a 4" diameter water cooled brass jacket resting on top of fire brick. The beryllia brick to be tested was placed inside the jacket between two other bricks of approximately the same density and a globar was inserted through the center of the bricks. Thus by introducing heat to the center of the brick and cooling the outer surface of the brick by circulating water through the brass jacket, various temperature gradients could be maintained between the inside and the outside of the

*Fabricated by Norton Company at Niagara Falls by placing the beryllia powder in a graphite mold, then heating the mold by resistance methods to 1600°C - 2100°C and finally applying a pressure of 1000 - 2000 pounds $inch^{-2}$ until the piece has reached the desired dimensions.

brick. The temperatures were measured by thermocouples cemented to the inside and the outside of the brick. It is quite possible, however, that the readings of the inside surface temperature are as much as 50° low.

A few preliminary experiments have been performed and the data are summarized in Table I. There is as yet insufficient data to permit a decision as to whether annealed bricks are superior to unannealed bricks in their resistance to thermal stress.

TABLE I

Effect of Annealing on Resistance of Beryllia Bricks to Thermal Stresses

Brick No.	Type of BeO Powder	Treatment	Run No.	Maximum Temperature Difference between Inside and Outside (°C)	Maximum Outside Temperature (°C)	Remarks
1102	Brush G.C.	Unannealed	1	90	500	No cracks
			2	175	500	No cracks
			3	210	700	Cracked
1105	Brush G.C.	Unannealed	1	95	500	No cracks
			2	195	680	Cracked
1109	Brush S.P.	Annealed*	1	275	575	No cracks
			2	250	625	Cracked
1115	Brush G.C.	Unannealed	1	195	628	Cracked
1108	Brush S.P.	Annealed*	1	295	475	No cracks

*Heated at ca. 1400°C for 2 - 3 hours (24 hour heating and cooling cycle) by Norton Company of Worcester, Mass.

1.1.3 Resistance of Fuel Tubes to Thermal Stresses (L. W. Fromm, T. G. Drugas, R. W. Phillips)

The general equations relating temperatures and thermal stresses in power pile fuel rods to their physical properties are given in CP-3493 (C. A. Hutchison, Jr., 4/15/46). Numerical calculations indicate that the maximum compressive and tensile stresses in solid circular cylindrical fuel rods in a power pile operating at 4000 kw are 38.3×10^7 dyne cm^{-2}. In a pile operating at 100,000 kw they are 9.58×10^9 dyne cm^{-2}. The

maximum compressive and tensile stresses in hollow circular cylindrical fuel rods operating at 100,000 kw are 64 x 10^7 dynes cm^{-2} and 128 x 10^7 dynes cm^{-2}, respectively.

Since the magnitudes of these thermal stresses are obviously of great importance, experiments were initiated to verify these calculations and also to determine the actual effect of such stresses on BeO-UO_2 fuel tubes. Efforts were also made to determine whether the spalling strength of beryllia tubes was increased appreciably by different manufacturing techniques or by the inclusion of various additives with the beryllia.

The apparatus used in these experiments was modified considerably during the course of the work. In the first experiments it consisted of a water-cooled brass jacket resting on top of fire brick. The BeO tube to be tested (ca. 3" long x 1.6" OD x 0.9" ID) was placed inside the jacket between two other BeO tubes to minimize end effects and a globar with a 10" heating length was inserted through the center of the tubes. In some experiments the single globar was replaced with a bundle of three 5/16" diameter x 11" globars with 4" heating lengths. In later runs the brass jacket was replaced by a glass jacket and cooling was accomplished by blowing a stream of air or nitrogen in the annular space between the tube and the jacket. The total power input to the globar was measured and from this the power input to the fuel tube in question could be calculated. (This is, of course, only approximate since the end losses were considerable.) The temperature gradient in the fuel tube was measured experimentally between a thermocouple cemented to the outside wall and a thermocouple in a hole not quite touching the inner wall. From these data, an apparent thermal conductivity of the material can be calculated using the equation:

$$k = \frac{\nu \ell'}{2\pi \Delta T \ell} \ln \frac{r_2}{r_1}$$

where

k = thermal conductivity (cal sec^{-1} cm^{-1} $^oC^{-1}$)

ν = total power input to the globar (cal sec^{-1})

ΔT = measured temperature difference (^oC)

ℓ = length of the heating section of the globar

ℓ' = length of the fuel tube

r_2 = outer radius of tube

r_1 = radius of tube at inner thermocouple

From this value for the apparent thermal conductivity the total temperature difference between the inner and outer walls can be calculated using the same equation. Values for the apparent thermal conductivity as calculated in this manner are under no circumstances a measure of the true thermal conductivity. Their only use is in the calculation of the total temperature difference.

By increasing the power input to the globar, the tube was subjected to increasing temperature gradients, and therefore thermal stresses, until finally the tube failed. This point of failure was determined either by the sound of the cracking during the run or else by subsequent visual examination or inspection by means of the Zyglo technique. The total temperature difference existing at the time of tube failure is a measure of the relative spalling strength of the tube if the tubes which are being compared all have the same dimensions and differ only slightly in thermal conductivity as was true in these experiments.

It is also possible to calculate the maximum tensile stress to which the tube was subjected using the approximate equation:

$$\phi = \frac{Eb}{1-\sigma} \frac{(\Delta T)}{\ln \frac{r_2}{r_1}} \left(\frac{1}{2} - \frac{r_1^2 \ln \frac{r_2}{r_1}}{r_2^2 - r_1^2} \right) *$$

where

ϕ = circumferential stress (dynes cm^{-2})

E = Young's modulus (dynes cm^{-2}; see section 1.1.4 for values)

b = coefficient of thermal expansion (1×10^{-5} $^{o}C^{-1}$)

σ = Poisson's ratio (assumed to be 0.1)

ΔT = total temperature difference between r_1 and r_2

r_1 = radius of inner wall of tube

r_2 = radius of outer wall of tube.

The results of a number of representative runs are reported in Tables II, III and IV. Where two values for a sample are reported, these represent the upper and lower limits between which the actual value lies. Closer approximations are not possible with this apparatus.

As shown in Table II, the average tensile strength of hot-pressed high density (> 2.7 g cm^{-3}) BeO tubes lies between 1.6×10^9 and 2.3×10^9 dynes cm^{-2}. This value for tensile strength is to be compared with the reported value of 1×10^9 dynes cm^{-2} for hot-pressed BeO-10% UO_2 tubes (density = ca. 3.0 g cm^{-3}) as determined from the bursting pressure of hollow cylinders (CT-3528, J. R. Gilbreath and S. R. Gaarder, 5/20/46). As determined by these experiments, there appears to be little correlation between density and spalling resistance in this range. On the other hand, the spalling resistance of hot-pressed tubes having a density

*See CP-3493 for the derivation of the corresponding general equation. It should be pointed out that these equations apply strictly only to the case of an infinitely long tube.

TABLE II

Relative Spalling Strength of Hot-Pressed BeO Tubes

Sample No.	Type of BeO Powder[b]	Density (g cm^{-3})	Temperature Gradient[a] (°C)	Outer Temp. (°C)	Maximum Tensile Strength (10^9 dynes cm^{-2})
1	Fused	2.290	139.1-205.9	875	
2	Fused	2.379	125.2-187.0	865	
3	Fused	2.484	117.1-175.3	765	
Avg.			127.1-189.4		
4	Metal	2.734	87.5-139.6	810	1.12-1.82
5	Metal	2.745	104.6-167.3	901	1.47-2.19
6	Metal	2.750	126.5-202.0	935	1.67-2.64
7	Metal	2.802	107.3-171.4	934	1.50-2.40
8	Fluorescent	2.896	83.4-123.4	840	1.26-1.88
9	Metal	2.951	133.7-198.1	1092	2.14-3.15
10	Metal	2.951	123.2-182.1	--	1.96-2.90
11	Metal	2.955	70.1-103.8	967	1.12-1.66
12	Metal	2.966	117.6-174.2	908	1.91-2.83
13	Metal	2.975	104.7-155.0	932	1.70-2.52
14	Metal	2.985	99.2-146.9	851	1.62-2.38
Avg.			105.3-160.3		1.6 -2.3

(a) This is the calculated temperature difference between the inner and outer walls of the tube.

(b) Metal and Fluorescent grades are low fired BeO powders made by the Clifton Company.

TABLE III

Relative Spalling Strength of Hot-Pressed BeO Tubes Containing 2% Al_2O_3, 2% SiO_2, or 2% CaO

Sample No.	Type of BeO Powder(b)	Density (g cm^{-3})	Temperature Gradient(a) (°C)	Outer Temp. (°C)
With 2% Al_2O_3				
15	G.C.	2.867	87.1-135.8	993
16	G.C.	2.874	133.2-207.7	981
17	G.C.	2.879	99.9-155.5	1025
18	Metal	2.969	149.9-221.9	970
19	Metal	2.975	104.1-153.9	985
20	Metal	2.982	110.9-172.6	836
21	Metal	2.996	82.3-121.9	922
22	Metal	2.998	87.2-128.9	928
23	Metal	3.012	89.8-132.9	923
24	Metal	3.014	116.8-172.9	965
Avg.			106.1-160.4	
With 2% SiO_2				
25	G.C.	2.393	77.9-115.5	755
26	G.C.	2.407	84.7-125.6	780
Avg.			81.3-120.6	
27	Metal	2.892	86.6-128.3	781
28	Metal	3.088	76.2-112.8	894
29	Metal	3.121	86.4-127.8	819
Avg.			83.1-122.9	
With 2% CaO				
30	G.C.	2.970	126.9-188.0	1061
31	G.C.	2.983	107.0-158.3	820
32	G.C.	2.988	125.1-185.2	964
33	G.C.	2.995	120.6-179.0	867
Avg.			119.9-177.6	

(a) This is the calculated temperature difference between inner and outer walls of the tube.

(b) G.C. grade is a low fired BeO powder made by the Brush Co.; Metal grade is a low fired powder made by the Clifton Co.

TABLE IV

Effect of Composition
on Relative Spalling Strength of BeO Tubes

Additives	Density ($g\ cm^{-3}$)	No. of Samples	Temperature Gradient* (°C)
		Hot-pressed	
None	<2.5	3	127.1-189.4
None	>2.7	11	105.3-160.3
2% Al_2O_3	>2.8	10	106.1-160.4
2% SiO_2	<2.5	2	81.3-120.6
2% SiO_2	>2.8	3	83.1-122.9
2% CaO	>2.9	4	119.9-177.6
10% Graphite	--	1	245.3-363.3
20% Graphite	--	1	407.5-603.0
		Ceramically fired	
None	<2.5	2	259.0-375.1

*Average values.

of less than 2.5 g cm^{-3} may be somewhat greater as indicated by the somewhat larger temperature differentials to which the tubes were subjected before failure occurred. The presence of 2% Al_2O_3, 2% SiO_2 or 2% CaO in the hot-pressed BeO tubes does not appear to increase the spalling resistance (Table III). Tubes containing various other additives including 2% ZrO_2, 2% Na_2O-Al_2O_3, 2% K_2O-Al_2O_3, and 10% SiC were also tried. None of these showed any significant improvement in resistance to thermal spalling. However, two samples of hot-pressed BeO containing graphite showed a very significant factor of improvement (Table IV). A tube containing 10% graphite showed a two-fold increase and a tube containing 20% graphite a four-fold increase over pure BeO in strength. Two tubes made by ceramic firing from coarse grained BeO also showed a significant two-fold increase in strength over hot-pressed BeO. It was found that these samples did not crack suddenly (as was the case with hot-pressed materials) but very slowly. After cracking, one of these samples was subjected to a temperature gradient of 817°C, yet no further cracks appeared. Several hot-pressed pure BeO tubes which had been annealed at 1700°C were also tested but showed no improvement over non-annealed samples.

In view of the increased spalling resistance of hot-pressed BeO-20% graphite, a test was run in which such a tube was heated by passing an electric current through the sample itself. At the peak of the test, 6000 kva were dissipated by the specimen at a temperature of 1200°C - 1500°C. Cooling was accomplished with a stream of nitrogen. This power dissipation is 1.82 times the power dissipated by one 3" fuel rod in a pile of 504 six foot channels running at 40,000 kw. A few small cracks resulted but none that greatly weakened the sample. An additional test was made in like manner on a solid graphite rod (3/4" diameter and 5.0" long). Again 6000 kva were dissipated but no cracks of any kind appeared in the sample.

The presence of cracks in a tube might so relieve the stresses as to make it possible to expose the tube to subsequent thermal stresses without additional degradation. In order to test this possibility several tubes were subjected to recurrent heating and cooling cycles. A hot-pressed tube made from metal grade BeO powder was subjected to 32 such cycles. For the first three cycles heating and cooling were carried out at a controlled rate of 10°C/minute, and the sample was examined under Zyglo after each cycle. In the remaining cycles, heating and cooling were done as rapidly as possible (heating - ca. 40°C/minute; cooling - ca. 20°C/minute). Initial cracking was noted on the first cycle at a total temperature difference between inner and outer wall of about 150°C, with an outer temperature of 908°C. Subsequent cycles did not cause excessive damage other than slight widening of the cracks resulting from the initial heating. Similar recycling tests were also run on two BeO tubes which had been annealed at 1700°C. These annealed tubes shattered completely after five and ten cycles respectively.

1.1.4 Variation of Elastic Modulus of Beryllia with Density (J. D. Karp)

Preliminary studies have been made to determine possible correlation between the elastic modulus and the density of beryllia shapes. A series of prisms were made from various beryllia bricks and hollow cylinders representing diversified methods of manufacture.

In order to determine the elastic modulus a dynamic method of measurement was used which involved determining the velocity of propagation of an elastic wave by observing the resonance vibration frequency of a test specimen of suitable dimensions (ca. 0.46 cm x 0.46 cm x 4.4 cm). This method is a modification of that described in several papers including that of L. W. Balamuth (Phys. Rev. 45, (1934), 715-720).

The sample to be measured is made part of a composite oscillator by attaching it to a piezo-quartz crystal by means of beeswax. The system, quartz-sample, is driven by a harmonically varying potential of constant amplitude but of adjustable frequency applied between the silvered faces of the piezo-quartz. As a result of the harmonically varying piezo-electric stress induced in the quartz, the entire oscillator is caused to assume a state of forced longitudinal vibration. The resonance frequency of the composite oscillator is then determined by measuring the amplitude of the current in the quartz circuit as a function of the applied frequency. In the region of the resonance point of the composite oscillator, the current flowing to the quartz rises to a maximum, falls to a minimum, and then regains its previous value. From this value for the resonance frequency of the composite together with the known resonance frequency of the quartz crystal, the resonance frequency of the sample can be calculated. The elastic modulus of the sample can then be calculated from the equation:

$$E = 4\rho r^2 \ell^2$$

where E = Young's Modulus (dynes cm^{-2}),

ρ = density of the sample (g cm^{-3}),

f = resonance frequency of the sample,

ℓ = sample length in cm.

The results of the elastic modulus measurements on seventeen prisms cut from beryllia shapes of various densities are reported in Table V. An apparent linear correlation, illustrated in Figure 1, was obtained between the modulus and the density of beryllia. The only value for ostensibly pure beryllia which is seriously out of line is that for a sample of density 1.904. The source of this material is unknown and the deviation is probably due to some composition or manufacture variable as yet undetermined.

The steady state thermal stresses in solid or hollow circular cylinders, assuming an isotropic, elastic, substance, are directly proportional to the elastic modulus and inversely proportional to the thermal conductivity. Thus, all other quantities being equal, a condition of low elastic modulus is desirable in considering thermal stresses.* In the course of efforts designed to increase the resistance of beryllia to thermal stresses, a series of samples were prepared containing the additives silica, lime, alumina, and graphite. It was hoped that these additives would behave

*It should be pointed out however, that as the thermal stresses are lowered by using material of decreased elastic modulus the tensile strength may be lowered also, so that no real gain is obtained in thermal spalling strength.

TABLE V

Influence of Density on Elastic Modulus of BeO Shapes

Sample No.	Source and Composition	Density ($g\ cm^{-3}$)	Elastic Modulus (10^{10} dynes cm^{-2})
1	Unknown	1.904	260
2	Argonne - pressed from Brush S.P. powder and fired at 1500°C	1.981	41
3	McDanel Co. - made from Clifton powder (60 mesh)	2.078	70
4	Argonne - pressed from Brush S.P. powder and fired at 1800°C	2.245	93
5	McDanel Co. - made from Clifton powder (200 mesh); heated to 1500°C in steam	2.229	115
6	Norton Co. - hot-pressed BeO tube containing 20% graphite	2.534	105
7	Norton Co. - hot-pressed from Brush S.P. powder	2.61	227
8	Norton Co. - hot-pressed from Clifton Metal grade and Brush S.P. powders	2.720	283
9	AC Spark Plug Co. - pressed from Clifton powder and gas fired	2.80	304
10	Norton Co. - hot-pressed from Brush S.P. powder	2.839	320
11	Same as #10	2.914	331
12	Norton Co. - hot-pressed from Clifton Fluorescent powder	2.943	340
13	Norton Co. - hot-pressed BeO tube	2.963	362
14	Norton Co. - hot-pressed BeO tube containing 2% lime	2.961	362
15	Norton Co. - hot-pressed BeO tube containing 2% silica	2.973	357
16	Norton Co. - hot-pressed BeO tube containing 2% alumina	3.002	367
17	Norton Co. - hot-pressed Uranium oxide tube	8.5	429

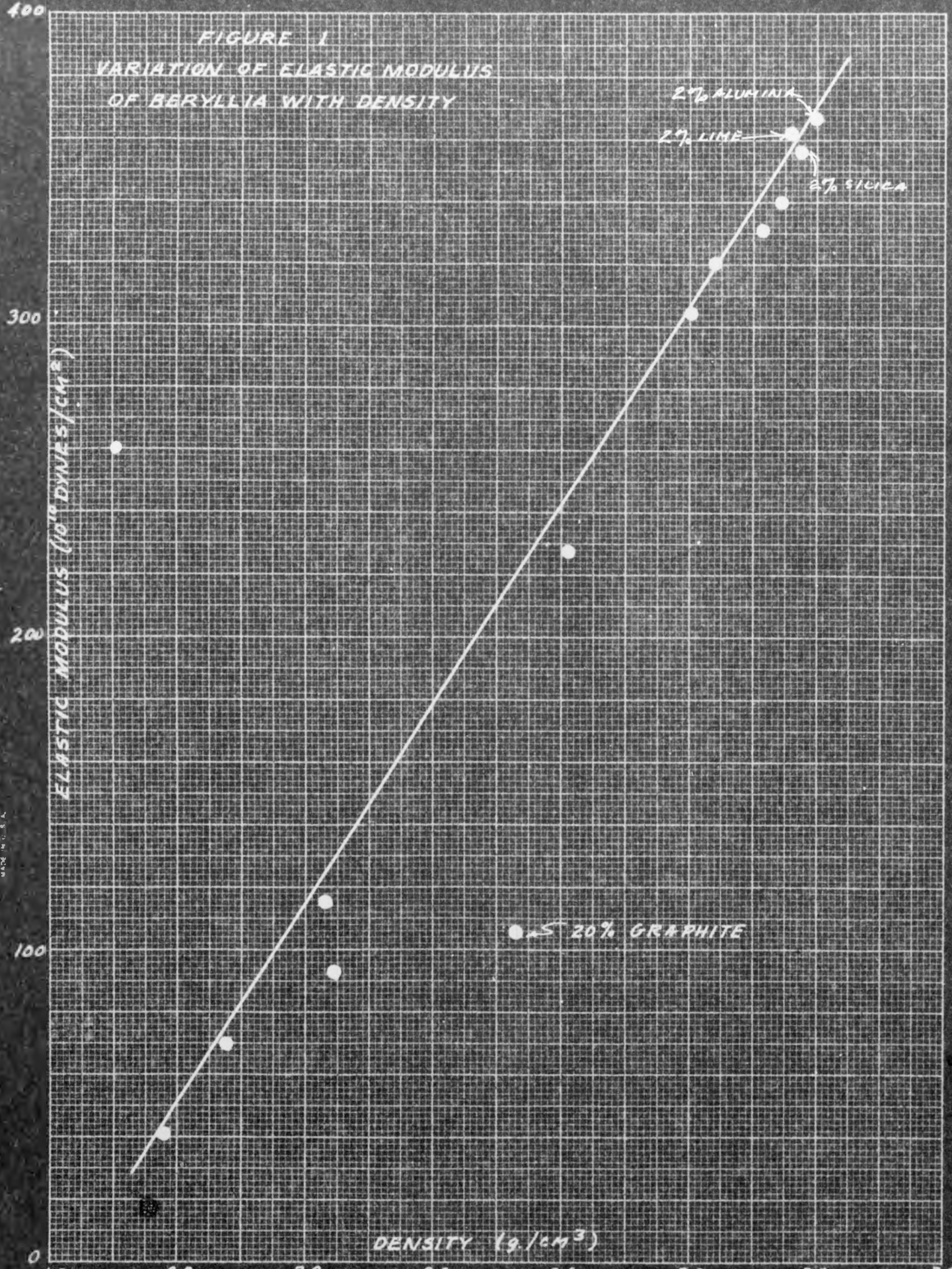
FIGURE 1
VARIATION OF ELASTIC MODULUS OF BERYLLIA WITH DENSITY
2% ALUMINA
2% LIME
2% SILICA
20% GRAPHITE
ELASTIC MODULUS (10^{11} DYNES/CM^2)
DENSITY (g./c.M^3)
400
300
200
100
0
1.8
2.0
2.2
2.4
2.6
2.8
3.0
3.2

as binders thereby inhibiting thermal crack-up. The elastic modulus of four such samples containing 2% SiO_2, 2% CaO, 2% Al_2O_3 and 20% graphite, respectively, were measured (see Table V and Figure 1). Except for the BeO-20% graphite they showed no difference in behavior from that of pure BeO. The addition of graphite, however, resulted in a lowered elastic modulus and this material therefore should be more resistant to thermal crack-up than pure BeO. This was verified by the experiments reported in section 1.1.3 of this report.

1.2 Reaction Between Beryllia and Steam (M. G. Berkman)

The investigation of the reaction between beryllia and steam was undertaken after it had been noted that at high temperatures beryllia was transported from one point in an apparatus to another in the presence of steam.

The first experiments of this investigation dealt with the determination of the effect of temperature on the rate of reaction between beryllia and steam. A report on this study is contained in Bi-weekly Abstract ANL-OCS-87, 11/13/46, pp. 3-5.

Subsequent experiments carried out on the reaction of beryllia with steam may be divided into four groups. These deal with:

(1) The effect of steam flow rate on the beryllia-steam reaction at 1500°C (Table VI).

(2) The effect of steam flow rate on the beryllia-steam reaction at 1400°C (Table VI).

(3) The effect of nitrogen gas on the beryllia-steam reaction (Table VII).

(4) The effect of hydrogen gas on the beryllia-steam reaction (Table VII).

1.2.1 General Experimental Procedure

In all runs the beryllia samples consisted of 5-gram pellets pressed from Brush high-fired beryllia powder, .5 ml 6N nitric acid being used as a binder. The pellets were dried at 100°C for 18 hours and then fired at 1650°C for one hour.

The beryllia pellet was placed on a platinum tray, and inserted into a sillimanite (mullite) tube which was heated by a Burrell furnace. Steam was then passed over the pellet which was maintained at a given temperature. The time for each run was 2½ hours in all cases. A preheater and cooler were provided for the steam. A sketch of the apparatus is included as Figure 2.

1.2.2 Effect of Steam Flow Rate

The data indicate that the rate of reaction of beryllia with steam increases

TABLE VI

Effect of Steam Flow Rate on the BeO-Steam Reaction

Run No.	Amount of H_2O Condensed (ml/min)	Steam Flow* Rate (liters/min)	Temp. (°C)	Weight % BeO Lost
28	0.1	0.81	1500	0.93
29	0.1	0.81	1500	0.90
19	0.25	2.02	1500	1.00
18	0.5	4.05	1500	1.21
25	0.5	4.05	1500	1.17
24	1.0	8.10	1500	1.45
14	2.0	16.20	1500	1.58
36	6.0	48.60	1500	2.10
37	0.6	4.58	1400	0.45
38	1.0	7.63	1400	0.52
13	2.0	15.26	1400	0.64

*Volume flow rate over sample in furnace, that is, at the furnace temperature.

TABLE VII

Effect of Nitrogen or Hydrogen Gas on the BeO-Steam Reaction

Run No.	Amount of H_2O Condensed (ml/min)	Steam Flow Rate (liters/min)	N_2 or H_2 Flow Rate (liters/min)	Partial Pressure H_2O (mm Hg)	Temp. (°C)	Weight % BeO Lost
33	2.0	16.2	3.0 N_2	640	1500	1.15
34	1.0	8.1	3.0 N_2	555	1500	0.91
32	0.14	1.1	3.0 N_2	208	1500	0.28
31	0.016	0.13	3.0 N_2	32	1500	0.05
35	2.0	16.2	1.5 N_2	695	1500	1.34
42	2.0	16.2	3.0 H_2	640	1500	1.32
41	0.8	6.5	3.0 H_2	520	1500	1.10
30	1.5	11.5	2.8 N_2	610	1400	0.52
40	1.0	7.6	2.8 N_2	555	1400	0.40

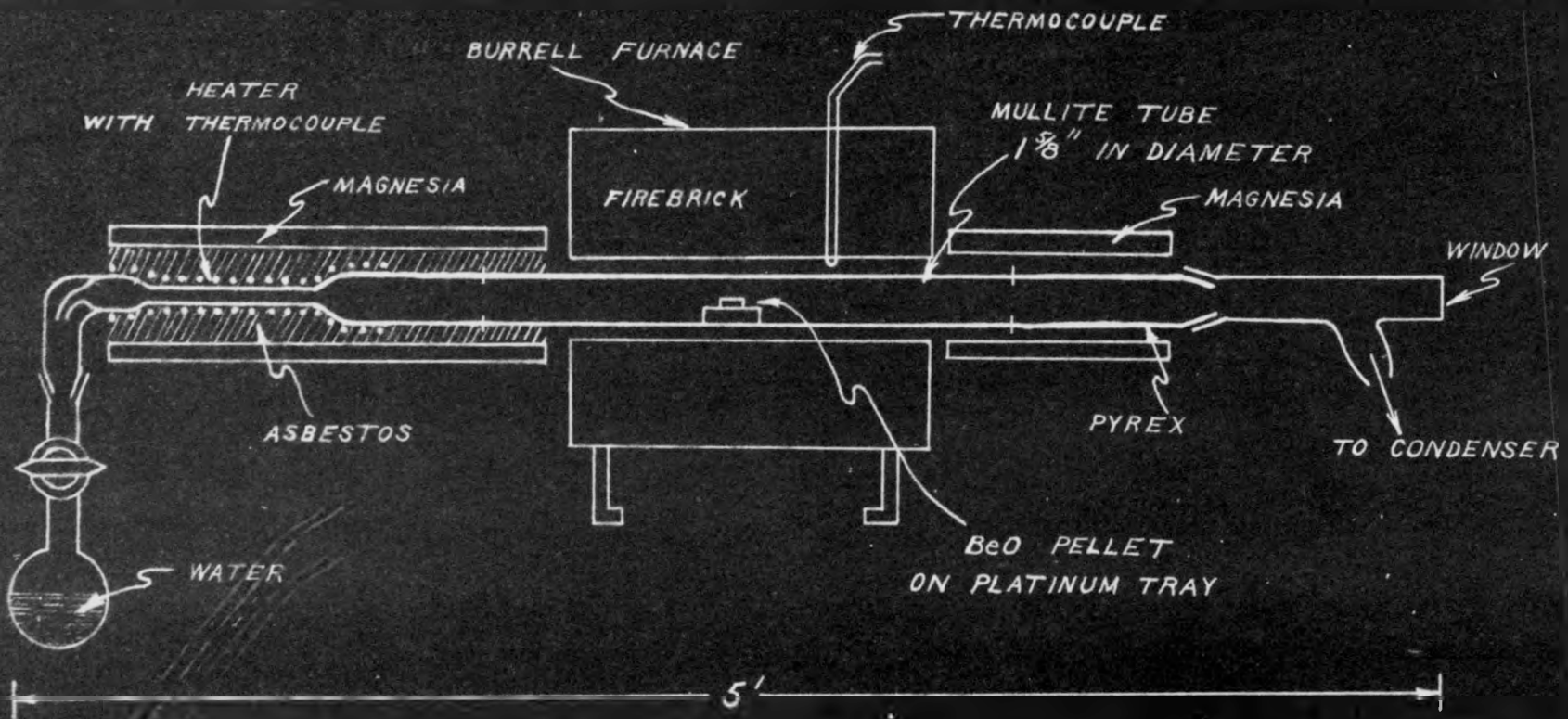

FIGURE 2

APPARATUS FOR BERYLLIA-STEAM REACTION

as the rate of flow of steam is increased. At a given steam temperature (at constant pressure) the effect of increasing the mass rate of flow of steam is to increase the rate of removal of beryllia from the sample. The rate of removal of beryllia from the sample, however, is not proportional to the steam flow rate, and, as the steam flow rate increases, the rate of removal of beryllia increases less rapidly (Figure 3).

In the steam flow rate experiments carried out, the extent of reaction (during the 2½ hour reaction period) was greater at 1500°C than at 1400°C (Table VI).

1.2.3 Effects of Nitrogen and Hydrogen Gas

The effect of decreasing the partial pressure of steam from one atmosphere to a lower value by the addition of either nitrogen or hydrogen is to decrease the rate of reaction with beryllia. The effect seems to be somewhat greater with nitrogen gas than with hydrogen. These results indicate that hydrogen does not enter into the mechanism of the reaction.

1.2.4 Interpretation of Results

There are as yet insufficient data to determine the actual mechanism of the steam-beryllia reaction. However, one might assume as a working hypothesis that the volatilization takes place through the following high-temperature reaction

$$BeO + H_2O \longrightarrow Be(OH)_2\uparrow$$

where the $Be(OH)_2$ is volatile and stable at the high temperatures and in the presence of water vapor. On the other hand, when the reaction product comes in contact with a cooler surface outside the furnace, the reverse reaction takes place. In agreement with this hypothetical reaction no appreciable influence on the rate was observed by adding hydrogen or nitrogen to the steam other than a slight decrease in rate which may be attributed to the corresponding increase in the volume flow rate of steam (see next paragraph).

One might conclude further that if the steam flow rate were slow enough so that saturation of the volatile species is attained, the steam would carry away $Be(OH)_2$, or any other volatile species, at the rate given by equilibrium vapor pressure. Within this saturation range the rate of removal of BeO would be proportional to the flow rate of the steam. At higher flow rates the steam would not be saturated and deviations from proportionality would occur. This is in agreement with the data if one assumes that the linear or proportional range (saturation range) lies at still smaller flow rates than were used. Thus, data at smaller flow rates are desired. From such data it may be possible to calculate the vapor pressure of the volatile species.

FIGURE 3

STEAM FLOW RATE VS WT % BeO LOST
(AT 1500°C)

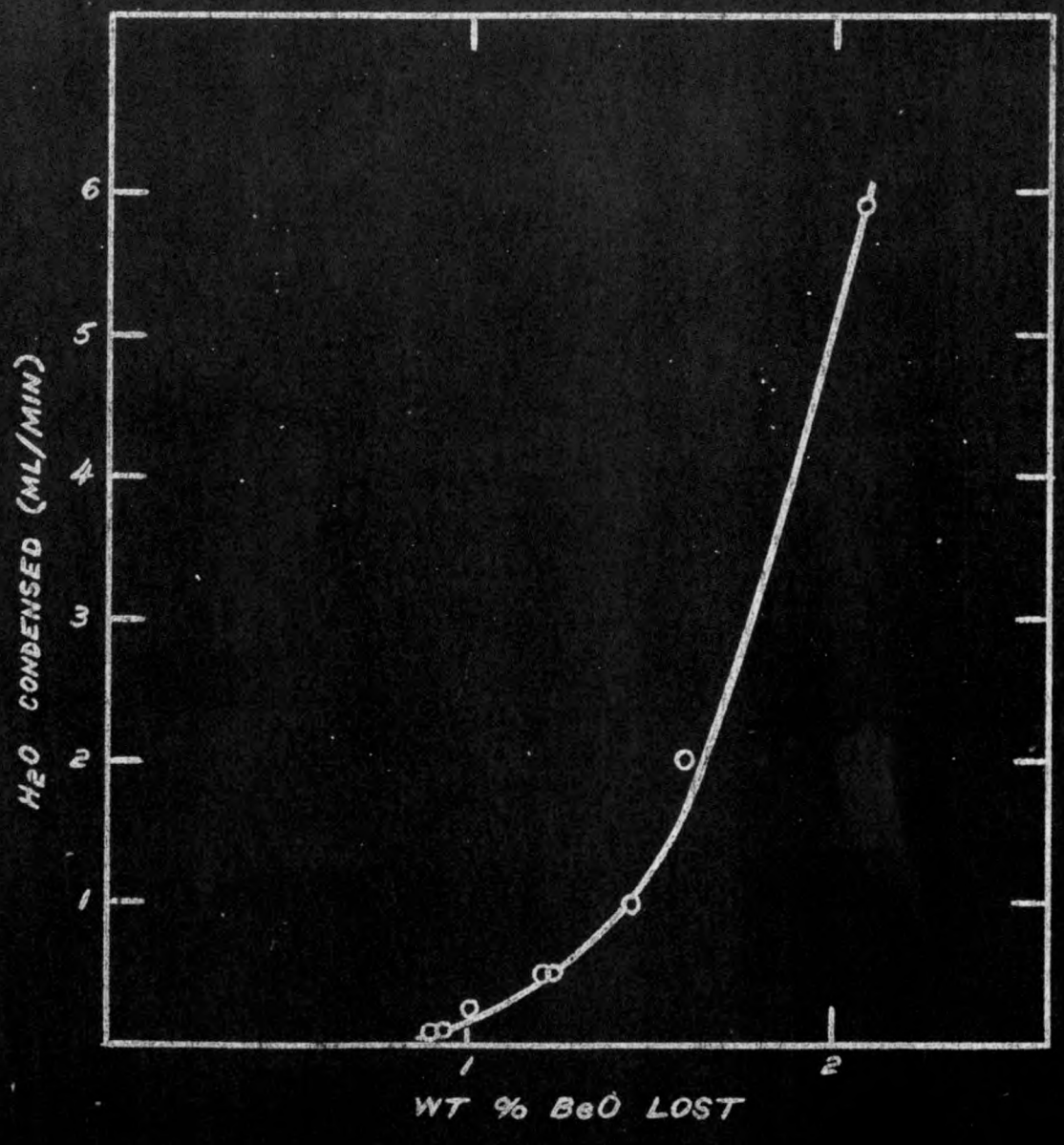

1.3 Effect of Heating on Fuel Materials (J. G. Malm, D. K. Miller)

1.3.1 Effect of Heating in Air on the Dimensions of $BeO-UO_2$ Materials

Measurements of the linear dimensions of hot-pressed $BeO-UO_2$ pellets and cylinders before and after irradiation at HEW show an increase in length of approximately 0.5% after irradiation (see section 1.4). Since it is known that oxygen reacts with UO_2 at elevated temperatures with attendant changes in physical properties and since a small amount of oxygen was present in the sample cans, experiments were initiated to determine the effect of heating similar samples under the conditions of temperature and oxygen concentration which might have obtained in the sample cans.

Norton hot-pressed high density $BeO-10\%$ UO_2 cylinders (0.25" x 0.25") were sealed in quartz capsules under known air pressures, and heated in a muffle furnace, temperatures being recorded by means of a thermocouple placed adjacent to the sample.

Table VIII lists the results of the preliminary heatings of these samples. The maximum mole ratio of oxygen/uranium in the bombardment cans has been estimated to be ca. 0.007; this would be equivalent to 4 cm^3 air at 40 mm pressure/0.6 g pellet. From the results presented in this and in the subsequent tables it will be seen that an appreciably greater amount of air was necessary to produce a significant length increase.

The data of Table IX show the change in length as a function of time. Apparently if there is any appreciable oxidation, with resultant expansion, it takes place rapidly at these temperatures.

For sample Nos. 50-56 listed in Table X heatings were carried out at various pressures, the amount of air present being varied by varying the size of the quartz capsule containing the sample. The expansion varies markedly with the amount of air present, but seems to be relatively independent of the pressure over the range studied (0.25-1.0 atm).

Table XI tabulates the results of heating Norton $BeO-UO_2$ prisms (1.75" x 0.25" x 0.25") in various concentrations of air and at various temperatures. No measureable change in linear dimensions was observed.

The changes in length resulting from heating $BeO-UO_2$ cylinders at 500°C for 45 days are shown in Table XII.

To summarize, small changes in length of mixed oxide samples were observed in some cases but these were invariably smaller than those observed after HEW irradiations. Since the conditions in these experiments were more favorable for oxidation from both the point of view of temperature and oxygen pressure than any conceivable conditions during irradiation, it must be concluded that irradiation was the principal cause of the expansion of the $BeO-UO_2$ samples.

TABLE VIII

Expansion of BeO-10% UO_2 Cylinders on Heating in Air

Sample No.	Volume of Tube (cm^3)	Pressure (mm Hg)	Temp. (°C)	Time at Temp. (hrs)	Original Length of Sample (inches)	Length after Heating (inches)	Length Change (inches)	Per Cent Expansion
4	3.7	752	540	64	0.2497	0.2502	0.0005	0.20
32	2.5	750	525	65	0.2471	0.2471	--	--
35	2.5	750	525	65	0.2501	0.2501	--	--
8	3.6	372	540	64	0.2430	0.2436	0.0006	0.25
36	4.7	369	525	65	0.2466	0.2470	0.0004	0.16
24	4.4	366	525	65	0.2465	0.2472	0.0007	0.28
5	3.8	188	540	64	0.2386	0.2387	0.0001	0.04
13	2.8	74	540	64	0.2385	0.2385	--	--
16	3.2	750	712	65	0.2595	0.2599	0.0004	0.19
37	5.0	750	712	65	0.2407	0.2417	0.0010	0.41
28	3.6	369	712	65	0.2466	0.2468	0.0002	0.08
30	3.6	368	712	65	0.2470	0.2473	0.0003	0.12
11	2.8	373	720	65	0.2321	0.2326	0.0005	0.22
10	3.2	188	720	65	0.2383	0.2384	0.0001	0.04
6	2.8	75	720	65	0.2501	0.2501	--	--

TABLE IX

Expansion of BeO-10% UO_2 Cylinders
on Heating in Air as a Function of Time

Sample No.	Volume of Tube (cm^3)	Pressure (mm Hg)	Temp. (°C)	Time at Temp. (hrs)	Original Length of Sample (inches)	Length after Heating (inches)	Length Change (inches)	Per Cent Expansion
18	3.2	371	506	20	0.2470	0.2471	0.0001	0.04
26	5.3	376	506	20	0.2386	0.2390	0.0004	0.17
21	5.8	368	506	45	0.2406	0.2412	0.0006	0.25
29	4.3	376	506	45	0.2418	0.2420	0.0002	0.08
20	3.4	369	506	92	0.2429	0.2431	0.0002	0.08
25	4.7	378	506	92	0.2418	0.2423	0.0005	0.20
19	3.4	369	506	189	0.2419	0.2421	0.0002	0.08
33	5.3	386	506	189	0.2385	0.2391	0.0006	0.25

TABLE X

Expansion of BeO-10% UO_2 Cylinders
on Heating in Air as a Function of Pressure

Sample No.	Volume of Tube (cm^3)	Pressure (mm Hg)	Temp. (°C)	Time at Temp. (hrs)	Original Length of Sample (inches)	Length after Heating (inches)	Length Change (inches)	Per Cent Expansion
50	2.34	750	516	17	0.2384	0.2391	0.0007	0.29
51	4.56	750	516	17	0.2376	0.2458	0.0082	3.23
52	10.00	750	516	17	0.2377	0.2529	0.0152	6.00
53	10.3	369	516	17	0.2597	0.2630	0.0033	1.25
54	5.06	369	516	17	0.2470	0.2479	0.0009	0.36
55	2.36	368	516	17	0.2387	0.2393	0.0006	0.25
56	10.4	182	516	17	0.2428	0.2441	0.0013	0.53

TABLE XI

Expansion of BeO-UO_2 Prisms on Heating in Air

Sample No.	Volume of Tube (cm^3)	Pressure (mm Hg)	Temp. (°C)	Time at Temp. (hrs)	Original Length of Sample (inches)	Length after Heating (inches)	Length Change (inches)	Per Cent Expansion
C-34(b)	5.7	757	500	89	1.7297	1.7297	--	--
C-33(b)	5.7	375	500	89	1.7304	1.7303	--	--
C-35(b)	7.2	371	500	89	1.7304	1.7302	--	--
C-36(c)	5.8	180	496	213	1.7300	1.7300	--	--
C-8(a)	4.6	742	706	213	1.7396	1.7396	--	--
C-23(c)	5.2	742	706	213	1.7338	1.7338	--	--
C-24(c)	5.3	363	706	213	1.7367	1.7367	--	--
C-32(c)	7.0	361	706	213	1.7292	1.7292	--	--

(a) BeO-10% UO_2 low density prism.

(b) BeO-2% UO_2 high density prism.

(c) BeO-2% UO_2 high density prism.

TABLE XII

Expansion of BeO-10% UO_2 Cylinders on Prolonged Heating in Air

Sample No.	Volume of Tube (cm^3)	Pressure (mm Hg)	Temp. (°C)	Time at Temp. (hrs)	Original Length of Sample (inches)	Length after Heating (inches)	Length Change (inches)	Per Cent Expansion
40	4.5	190	500	1080	0.2470	0.2471	0.0001	0.04
41	3.7	190	500	1080	0.2388	0.2388	--	--
42	3.6	190	500	1080	0.2428	0.2428	--	--
43	3.8	190	500	1080	0.2419	0.2422	0.0003	0.12
44	4.3	190	500	1080	0.2470	0.2472	0.0002	0.08
45	4.0	190	500	1080	0.2432	0.2432	--	--
46	3.3	77	500	1080	0.2386	0.2388	0.0002	0.08
47	3.4	77	500	1080	0.2496	0.2497	0.0001	0.04
48	4.3	77	500	1080	0.2383	0.2385	0.0002	0.08
49	5.8	77	500	1080	0.2418	0.2418	--	--

1.3.2 "Life" Tests

"Life" tests refer to the long-time heating tests on Norton BeO-10% UO_2 hot-pressed pieces as a final check on the rate of volatilization of uranium in a purified helium stream. The apparatus and procedure used was similar to that employed in preceding volatilization tests on such samples and is described in MUC-CAH-46 (C. A. Hutchison, Jr. and J. G. Malm, 6/25/46). A successful long run was never obtained and work on this was discontinued in favor of volatilization tests on graphite samples.

1.3.3 Volatilization Tests on Impregnated Graphite

Volatilization tests in a purified helium stream were begun on uranium-containing graphite samples, the heatings being carried out in a mullite tube at 1450°C. However, reaction of the graphite with the mullite at these temperatures indicates the desirability of using induction heating in further work on this problem.

1.3.4 Miscellaneous

A sample BeO-10% U_3O_8 piece containing 0.53% silicon in the form of SiO_2 prepared at the Battelle Memorial Institute by ceramic firing was examined for the loss of uranium and the appearance of cracks after heating in oxygen. Heating was carried out in a mullite tube in a globar furnace with water-free tank oxygen passing over the sample. At 1500°C, 35% of the uranium was volatilized in 7.8 hours. The sample was unusual, however, in that it showed no signs of cracking on heating from room temperature to 1500°C in oxygen.

delete entire section 1.4

[redacted]

+000 29A

1.5 Diffusion of Xenon Fission Products from BeO-UO_2 Materials (J. E. Wilson, O. C. Simpson)

Experimental measurements of xenon diffusion from beryllia fuel rod material are being continued. The material used is 10% U_3O_8-90% BeO of density ca. 3.1 g cm^{-3}, manufactured by the Norton Company by the hot-pressing technique.

1.5.1 Method and Procedure

A cube sample of the fuel rod material approximately 1 cm on an edge was irradiated in the Argonne CP-3 pile, placed in a furnace at the desired temperature, and a stream of helium passed over it and through a thin-walled cell adjacent to a Geiger-Muller tube. The total xenon which escaped was calculated from the helium flow rate and the GM counts.

Each sample was allowed to cool 4 days after irradiation before making a run. Principally 5d Xe is left after 4 days cooling, the remaining 9h Xe causing an error of about 5%. It was found that the other principal fission products which diffuse out at 1000°C are Te and I. These were removed from the helium stream by passage over clean copper turnings at 250°C, the I and Te reacting strongly with the hot copper. New copper turnings were used after every 3 runs.

The helium was purified by passing it over activated copper catalyst on infusorial earth to remove oxygen, then over copper turnings cooled to liquid air temperature to remove water. The rate of flow of the purified helium was measured with a capillary type flow meter, the pressure difference between the two ends of the capillary being measured by a mercury manometer. The relation between flow rate and manometer reading was established by measuring the time to pass known amounts of gas at various pressure readings.

The sample was heated in a platinum boat inside a mullite tube placed in a Burrell furnace. The linear rate of helium flow directly over the sample was approximately 1 cm/sec.

When it was desired to start a run, the platinum boat with the sample was pushed into the hot furnace by a magnetic arrangement. After passing over heated copper turnings the helium containing the active xenon was passed through a small cylindrical pyrex cell about 3 cm in diameter and 2 cm deep, the bottom of the cell having a thin mica window. This window was directly against the window of the Geiger-Muller tube which was connected to a scaler.

Each run was of three hours duration and the counting rate was measured frequently during this time, the flow rate being held constant. By plotting

counting rate versus time and integrating graphically, the total count for the run was obtained. From this it was possible to calculate the total number of 5d Xe atoms passing through the cell. Since the total number of Xe atoms originally present in the sample could be calculated from the pile neutron flux and time of sample irradiation, it was then possible to calculate the percent of original Xe which diffused out in three hours.

1.5.2 Experimental Results

Data for the runs at 1000°C considered free of major experimental errors are presented in the following table:

TABLE XXVII

Diffusion of Xenon from $BeO-UO_2$ at 1000°C

Run No.	Temperature (°C)	Percent Xenon Diffused out in 3 hours
29	1000	0.1
35	1000	0.2
36	1000	0.1
37	1000	0.1

These results may be compared with the 1.4% previously found to diffuse out at 1450°C and ca. 0.4% at 1400°C.

Another test for the diffusion of less volatile products, principally iodine and tellurium, has also been made. A nickel plate 12" long placed next to the fuel rod sample in a 3 hour run at 1000°C was tested for activity by J. Seiler (see section 1.6 of this report). A total activity of roughly 10,000 c/m was found. This is to be compared with the several million c/m found in a previous similar experiment at 1450°C.

1.5.3 Calculations of Steady State Activity in Pile Coolant

The steady state activity due to 5d and 9h Xe in the coolant of the operating high temperature pile was calculated for "bamboo" shaped fuel rods of 0.043" wall thickness (see section 1.11.2 of this report). The pile was assumed to operate at 4000 kw power, with 3000 liters of helium coolant. The temperature of the fuel rods was assumed to be 1450°C, and the diffusion constant for Xe was taken to be 2.3×10^{-8} cm^2/min (calculated from the 1.4% of 5d Xe diffused out at 1450°C in 3 hours).

The calculation was made with the help of two assumptions. (1) Mathematically these thin-walled fuel rods were treated as a single infinite sheet, since use of cylindrical functions leads to unduly complex numerical computations. (This assumption is justified by the fact brought out in the calculation that the r.m.s. distance of diffusion of 5d Xe before dying is 0.0155 cm = 0.006", a distance considerably smaller than the wall thickness.) (2) Concentration of active Xe at the surface of the fuel rod was taken as zero. This is the safest assumption since this gives most rapid diffusion from the rod. Actually the Xe concentration at the surface of the rod is an unknown function of Xe concentration in the coolant. The assumption is also justified by the calculation itself, which showed a low concentration of Xe in the coolant because of its relatively large volume and because 90% of the 5d Xe remains in the rods in steady operation.

Let C represent the concentration of 5d Xe atoms in the fuel material. Its units are atoms cm^{-3}.

Let P represent the rate of production of the Xe atoms at the constant operating power level of the pile. The units of P are atoms cm^{-3} sec^{-1}.

For one dimensional diffusion of such radioactive atoms the differential equation is:

$$D\frac{\partial^2 C}{\partial x^2} - \lambda C + P = \frac{\partial C}{\partial t} \qquad (1)$$

where D is the diffusion constant in cm^2 sec^{-1} and λ is the radioactive decay constant in sec^{-1}. In line with assumptions (1) and (2) this equation is to be applied to the hypothetical case of a semi-infinite slab of fuel material of surface area S cm^2 equal to the sum of all the surface areas of all the fuel containing pieces which are at the high temperature. Now radioactive xenon atoms will emerge from this surface S by diffusion and will be rapidly distributed throughout the circulating coolant.

Let G be the total number at any time t of radioactive atoms in the coolant, assumed to be uniformly distributed, and let V be the total coolant volume in cm^3. The equation which expresses the fact that atoms are coming into the coolant by diffusion and are leaving by old age and death is:

$$\frac{dG}{dt} - \lambda G = SD\left(\frac{\partial C}{\partial x}\right)_{surf} \qquad (2)$$

where the gradient of the concentration is calculated at the surface of the slab as indicated in the following sketch.

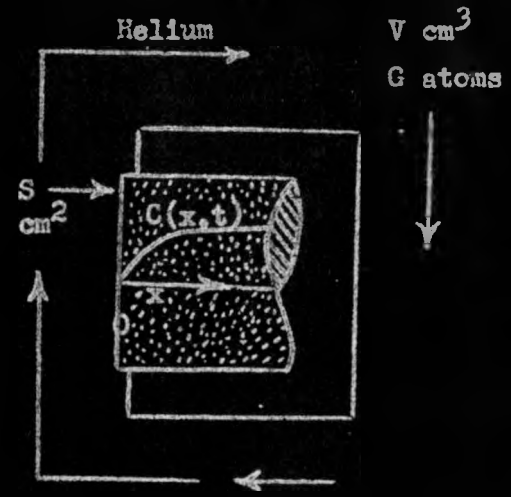

In order to get the steady state activity in the coolant, λG_∞, it is not necessary to solve equations (1) and (2) in detail. For large times, $t \cong \infty$, where steady state conditions obtain, equation (1) may be used to find the concentration $C(x,\infty)$ as a function of the distance inside the surface. The equation which holds is

$$D \frac{d^2C}{dx^2} - \lambda C + P = 0 . \qquad (3)$$

Therefore

$$C(x,\infty) = \frac{P}{\lambda} + Ae^{-ax} + Be^{+ax}, \qquad (4)$$

where $a = \sqrt{\frac{\lambda}{D}}$. Obviously $\left(\frac{dC}{dx}\right)_{x=\infty} = 0$, hence $B = 0$. Also it is assumed arbitrarily that $C(o,t) = 0$ from which it follows that $A = -\frac{P}{\lambda}$. The concentration distribution which holds in the steady state is therefore

$$C(x,\infty) = \frac{P}{\lambda}(1 - e^{-ax}). \qquad (5)$$

From equations (2) and (5) it follows that the activity of the coolant, λG_∞, in disintegrations per second is

$$\lambda G_\infty = SD\left(\frac{\partial C}{\partial x}\right)_\infty = \frac{PS}{a} = PS\sqrt{\frac{D}{\lambda}}, \qquad (6)$$

and the activity in curies per liter is

$$\frac{\lambda G_\infty}{V\ 3.7 \times 10^{10}} = \frac{PS\sqrt{\frac{D}{\lambda}}}{V\ 3.7 \times 10^{10}} \qquad (7)$$

The fraction f of the active atoms which are in the coolant under steady state conditions is given by

$$f = \frac{\lambda G_\infty}{Pv} = \frac{S}{va}\sqrt{\frac{D}{\lambda}} \qquad (8)$$

where small v is the volume of the fuel pieces. For thin-walled "bamboo" fuel rods the situation with respect to the fraction f is about the worst possible. In this case the ratio $S/v \cong 1/d$ where d is the wall thickness. Since $\sqrt{D/\lambda}$ is numerically equal to 0.0155 cm and d = 0.109 cm, f = 0.142. At 4000 kw power the number of Xe atoms produced per second (assuming 4.6% yield for the fission chain leading to 5d Xe) is approximately 5.75×10^{15} atoms/sec. If 14% of these atoms die in the coolant, the activity in the coolant will be

$$\frac{0.142 \times 5.75 \times 10^{15}}{3.000 \times 3.7 \times 10^{10}} = 7.4\ \beta\text{curies/liter.}$$

If one assumes about the same fission yield for the 9h Xe, an additional 2.0 βcuries/liter should be added to give 9.4 βcuries/liter.

Several remarks should be made at this point:

(1) If one assumes that the concentration at the boundary is not kept at zero but always remains equal to the concentration of active atoms in the coolant G/V, the analysis is not more difficult; the result is the same as equation (6) to a high degree of approximation. The truth about the boundary concentration probably lies between these two assumptions.

(2) The assumption that diffusion takes place as in a semi-infinite solid can be replaced by the better assumption that one has a plane sheet of thickness d with diffusion from both sides. Again, this more complex analysis is hardly worth the candle even for these thin-walled tubes and at the high temperature assumed here. For conventional shaped fuel rods and at a lower temperature, smaller D, the analysis presented here is still better.

(3) No attempt has been made to take account of the varying temperature from end to end of the pile. Since the diffusion constant changes rather rapidly with temperature only a fraction of the total surface is really effective in giving activity to the coolant. By the use of the experimental relation D(T) between the diffusion constant and the temperature, one can correct equation (6) as follows:

$$\lambda G_{\infty} = \int \frac{P}{\sqrt{\lambda}} \sqrt{D(T)} \, \frac{dS}{dT} \, dT \, . \qquad (9)$$

Since the surface dS will always be some peripheral length L times dh where h is a vertical distance, and since dT/dh will be approximately constant equation (9) can be written

$$\lambda G_{\infty} = \frac{LP}{\sqrt{\lambda}\,(dt/dh)} \int D^{\frac{1}{2}} \, dT \, . \qquad (10)$$

(4) An alternate derivation of equation (6) can be made as follows: The average (r.m.s.) distance that a particle diffuses in a direction x in time t is given by

$$\sqrt{\overline{\Delta x^2}} = \sqrt{2Dt} \qquad (11)$$

This equation follows from the particular solution of the one dimensional diffusion equation with no decay and no production rate. Thus

$$C(x,t) = \frac{1}{2\sqrt{\pi Dt}} e^{-\frac{x^2}{4Dt}}$$

represents the probability that a particle which is at point $x = 0$ at time $t = 0$ will be at point x at time t. The m.s. distance is then

$$\frac{1}{2\sqrt{\pi Dt}} \int_{-\infty}^{\infty} x^2 \, e^{-\frac{x^2}{4Dt}} \, dx = 2 \, Dt \, .$$

The average volume from which radioactive atoms can diffuse before dying equals $S\sqrt{2D\tau}$ where τ is the average life. Probably the best average life to take would be the r.m.s. life since time enters the equation under the radical. The r.m.s. life equals $\sqrt{2/\lambda}$. If this volume element is at the surface of a fuel rod one-half, on the average, of the atoms which leave the volume will enter the coolant through the surface. Now the number produced per second in the volume element $= PS\sqrt{2D\tau}$. At steady state half of this number will enter the coolant and die there each second. The other half diffuses into the interior of the fuel rod and dies there. Hence

$$\text{Disintegrations/sec in coolant} = \frac{PS\sqrt{2D\tau}}{2} = PS\sqrt{\frac{D}{\lambda}} \, . \qquad (12)$$

1.5.4 Distribution of Activity Through Coolant Ducts

Another question of considerable interest is whether the less volatile fission products are completely spread around the coolant path or whether they strike and stick to the wall rather close to the pile because of their low volatility. The following equation from Einstein and Stokes

can be used to obtain an answer:

$$\overline{\Delta x^2} = \frac{RT}{N} \cdot \frac{\Delta t}{3\pi\eta r}$$

$\overline{\Delta x^2}$ gives the average square distance of diffusion of a particle through the coolant gas in the x direction in time Δt. The viscosity for helium, η, was taken as 1.9×10^{-4} cm^{-1} g/sec, the value at room temperature and atmospheric pressure; actually the gas leaving the pile would be at about 1300°K. The equation holds strictly for a particle moving in a perfectly homogeneous medium at res , but will give a reliable estimate of order of magnitude in the present case. It can also readily be shown that the "immovable layer" of gas atoms at the wall has a thickness of a much smaller order of magnitude than the average diffusion distance and should have little effect on the result for that reason. Consider the first five feet of 1.5 ft diameter pipe leaving the pile. With a linear velocity of 270 ft/sec the wall is available to a 5 ft long volume of gas for 0.0185 sec. During this Δt,

$$\overline{\Delta x} = 10^{-2} \text{ cm}$$

From this value the percent of the total number of atoms striking the wall is 0.04%. Then, assuming that each time a fission product atom strikes the wall it adheres permanently (maximum efficiency), only 0.04% of the active fission products would stick to the wall in the first five feet past the pile. Thus it can be seen that most of the activity would be swept on to be trapped perhaps on the greater surface available in the heat exchanger and the circulation pump.

1.6 Diffusion of Fission Products Other Than Xenon From BeO-UO_2 Fuel Materials

(A. Dudley, J. A. Seiler)

The following describes certain experiments made in cooperation with J. Wilson to determine the radioactive nature of fission products other than xenon which might diffuse from dense BeO-UO_2 pellets into the pile coolant gas at the high temperature at which the pile is to operate.

In an initial scouting experiment an attempt was made to determine the amount of fission products which had diffused out of neutron irradiated pellets of BeO-UO_2 after heating them at 1400°C in a stream of helium gas. This was accomplished by dissolving weighed portions of the pellets before and after heating, and seeking the decrease in the individual fission product activities. The total amount of activity which diffused from the pellets was so small that it could not be detected as the difference between the activities of the solutions of the heated and unheated portions. Maximum preliminary estimates indicated that less than 0.1% of the fission product activity (exclusive of rare gases which were not measured by this method) diffused from the pellets in fourteen hours of heating at 1400°C; furthermore, only I activity could be found in the traps on the downstream side of the system.

1.6.1 Experimental Method

The method of dissolving the $BeO-UO_2$ pellets for fission product assay may be of interest. Dissolution was best accomplished by immersing the pellets in conc. HF in a Pt dish, adding one cc of conc. HNO_3 and keeping the temperature near the boiling point. More acid mixture was added until solution was complete except for the few milligrams of black residue (presumed to be graphite flakes from the surface of the pellet). The HF was then metathesized with 6N HNO_3, heated almost to dryness to remove practically all the HF and finally taken up in strong HNO_3. It was then boiled for a few minutes with a little HCl, cooled, and made up to volume. Most of the graphite residue was oxidized off by the HNO_3 treatment. The above procedure gives a solution in which the fission products are stably retained without becoming adsorbed on the walls, and in which chemical exchange with the carriers seems to be satisfactory. It is probable that much of the I activity is lost by volatilization in the dissolving. To dissolve a solid piece of the dense mixed oxide weighing about one-half gram takes about 90 minutes. If the pellet is crushed in a mortar dissolving may be completed in fifteen minutes.

Subsequent experiments concern efforts to isolate, identify and estimate qualitatively the amounts of fission products volatilized from the heated pellets by collecting the evolved activity in cool portions of the line. The apparatus for heating the pellets in flowing helium has been described by Wilson (see section 1.5 of this report).

A fission product trap consisting of heated copper turnings was placed near the hot furnace tube and on the downstream side. The activity was found to have collected entirely on the first few inches of copper turnings. The fission products were leached from the turnings, washed, and analyses carried out. Some difficulty was occasioned by the interference of copper with the analysis since it was almost impossible to remove all the activity from the copper turnings without completely dissolving the copper. It was also difficult to check the amount of fission product activity which deposited on the glass tubing between the pellet and the copper turnings. To see if fission products were deposited on the glass tubing between the heated pellet and the copper turnings, in some of the experiments a cylinder made of a doubled sheet of rolled Pt foil about 24 cm long was inserted near the $BeO-UO_2$ pellet. The arrangement of the sample, Pt cylinder and copper turning trap is shown in Figure 5. After heating the pellet, the inner layer of the Pt foil was detached from the outer layer. Strips about one cm square were made by rolling the platinum cylinder out flat and cutting crosswise (perpendicular to the axis of the cylinder) into strips 1 cm wide, then cutting each strip into 1 cm squares. The squares were weighed (to normalize the area) and were mounted on cardboard for following their decay on a thin window GM tube. Aluminum absorption curves were also taken.

1.6.2 Experimental Results

The activity deposited on the copper turnings was very slight, hardly enough to appreciably increase the background when the turnings were held close to a GM tube. The "upstream" half of the copper was dissolved in

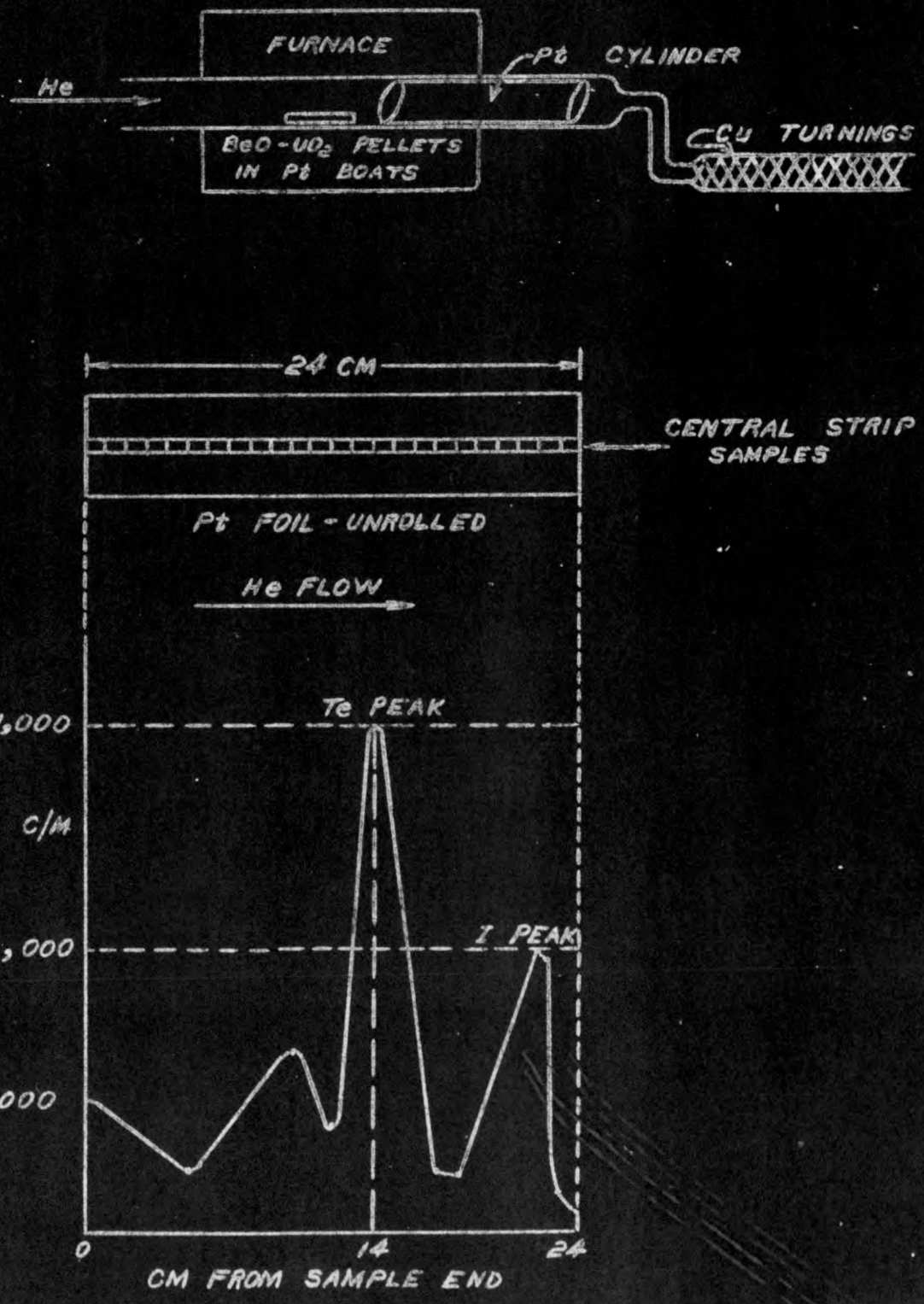

Figure 5

Diffusion of Non-Gaseous Fission Products from $BeO-UO_2$ Cylinders

HNO_3, gross beta samples were prepared by evaporating aliquots, and I and Te analyses were performed on other aliquots. The Te sample gave only a few counts, corresponding to less than 0.01% of Te activity in the sample. Neither the gross beta sample nor the I sample showed any activity at all, although, of course, the gross beta sample was only a small (1/100) aliquot of the copper solution. Whatever traces of I activity might have been present on the copper were presumably lost by volatilization as the copper was dissolved. Leachings on the "downstream" half of the turnings with various dilute acids showed no evidence of fission product activity.

More highly activated pellets were tried next. All precautions for I and Te exchange with their chemical carriers were taken. The major portion of the activity was found to deposit on the first few centimeters of tightly packed copper turnings; the rest of the copper had only trace amounts of I activity. The turnings were washed and leached to remove the activity and analyses were made for some of the fission products. All analyses were negative except those for I and Te whose total accounted for the entire activity found as determined by a gross beta sample from the leaching solution. An analysis of the I decay curve showed some 2.4h component which grows from 77h Te. Since the copper leaching was performed more than 24 hrs after the pellet heating took place, the 2.4h I could not have been present in the copper solution in a detectable amount unless it had been formed by the decay of the 77h Te in the solution. Some Te presumably is evolved from the pellet. The rest of the I activity is mainly 8d I plus a small fraction of 22h I.

The deposition of activity on the Pt cylinder was non-uniform. When the Pt cylinder was opened and laid flat, the majority of the activity lay along a central strip (Figure 5). From this central strip 24 samples were prepared and followed on CM tubes. The relative activities of these central sections show some 77h Te near the upstream edge which increased progressively lengthwise along the strip until it reached a maximum at around the middle (Figure 5). The downstream half of the strip showed only 8d I; the maximum activity was reached near the end of the strip. The copper turnings immediately downstream from the Pt foil showed a very small amount of I activity on the first few millimeters.

Aluminum absorption and decay curves proved to be identical with standard 77h Te and 8d I curves. Although no chemical analyses were made the identification may be considered certain. Figure 5 shows the rolled out Pt cylinder, the 24 samples from the center strip and the graph showing the distribution of fission product activity along the length of this strip.

Within the sensitivity limitations of these experiments it may be seen that no fission product other than I and Te activity (and of course the rare gases) diffused out of the high density $BeO-UO_2$ pellets when they were heated at 1400°C for three hours, and that the diffusion of these activities is very slow. The distribution of the activities on the Pt foil is in the anticipated order, the less volatile Te depositing almost completely on the initial portion of the Pt foil cylinder which is at a temperature perhaps only a few hundred degrees cooler than the sample itself. The outer end of the Pt foil is at about 200°C to 300°C (estimated)

and the major portion of the I activity was deposited here. Roughly of the order of 0.1% of the total I and Te activities present in the dense pellet were volatilized off in this experiment.

1.7 Impregnation of Graphite with Uranium Compounds for Use as Fuel Rod Materials (C. A. Boyd, P. F. Dismore, D. N. Schultz, M. T. Walling)

Graphite is being considered as an alternate material for the fabrication of fuel tubes to be used in the Daniels High Temperature Pile. A question then arises as to the method by which the enriched uranium should be incorporated into the graphite.

One possible method of accomplishing this would be to make up a mixture of carbon flour and U_3O_8 powder and then graphitize the composite by heating to a high temperature. The following preliminary experiment was carried out. Powdered graphite was added to a solution of uranyl nitrate hexahydrate and the mixture evaporated to a thick paste. This was packed into a beryllia tube and baked overnight at 400°C whereby the remaining water was removed and the nitrate decomposed. The temperature of the oven was then raised to 1450°C and held there for a few hours. When the sample was removed from the furnace it was found to be in the form of a fine powder. This method of attack was abandoned at this stage at the Argonne National Laboratory since it was obvious that to produce coherent material it would be necessary to mix the powders in pitch and actually regraphitize in very high temperature furnaces which were not available. Therefore, the Argonne National Laboratory has interested the Norton Co., Battelle Memorial Institute, and the National Carbon Co. in this phase of the work.

Another suggested method of incorporating uranium into graphite requires that the graphite be fabricated in the desired shape and then soaked in a solution of a uranium salt. This would allow the solution to penetrate the pores of the graphite, where the salt would be deposited upon drying. The salt used would be selected to be unstable at a reasonably low temperature decomposing into an oxide which would be more stable.

Accordingly a project was initiated at ANL to investigate the feasibility of impregnating graphite with uranium compound.

The work to be described in the present report includes the results of preliminary experiments studying the general nature of the process and the effect of some of the more obvious variables upon the extent of the impregnation.

1.7.1 Impregnation with Molten Uranyl Nitrate Hexahydrate

Uranyl nitrate hexahydrate, when heated to 60°C, dissolves in its water of hydration. Consequently, tests were made using such a solution for the impregnation. After treatment with the solution the samples were fired at 800°C to convert the $UO_2(NO_3)_2 \cdot 6H_2O$ to U_3O_8. The process could be repeated to increase the percentage of U_3O_8 in the graphite.

Although large percent weight increases were observed for the samples (as great as 19%), the amount deposited was extremely nonreproducible.

This was thought to be due in part to the fact that during the firing step noticeable quantities of uranium salt melted and migrated to the surface.

A study was made of the distribution of uranium in a graphite rod of density 1.56 g/cc which had been impregnated by this method. The rod, which contained 29 g of U_3O_8 per 100 cc of graphite calculated on the basis of the weight increase, was turned off to various depths on a lathe and the shavings collected and analyzed for uranium content. The results are shown in the following table.

Location of Sample Measured from Original Surface of Rod	Percent U in Sample	g U_3O_8 per 100 cc of Graphite
0 - 1 mm	15.8	35.7
1 - 2.5 mm	14.9	33.8
2.5 - 4 mm	12.5	28.2

It is obvious that the uranium content in the center must be a great deal less than the average. This was confirmed through examination of the impregnated samples by X-ray which showed low concentration zones at the center of the shape.

1.7.2 Impregnation with an Ether Solution of Uranyl Nitrate

Other studies were made using uranyl nitrate dissolved in diethyl ether as the impregnating solution. This solvent was selected for the following reasons:

(1) It was thought that the lowered surface tension and viscosity might improve the penetration of the solution into the graphite.

(2) The uranyl nitrate in ether solution contains only a very small amount of water. It was felt that this might prevent the melting and migration of uranium salt to the surface during firing.

In general, the samples used were cylinders approximately 1 cm in diameter and 2 cm long. These were boiled in distilled water to remove any powdered graphite sticking to them. They were then heated to 800°C in an atmosphere of tank helium to remove the water and make the samples more absorbent. After cooling, the samples were weighed and then refluxed in an ether solution containing 39 g of $UO_2(NO_3)_2$ per 100 cc of solution for one-half hour. These were then fired in a tube furnace at 800°C in an atmosphere

of helium for one-half hour to convert the uranyl nitrate to oxides of uranium. After cooling, the samples were reweighed. It was found that the samples increased approximately 3% in weight although there was a reasonably large scatter of the values about the average.

Tests were also made to ascertain if the spread in the percent weight increase, observed in samples treated in the same manner, could be reduced by using lower solution concentrations and by recycling the graphite sample through the impregnation process. Four runs of three samples each were made using different ether-uranyl nitrate concentrations. Each set of samples was recycled four times through the process, the weight percent increase being determined after each cycle. The results of these tests are summarized in Figure 6.

It will be noticed in this graph that the samples which deviate from the average for the first impregnation also deviate in the same direction for succeeding ones. This indicates that the observed scatter is mainly due to variations in the graphite itself and not due to variations in the impregnation process.

During the above tests it was found that the ether solutions gradually formed a colloidal black precipitate after prolonged refluxing. Investigation of this instability showed that the decomposition could be inhibited by increasing the free acid content but could not be prevented entirely. This decomposition was greatly accelerated at the boiling point.

X-ray examination of samples prepared by impregnation from ether solution showed that although the uranium was deposited more or less uniformly throughout the sample, there were "empty" zones distributed at random throughout the structure where the uranium content was lower.

1.7.3 Impregnation with Hexane, Acetone, and Water Solutions of Uranyl Nitrate

Tests were made using hexane and acetone as solvents for the impregnating solution. Approximately the same results were obtained with these solvents as had been obtained earlier with ether. These solutions also exhibited instability at elevated temperatures.

The effect of time of refluxing the graphite in the impregnating solution upon the amount of uranium taken up was also studied. An acetone solution containing 86 g of $UO_2(NO_3)_2$ per 100 cc solution was used. Although the variation among individual samples is reasonably large it appears that there is no appreciable increase in the amount of uranium taken up after 30 minutes of impregnation. The results are shown in the following table.

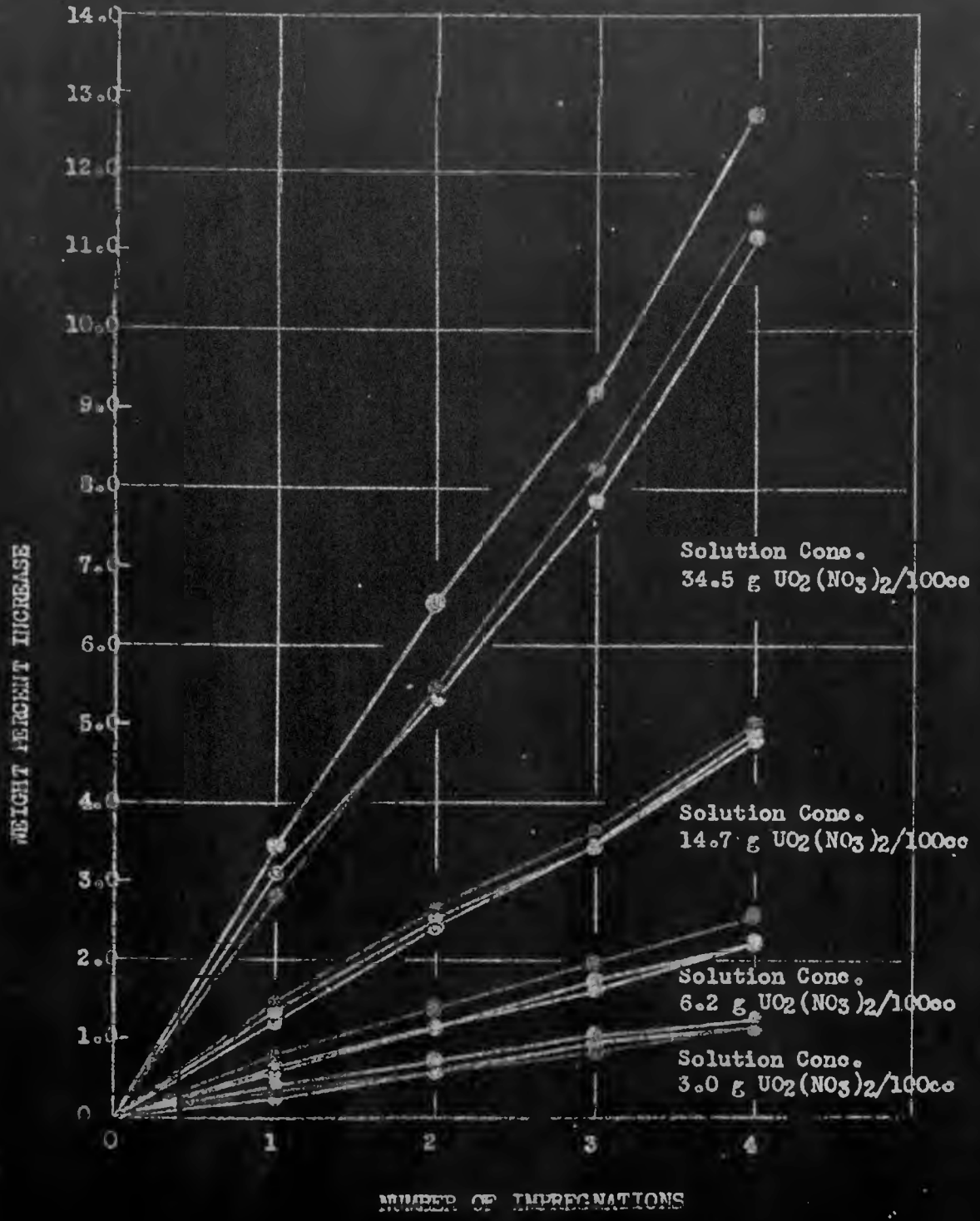

Figure 6

Variation of Wt Percent Increase for AGOT-K Graphite Samples With No. of Impregnations for Several Concentrations of Ether - $UO_2(NO_3)_2$ Solutions

Time of Impregnation	Percent Wt. Increase
10 minutes	2.78 3.79 2.90
30 "	3.37 3.26 2.86
60 "	3.20 3.38 3.20
120 "	3.66 3.22 3.14

The use of water as a solvent was tried early in the program. However, at that time the amount of uranium needed in the fuel tube was thought to be of such a magnitude that a very concentrated solution was required, and considerable migration of the deposited uranyl nitrate hexahydrate occurred during firing. With the lowering of the required amount of uranium, this difficulty may be minimized and tests will be made to see if water can be used as an impregnating solvent under the new requirements. It should be pointed out that water solutions of uranyl nitrate are far more stable than solutions made with organic solvents. Also, if slightly acid aqueous solutions are used, the uranyl nitrate deposits as the tri- or di-hydrate which may cut down the tendency to migrate during drying.

1.7.4 Miscellaneous Tests

Some tests were made to investigate the effect of immersing the graphite in the impregnating solution under vacuum and then allowing a return to atmospheric pressure. This was done by evacuating a chamber containing the graphite for one hour after which an ether solution of uranyl nitrate was suddenly flushed over the sample. The pressure was then returned to atmospheric. No greater amounts of impregnation were obtained in these tests than had been obtained earlier by refluxing in an equivalent solution for 30 minutes.

Preliminary tests were also made to determine the effect of long time heating upon the impregnated graphite. In the first test a sample containing 9.2% U_3O_8 was heated in a stream of purified helium for a total of 30 hours at 1040°C. At the end of this time the sample had lost 1.1% of its weight while a control sample of plain graphite lost only 0.4% of its weight. Gas analyses run on the entrant and exit gases gave the following results:

	Entrant Gas (%)	Exit Gas (%)
CO_2	0.02	0.04
CO	0.03	0.10
O_2	0.05	0.04

Another similar test run at 1390°C for sixty hours gave the following results:

	Entrant Gas (%)	Exit Gas (%)
CO_2	0.03	0.03
CO	0.02	0.62
O_2	0.02	0.03

It is seen that in both of these tests there is a considerable increase in the CO content in the exit gas with little change in the free oxygen content. This suggests that the graphite may be reducing the U_3O_8 to a lower oxide or possibly carbide.

Preliminary tests undertaken to determine the feasibility of recovering uranium from impregnated graphite indicate that about 90% of the uranium can be leached out of the graphite by digestion in dilute nitric acid at 90°C. Further experiments are planned.

Samples of beryllia (a possible fuel tube material) of density 2.06 g/cc were treated with uranyl nitrate by refluxing in an ether solution, followed by heating to convert to the oxide. These samples absorbed 4.8% U_3O_8 as shown by weight increases. A brown oxide layer appeared on the surface.

1.7.5 Conclusions

(1) It is possible to impregnate graphite with uranium oxides by refluxing in a solution of uranyl nitrate and then firing to convert the compound to the oxide.

(2) The deposited uranyl nitrate hexahydrate shows a tendency to migrate to the surface upon firing, especially if the concentration is high.

(3) Organic solvents give reasonably uniform impregnations as compared with use of molten hexahydrate. However, the solutions are unstable and cannot be used for more than fifty hours reflux time.

(4) Upon heating impregnated graphite to elevated temperatures (above 1000°C) an apparent reduction of the U_3O_8 occurs.

(5) Tests should be continued to investigate the feasibility of impregnating large scale fuel tubes.

1.8 Vapor Pressure of Beryllium Oxide (N. D. Erway, R. L. Seifert)

The vapor pressure of beryllium oxide has been measured in the temperature range 1950°C to 2150°C by a modified Knudson effusion method using radioactive Be^7 as a tracer. In this temperature range the vapor pressure is given by the equation:

$$\log_{10} P_{mm} = 18.32 - \frac{34,230}{T} - 2 \log_{10} T$$

The boiling point is estimated to be about 4300°C with a molar entropy of vaporization at the boiling point of about 26 calories/degree. A report has been written (CF-3626, by N. D. Erway and R. L. Seifert, 9/24/46) detailing the method and giving the experimental results obtained from these measurements.

1.9 Spectral Emissivity and Total Emissivity of Beryllium Oxide (R. L. Seifert)

A report has been written (CF-3649, by R. L. Seifert, 10/25/46) detailing the method and the experimental results obtained on the measurement of the spectral emissivity and the total emissivity of hot-pressed beryllia in the temperature range 1200°K to 2150°K. Essentially two types of hot-pressed BeO were used in these experiments, a sample of the black material as it comes directly from the graphite molds used in the hot-pressing operation, and a sample of similar material which had been whitened by subsequent annealing in air.

The spectral emissivities were measured by comparison with a reference surface of platinum plated directly onto part of the beryllia surface. The spectral emissivity ($\epsilon_{0.665,\mu}$) was found to vary from 0.542 at 1200°K to 0.587 at 1900°K to 0.235 at 1900°K for the whitened samples of beryllia. The complete curves are presented in the above mentioned report.

The total emissivity of these samples was measured with a total radiation pyrometer, with suitable modifications of the customary apparatus being made to permit the attainment of high temperatures. The total emissivity (ϵ_{total}) of the "black" material varied from 0.665 at 1200°K to 0.931 at 2000°K whereas the total emissivity of the annealed "white" material varied from 0.336 at 1200°K to 0.475 at 2150°K. The complete curves are presented in the above mentioned report.

1.10 Power Pile Mock-up Unit (N. Dawson, D. H. Miller, W. Salmon, M. T. Walling, Jr., H. Woolf)

The power pile mock-up unit has been rebuilt in preparation for a series of runs in which the simulated operation of a helium cooled pile will be studied over several temperature ranges and power levels.

Pile materials placed in the unit for three runs include sixty hot-pressed BeO hexagonal bricks, including both 3" and $4\frac{1}{2}$" bricks, annealed and unannealed bricks, and a like number of hot-pressed mixed-oxide "fuel" tubes including both 10% UO_2 and 2% UO_2 tubes. These shapes were weighed, micrometered and inspected for cracks by the "Zyglo" technique before installation in the unit. The uranium contents of several representative "fuel" tubes and the densities of a number of bricks and tubes were also determined before installation.

A helium purifier consisting of an electrically-heated furnace packed with copper wool has been set up in a by-pass position on the outlet side of the blower. A "De-Oxo" indicator, a continuous-recording indicating oxygen meter manufactured by Baker & Co., has also been installed to measure the oxygen content of the helium in the mock-up coolant system. The mock-up has now been equipped with a flight recorder (a 96 point Brown strip-chart potentiometer obtained from Wright Field, Dayton, Ohio) which will be used to record continuously the emf's of the twenty-five mock-up thermocouples.

Under-over current relays and accessory equipment have been inserted in the electrical circuit. These relays, which automatically shut down the mock-up furnace and blower in the event of any gross changes in the heating current, were installed as protection for the pile materials housed in the mock-up furnace. Experience has shown that these materials are quite susceptible to thermal shock.

Preliminary runs made for the purpose of testing the new equipment indicate fairly satisfactory operation. Oxygen contents of less than 0.001% (the lower limit of the "De-Oxo" meter) have been obtained under steady-state conditions in which less than 5% of the circulating helium was diverted through the purifier unit.

The results of these preliminary runs will be reported at a later date, along with the series of runs which will begin shortly.

1.11 Pile Design and Mechanisms (H. B. Fairchild)

1.11.1 Loading and Unloading Mechanism

Because of the prospect of bringing the temperature of the pile down to 750°C - 800°C with the resultant possibility of "canning" the fuel rods, loading and unloading problems are again being investigated. A mechanism for top of pile operation has been designed (ANL-OCS-18, from H. B. Fairchild to O. C. Simpson, 7/26/46) which can be manually operated with a wire cut-off device enabling the fuel rods to drop out the bottom of the pile into a hopper via a liquid seal. Various elements and compounds which may have possibilities for fulfilling the requirements of a liquid seal are being investigated, and a memo compiling the available data has

been written (ANL-OCS-66, from H. B. Fairchild to O. C. Simpson, 10/2/46). This report also contains the description of an alternate proposal for fuel slug removal entailing the use of a double gate gas lock instead of a liquid seal.

1.11.2 Determination of Pressure Drops

A memo has been issued (ANL-OCS-30, from H. B. Fairchild to O. C. Simpson, 7/22/46) on the theoretical treatments available for the calculation of the approximate pressure drops through a spherical pebble pile. The diversity of the solutions of the equations in the literature indicated the advisability of determining such pressure drops by actual experimentation (ANL-OCS-30 Supplement, from H. B. Fairchild to O. C. Simpson, 9/26/46). Four runs were made on 1" dia. spheres with complete repacking for each run. However, very little variation of fractional free space (or % void) was achieved in each case. Pressure drops through 1" dia. spheres (smooth surface) arranged in a 7" diameter column 1 foot high were observed throughout a range of flow rates whose maximum value was determined by the operating limit of the apparatus (ca. 0.012 lbs/sec flow of He). A typical equation for the pressure drop under such conditions is

$$\Delta p = 1274\ W^{2.038}$$

where

Δp = inches H_2O/foot

W = helium flow rate in lbs/sec

The observed values were ca. 50% of the theoretical values obtained from equations found in the literature with the exception of one equation derived by S. B. Burke and W. B. Plummer (Industrial and Engineering Chemistry, 20 (1928) 1199), where the agreement was very close.

Since the proposed design of the high temperature pile considers the flow of gas through channels containing fuel slugs, the gas flow characteristics through such a channel has been determined using various fuel rod designs. A memo has been issued (ANL-OCS-29, 7/19/46) describing the apparatus used, the data obtained, and some conclusions of such observations. Of eight designs tested, four showed more promise than the others from the standpoint of the least variation in gas flow with orientation of the fuel rod in the channel. One of these designs, "F-22" (a hollow cylinder without ribs: 1.500" OD, 0.625" ID, 6.0" long), has a further advantage over the other three in that it offers good area of contact to a gas film thus allowing for efficient heat dissipation. Although this design may offer only two point contact depending on the orientation, there is satisfactory coolant gas flow past the points of contact.

The pressure drops occasioned by alundum tubes 2 feet long were determined for comparison with the above designs, and the results appear in memo ANL-OCS-31 (from H. B. Fairchild to O. C. Simpson, 9/7/46). Alundum "bamboo" rods (0.627" OD, 0.301" ID) showed a greater pressure drop than previous designs. Alundum "cane" rods (0.420" OD, 0.335" ID), however, gave pressure drops comparable to previous designs.

1.12 BeO Pile Calculations (R. G. Sachs)

1.12.1 Computations on Transient Behavior of the BeO Pile

A memo has been written to Farrington Daniels (from R. G. Sachs, ANL-RGS-6, 8/28/46) on "The Transient Behavior of the BeO Pile". The reactivity of the BeO pile when it is at room temperature (not in operation) is expected to be at least 15% greater than at the operating level. Since it is not safe to make a sudden change in the reactivity of more than 0.1%, it will be necessary to start the pile slowly. The start-up schedule of the reactor and questions concerning its stability while in operation are discussed in this memo for the purpose of obtaining a preliminary idea concerning the design of a control system for the pile. This memo is not intended to be the basis for final decisions concerning the design of the pile, but rather as an indication of the considerations which will be involved in making such decisions.

The constants that have been used in this treatment correspond to a pile containing 0.0275 g of UO_2/g of BeO, with the uranium present as 30% U^{235}, but the qualitative results would probably not be changed in a serious way if the concentration were lowered. It is found that the pile may oscillate with increasing amplitude at all power levels. This is not important at low power levels because the start-up procedure can be such that oscillations do not occur until the operating level is attained. At the operating level, the worst features of the instability could be eliminated by introducing a temperature control on the coolant system. There would still be a tendency toward instability as a consequence of radiative heat transfer from the fuel rods to the moderator, but it is indicated that this instability will have a great enough relaxation time for it to be handled by means of control rods.

1.12.2 Changes in Calculations on BeO Pile Size and Experimental Requirements

It has recently been proposed that the density of loading of the BeO pile be reduced to 0.004 g of UO_2/g of BeO. In addition to this change, recent experiments by D. J. Hughes (CP-3562) indicate that the transport cross-section is nearly 6.2 barns rather than the value of 10 barns previously reported in MUC-KW-60 (from K. Way to R. G. Sachs, 4/12/46). New estimates have therefore been made of critical size (weight) and of the materials needed for the exponential, age and diffusion length experiments. A memo has been issued (ANL-RGS-2, from R. G. Sachs to F. Daniels, 8/7/46) concerning the changes thus made necessary in previous calculations given in MUC-RGS-AVM-5 (A. V. Martin to R. G. Sachs, 5/15/46) and MUC-RGS-2 (R. G. Sachs to J. E. Willard, 4/2/46).

(1) Critical Size of Pile — A rough estimate of the change in reactivity of the hot pile on the basis of the low density of loading now being considered and the correction in the transport cross section indicates that the critical size (weight) of the pile will be 1.7 times greater than reported in MUC-RGS-AVM-5.

(2) Physics Experiments Associated with Design of BeO Pile

(a) Exponential Pile Estimates of material needed on the basis of the new loading density and the corrected transport cross-section indicate a requirement of 2300 lbs of BeO bricks and 9.3 lbs of UO_2 containing ca. 1.3 kg of U^{235} for the exponential experiment.

(b) Age Experiment No change will be necessary in the amount of material estimated in MUC-RGS-2 for the age experiments; namely, ca. 1.5 tons of BeO about equally divided between hexagonal bricks and plugs.

(c) Diffusion Length Experiment It seems almost certain that the age experiment will be subject to interpretation only if the diffusion length in the same sample of pure BeO is measured. The amount required for the diffusion length measurement is increased by a factor of 2.0.

The material required for the three experiments is summarized in the following table:

	Weight of BeO Bricks	Weight of BeO Plugs	Weight of UO_2 (Containing 30% U^{235})
Exponential	2300 lbs	0	9.3 lbs
Age	1500 lbs	1500 lbs	0
Diffusion length	4000 lbs	4000 lbs	0

1.12.3 Effect of Impurities on Pile Size and Conversion (R. G. Sachs)

An estimate has been made (ANL-RGS-3, from R. G. Sachs to O. C. Simpson, 8/9/46) of the effect of introducing 10^{-6} parts of boron by weight into the pile moderator for a pile containing 0.004 g of UO_2/g of BeO. If it is assumed that the accepted absorption cross-section of BeO, namely, 0.01 barns, is due only to the beryllium, this amount of boron would increase the absorption of neutrons in the moderator by 18%. This increase in the absorption would lead to a decrease in k of 3% and a decrease in diffusion length of 1.5%. The corresponding change in the reactivity would be a reduction by about 5%. Thus the pile volume would be increased by ca. 7%. It is also to be expected that the conversion gain would be reduced by an amount of the order of 3%.

1.13 Procurement of BeO (C. A. Boyd, C. A. Hutchison, Jr., O. C. Simpson, J. E. Willard)

Negotiations have begun for procurement of BeO for the various experiments listed above to be carried out by Monsanto at Clinton Laboratories. Since all the original experimental work and contacts with the companies had been made at this site, it was requested that the Argonne National Laboratory continue to deal with the companies as go-betweens during the transition period. As a result of the above mentioned calculations on the effect of boron on the absorption of neutrons in the moderator, a specification of 0.5 ppm of boron (or equivalent in absorption cross-section) has been set on the BeO powder, and <1 ppm of boron (or equivalent) in the completed brick.

1.13.1 Procurement of Powder

The Clifton Products Company, Painesville, Ohio, has consistently produced powder of the purity specified, though the physical properties of their product seem to cause some difficulties in molding. The Brush Beryllium Company, Cleveland, Ohio, on the other hand, has been able to produce material which is very satisfactory for molding, but much of this has had a high boron content. Monsanto Chemical Co. has placed an order with Brush for 5000 lbs of their GC grade BeO, and will place a similar order with Clifton when it appears likely that one of the molding concerns will be able to use their material.

1.13.2 Procurement of Bricks.

An order has been placed with the Norton Company, for fabricating hexagonal bricks by hot-pressing in graphite molds at their Chippewa plant, Niagara Falls, Ontario, Canada, and annealing them at their Worcester, Massachusetts plant. Work will begin as soon as a sufficient quantity of acceptable powder can be obtained.

Contact has also been made with the AC Spark Plug Division of General Motors, Flint, Michigan, who have been experimenting with the production of hexagonal bricks (equipped with dowel pins) made by ceramic firing. Work has been started to decide upon a suitable grade of powder and to calculate shrinkage characteristics of this powder. Steel dies for bricks and dowel pins are being made by the shop at ANL and it is expected that they will be ready by the time the powder can be supplied. Because the shrinkage is different for each batch of powder the whole 5000 lbs must be procured before fabrication can begin.

1.13.3 Criteria for Acceptance of Material

(a) Acceptance of Powder Powder is to be sent to the spectrographic laboratory at ANL and will be accepted or rejected by Monsanto according to the resulting analyses. The ANL results have checked with the National Bureau of Standards and others in a national standardization program, and attempts are now being made, by preparing new standards,

comparing plates, etc., to bring agreement between the Norton Company analyses and ANL analyses. Since the Brush Beryllium Company has no facilities for analysis, and has no means of discovering why their powder varies so much in boron content, they are collecting samples from various points in their process using various methods of sampling and sending them to ANL for analysis.

(b) Acceptance of Bricks The specification of <1 ppm of boron or boron equivalent has been placed on the fabricated bricks. Acceptance of the bricks will be determined by the functional test to be run using the CP-3 pile, since spectrographic analyses of entire bricks is not practical and since early functional tests gave a value in agreement with the spectrographic analyses.

2 GRAPHITE PROBLEMS

2.1 Investigation of the Properties of Irradiated Graphite (Section written by H. A. Kierstead with the assistance of W. Primak and R. B. Lees, all three of whom joined the group in September)

Investigation of the properties of irradiated graphite is being carried out principally along three lines: measurement of the stored energy and its healing rate, determination of the activation energy spectrum for healing of resistance changes, and investigation of the effect of irradiation and of subsequent heating on the a_z lattice constant of graphite.

Stored energy is being measured by four different techniques. The most direct, and at present the most accurate, method is comparison of the heats of combustion of irradiated and unirradiated samples. This work is being done for the Argonne Laboratory by Prosen and Rossini at the National Bureau of Standards. Apparatus is now being constructed to measure the heat of dispersal of graphite in liquid potassium. This technique promises to be quicker and possibly more accurate than the heat of combustion. The Sykes method measures the rate of release of stored energy as the sample is heated at an approximately linear rate. The "dunking" technique is a calorimetric method of measuring the isothermal rate of release of stored energy.

delete

4000 52A

2.1.2 Measurement of Stored Energy from the Heat of Dispersal in Potassium (S. Gordon, L. A. Quarterman)

The observation made by L. Kelman (Metallurgical Division, Argonne National Laboratory) that graphite and Na-K alloy react suggested the possibility of determining the stored energy by comparing the heat of reaction for irradiated samples with that for unirradiated material. Alkali metal-graphite compounds were found to have been investigated previously [Fredenhagen and Cadenbach, Z. Anorg. Chem. 158, 249 (1926)]. Since sodium was reported to be unreactive, it was decided to use potassium alone. Considerable difficulty was encountered in devising a satisfactory calorimeter, and in developing a technique for manipulating the apparatus so that the potassium was not oxidized excessively. Some of the techniques and procedures thus far developed may be of interest.

Preparation of the Potassium Air was displaced from the filter apparatus (Figure 8) by nitrogen purified by passing it over hot copper. A cylinder of potassium, cut from a large chunk of metal with the aid of a corkborer, was then introduced into the chamber (A). The apparatus was evacuated and the potassium melted by induction heating. Nitrogen was now admitted, forcing the potassium through the filter into the lower bulb (B). After the potassium solidified, the lower bulb was sealed off at the constriction.

Introduction of Potassium and Graphite into the Calorimeter A piece of rubber tubing filled with nitrogen was placed over the tip of the potassium ampule, and the tip broken inside of the tubing. With the rubber tubing still attached, the ampule was tied to the wires (B) of the calorimeter cap, the tip pointed downward (Figure 9). While nitrogen was flowing through the apparatus, the rubber tube was removed from the tip of the potassium ampule, and the cap holding it was quickly lowered into position. The calorimeter was then partially evacuated and the potassium, melted by induction heating, flowed into the silica cup (C). The calorimeter was again filled with nitrogen. While the nitrogen was flowing, the cap was lifted, and the graphite sample (D), weighted with a piece of glass rod inserted into it, was attached to the fuse wire (E). The cap was replaced and the calorimeter evacuated. An oil bath maintained at 80 ± 0.02° was now brought up into position. When the calorimeter reached the temperature of the bath, 110 V was momentarily connected across the fuse wire causing the sample to drop into the molten potassium. Simultaneously a clock was started, and the EMF of the copper constantan thermocouple (F) was read periodically with a Type K potentiometer.

Calculations of the heat of dispersal were carried out in the usual manner for calorimetric experiments. A trial run has been made with this apparatus in order to develop the technique for manipulating it, but no values of stored energy have been obtained to date.

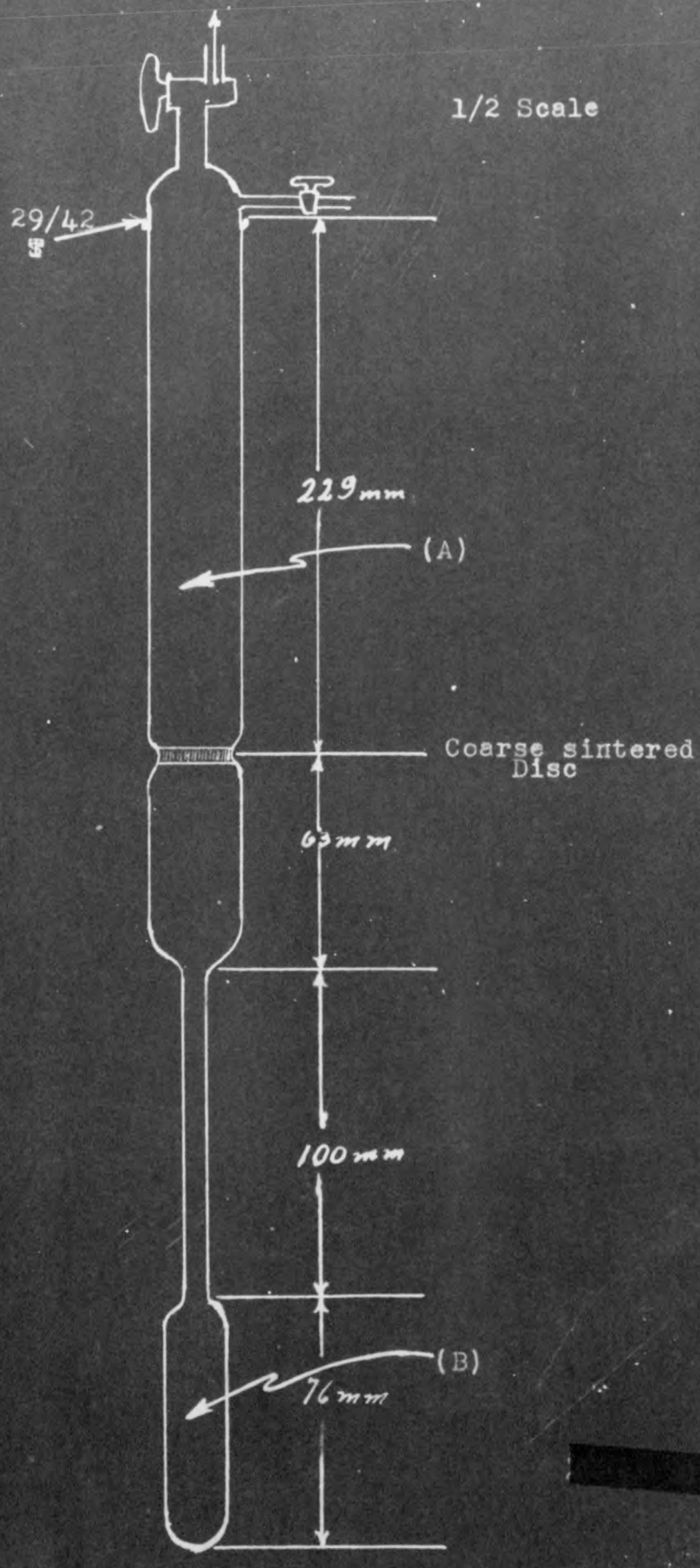

FIGURE 8
Potassium Filtering Apparatus 4000

FIGURE 9

Dispersal Apparatus
1/2 Scale

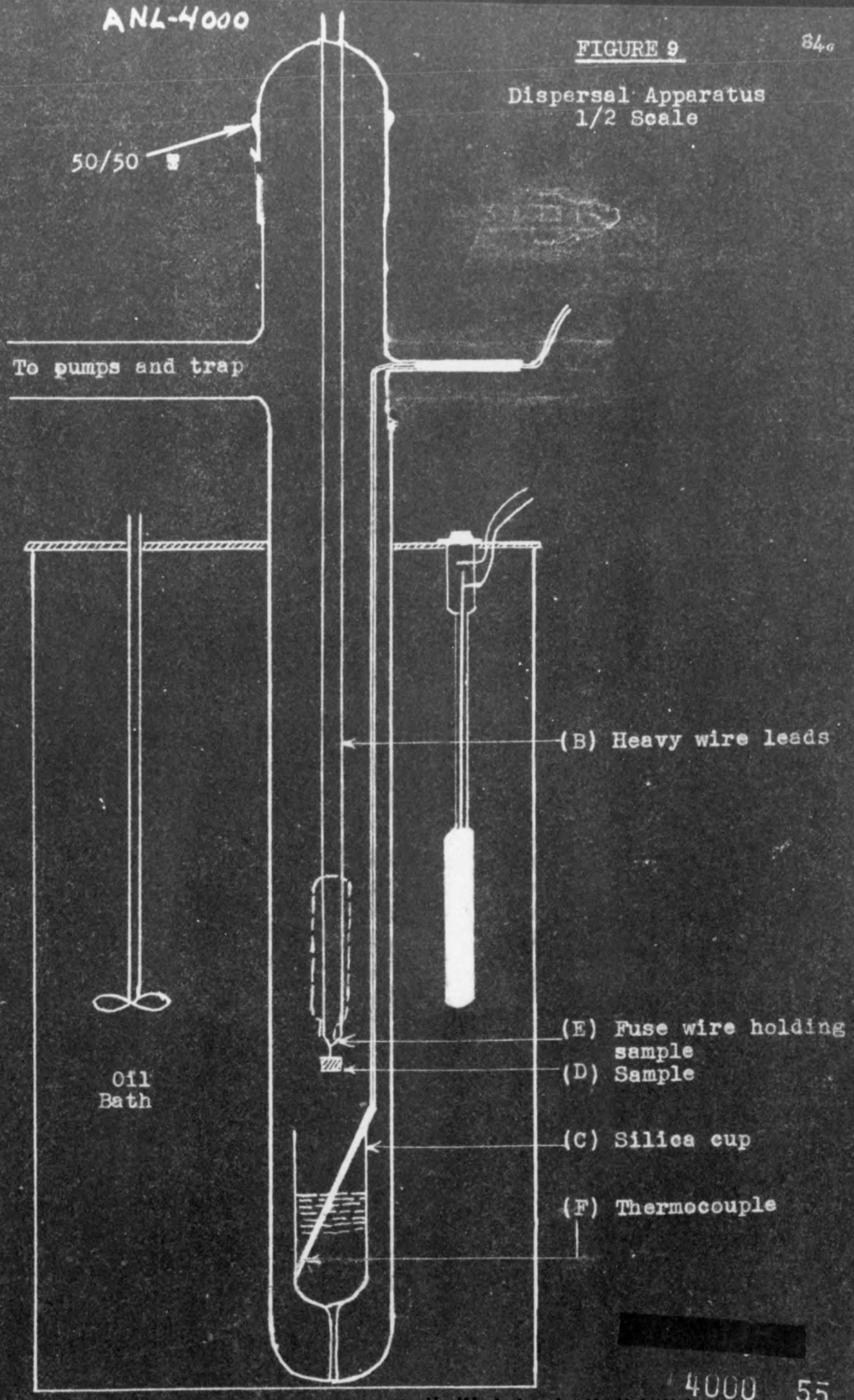

2.1.3 Measurement of Stored Energy by the Sykes Method (D. H. Gatley, R. B. Lees, R. C. Milham

The Sykes method depends upon the fact that stored energy is released as thermal energy when an irradiated sample is heated. In order to measure this thermal energy, the sample is placed in a cavity in a copper block in such a manner that it is partially insulated from the block by the gas space around it. For comparison purposes an unirradiated graphite sample is placed in a similar cavity. The block is then heated at a uniform rate by a furnace around it. The rate of heating of the sample will be given by

$$C_H \frac{dT_H}{dt} = K(T_B - T_H) , \qquad (1)$$

where C_H is the "apparent" heat capacity of the sample, T_H is its temperature, T_B is the block temperature, and K is the heat transfer constant of the insulating gas space. Similarly, for the unirradiated sample

$$C_C \frac{dT_C}{dt} = K(T_B - T_C) , \qquad (2)$$

where the same K is used since the two samples are identically arranged in the block. Combining equations (1) and (2)

$$\frac{C_H}{C_C} = \frac{T_B - T_H}{T_B - T_C} \frac{dT_C}{dT_H} . \qquad (3)$$

Now if the furnace is cooled and then reheated, the irradiated sample will have given up its stored energy in the first run, so it will now exhibit its true heat capacity, C_H'. For this second run then

$$C_H' \frac{dT_H'}{dt} = K(T_B' - T_H') , \qquad (4)$$

$$C_C \frac{dT_C'}{dt} = K(T_B' - T_C') , \qquad (5)$$

$$\frac{C_H'}{C_C} = \frac{T_B' - T_H'}{T_B' - T_C'} \frac{dT_C'}{dT_H'} . \qquad (6)$$

The relation between the true and "apparent" heat capacities of the irradiated sample may be obtained by observing that in the first run a true heat balance would be given by

$$C_H' \frac{dT_H}{dt} = K(T_B - T_H) - \frac{dS}{dt} , \qquad (7)$$

where S is the total amount of stored energy in the sample at time t. This must be true since the sample is heated by stored energy release as well as by the furnace. Substituting equation (1) in equation (7)

$$\frac{dS}{dt} = (C_H - C_H') \frac{dT_H}{dt} , \qquad (8)$$

or $$\frac{dS}{dT_H} = C_C\left(\frac{C_H}{C_C} - \frac{C_H'}{C_C}\right) , \qquad (9)$$

and $$\Delta S = \int_{T_1}^{T_2} C_C \left(\frac{C_H'}{C_C} - \frac{C_H}{C_C}\right) dT_H . \qquad (10)$$

The ratios of heat capacities required in this equation may be obtained from equations (3) and (6). If the rate of stored energy release is small compared to the heating rate of the furnace, $\frac{dT_C}{dT_H}$ and $\frac{dT_C'}{dT_H'}$ will not vary significantly from unity, under which conditions then

$$\frac{C_H}{C_C} = \frac{T_B - T_H}{T_B - T_C} , \qquad (11)$$

and $$\frac{C_H'}{C_C} = \frac{T_B' - T_H'}{T_B' - T_C'} . \qquad (12)$$

The temperature differences required are conveniently measured by differential thermocouples.

Apparatus The block is machined from solid copper as shown in Figure 10. In the top are bored two large cavities for samples, each with a small hole at the bottom on the center line to hold the alundum tube support, and an enlarged upper portion to accomodate the copper plugs (Figure 11). These copper plugs are coated with Aquadag before inserting; otherwise they are difficult to remove after the furnace has been heated. Also, three long holes are drilled in the block parallel to the center line to hold thermocouple tubes, and two tapped holes are provided to hold the upper insulating framework. This framework consists of five circular copper discs mounted at one inch intervals above the block as insulating baffles. The thermocouple wires pass through holes drilled in these disks.

In the side of the block are drilled six holes to hold small quartz or copper pegs to center the block in the furnace. The lengths of the pegs are adjusted to just fit into the furnace, as the diameter of the block increases slowly with use.

The vertical furnace (Figure 12) consists of an iron pipe closed at the bottom, and sealed at the top with a $\frac{1}{4}$" thick brass plate. The plate is bolted on with eight $\frac{1}{4}$" bolts, and is sealed with a neoprene gasket. It contains one central tube, 3/8" OD, for the evacuation and gas-filling line, and two small plastic insets drilled for two thermocouple wires on one side and four on the other. The wire leads and plastic insets are covered with Apiezon wax during a run to make the furnace completely air-tight. The iron pipe is held vertically in an alundum tube, wound outside with heating coils and insulated with three inches of fire-brick. The copper block rests upon three alundum pegs held vertically on the bottom of the iron pipe by three horizontal copper plates spaced with quartz tubes, providing bottom insulation similar

FIGURE 10. COPPER BLOCK

Full Scale

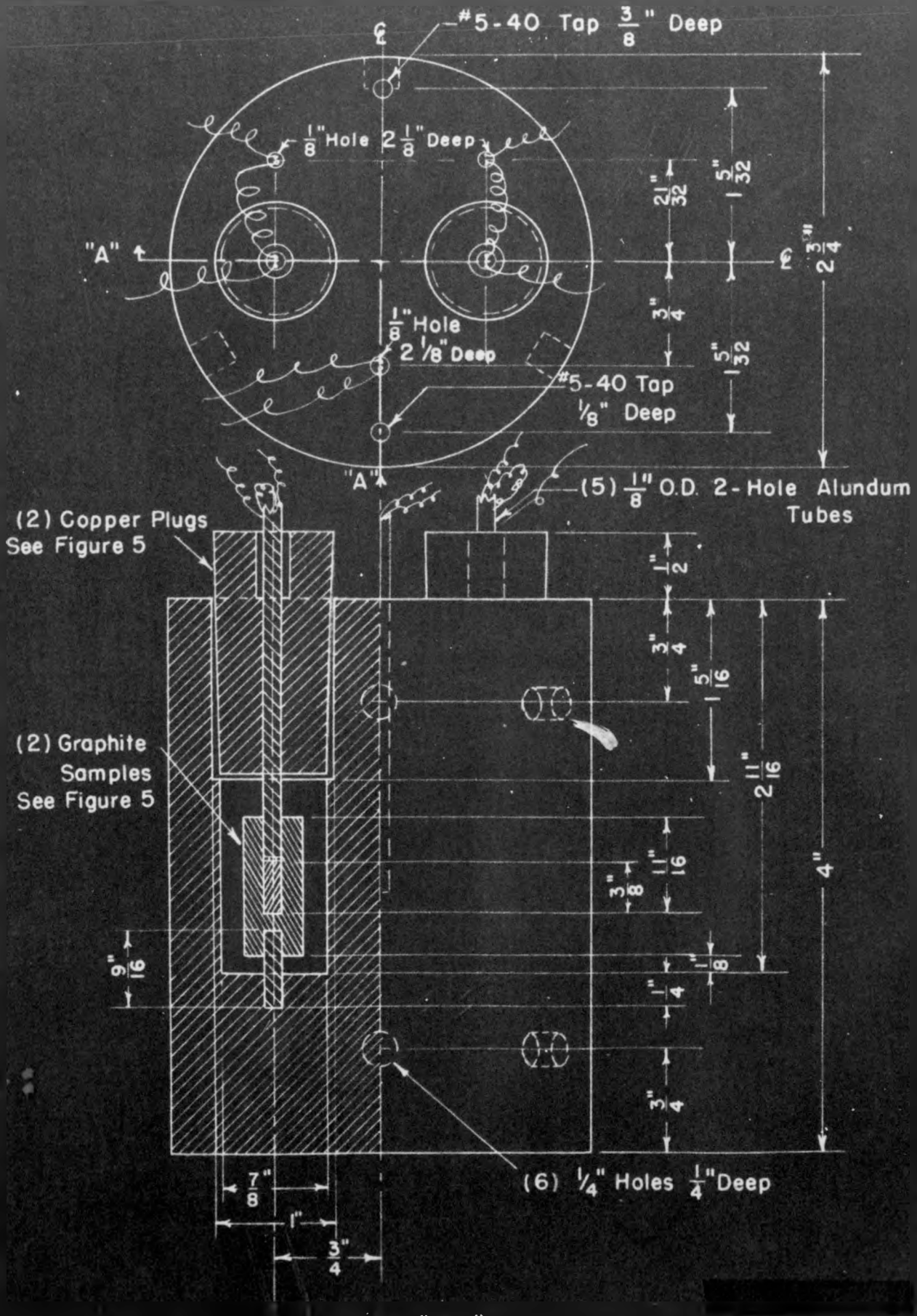

Section "A-A"

FIGURE 11

DETAILS OF SYKES APPARATUS

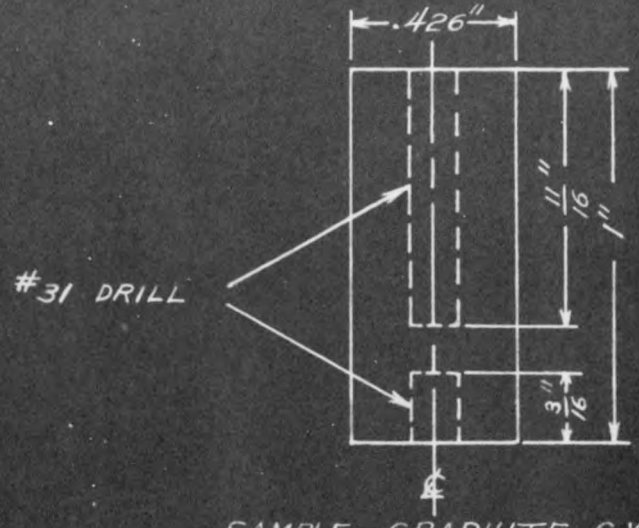

SAMPLE - GRAPHITE CYLINDER

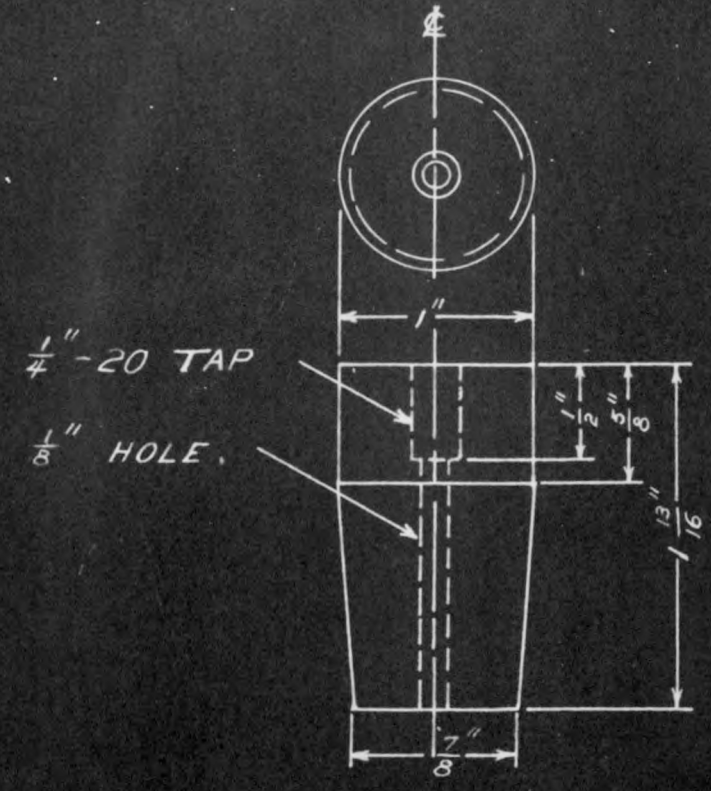

COPPER PLUG

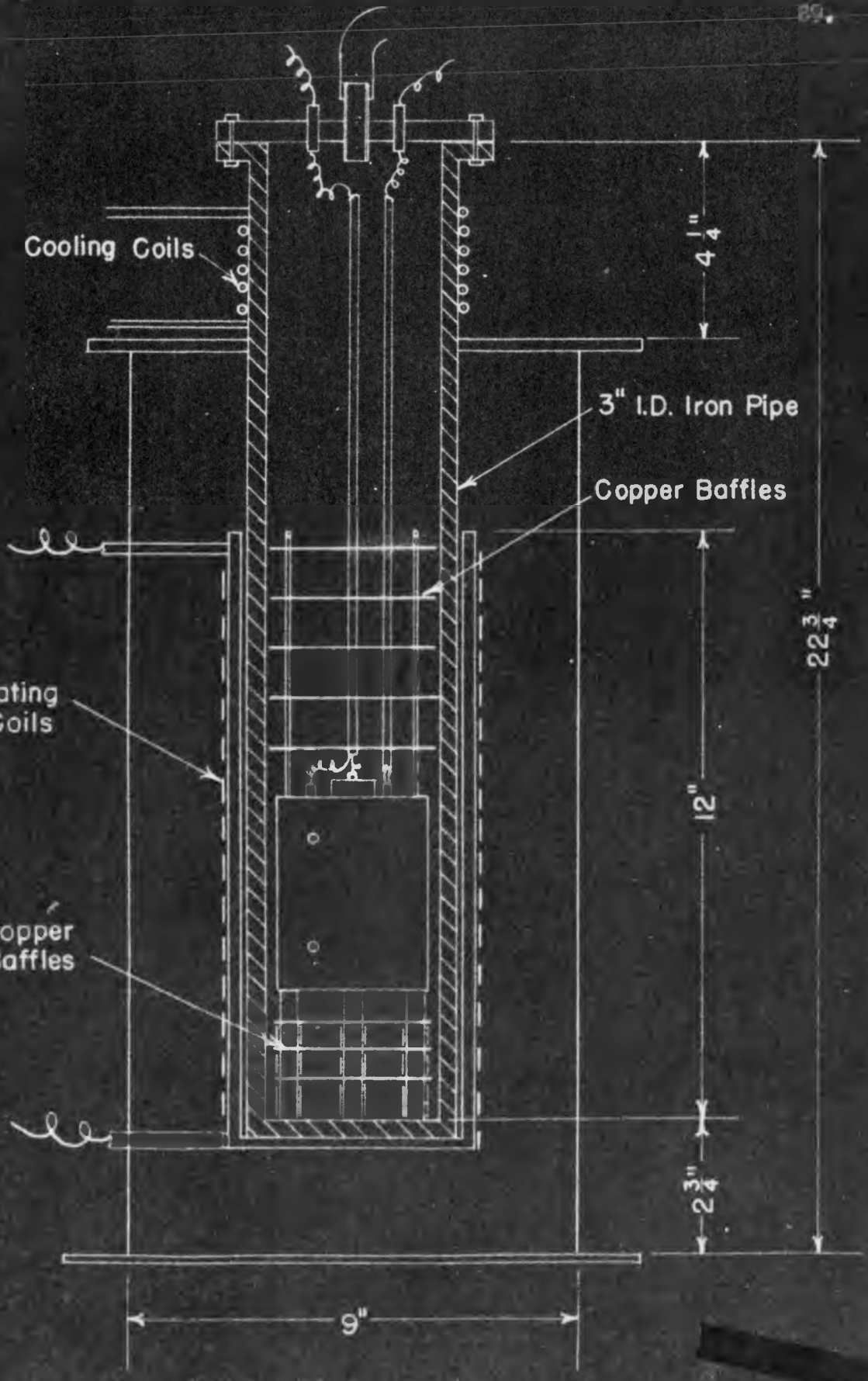

FIGURE 12

4000 60

ASSEMBLY OF FURNACE AND BLOCK.

to the discs at the top of the block. The top four inches of the pipe project from the furnace and are cooled externally with nine turns of ¼" Cu tubing through which cold water is circulated.

The temperature of the block is measured with a 28 guage iron-constantan thermocouple. The hot junction is soldered into a copper tube 2 3/4" long by 1/16" ID, which is closed at one end. This tube fits into a hole in the top of the block, so that the junction is about 3/16" from the bottom of the hole. The leads, insulated with cotton, are led from this tube through separate holes in an alundum tube which passes through the plastic insets on the top plate to an external cold junction.

The temperatures of the samples are measured by differential thermocouples, one junction being anchored in the block in the same manner as the hot junction for the measurement of the block temperature. The constantan lead, however, goes to the sample where it joins the second iron lead (Figure 10). A similar arrangement is made for the second sample. The sample junction terminates in a small copper well, 3/8" long, 7/64" OD, 3/64" ID, which just fits into the hole in the sample. This junction, soldered into the Cu well, is thus 5/8" below the top of the sample. From the copper well the iron and the constantan leads run through a short length of two hole alundum tubing which passes through a hole in the Cu plug, the constantan lead then going to the block junction where it joins the other iron lead. The four iron leads from the two differential couples are finally led through a 4-hole alundum rod (as was described earlier) to the outside of the furnace. The constantan lead from the block temperature couple runs to a constantan-iron junction in the ice bath and the iron lead from this same junction to an iron-copper junction in the ice bath. The other five leads from the apparatus are all iron and are joined to copper leads in an ice bath, in order to avoid spurious thermo-electric effects.

The three pairs of copper leads are connected each to a reversing double-pole, double-throw knife switch. The block temperature is then measured by a type K Leeds and Northrup potentiometer. From the switches the two differential leads run in parallel to a bank of resistances where 100, 250, 500, 750, 1000, or 1500 ohm resistances may be put in series with the circuit, and then to a Leeds and Northrup galvanometer having a 50 ohm damping resistance. (The galvanometer was mounted on a brick pier.) A separate Rubicon potentiometer is provided to calibrate the scale of the deflection galvanometer for the various resistances by application of a known EMF across the reversing switches in place of the thermocouple EMF's. For the 500 ohm resistance in series, the galvanometer sensitivity is 73 cm per millivolt.

The power to the furnace is provided by a 220 v line, reduced in a Variac transformer to the desired voltage level so that various rates of heating are available. In order to make the heating rate more linear, the current is passed through a motor-driven rheostat whose resistance is reduced from 7.5 ohms to zero in a period of 40 minutes.

Procedure When the samples and the block have been mounted in the furnace, the furnace is evacuated to about 0.1 mm of Hg by means of a

Cenco Hyvac pump, and filled with hydrogen at a few cm above atmospheric pressure. Then the power is turned on and the motor-driven rheostat is started. The differential thermocouples are read every minute, and the block thermocouple every five minutes. When the block reaches 700°C, the power is turned off and measurements are continued for a few minutes until the temperature begins to fall. The furnace is allowed to cool over night without disturbing the samples.

The next morning the furnace is evacuated and refilled with hydrogen, and a second run is made in the same manner as the first.

Results The results of a measurement on the T-bar (ANL's designation for the third of a series of Hanford stringer bars taken from side holes) are given in Figure 13, in which the ratio $\frac{C_H}{C_C}$, calculated from equation (11), is plotted against T_H. The unirradiated sample was ACCT-Kendall graphite. Three successive runs on the same sample are shown. It should be noted that the second and third runs are nearly identical, proving that no stored energy was released during the second run. A fourth run, not shown, also duplicated the previous two.

The fact that the first and second curves do not close at the high-temperature end indicates that stored energy was still being released at the end of the first run. Ideally, the first and second runs should close at the beginning, since no stored energy should be released until 130°C, the temperature of irradiation. The reason that they do not close is that the true heat capacity and the thermal conductivity of the sample change due to healing during the run. They are therefore not the same in the second run as they were in the first. To correct for this, the curve for the second run must be shifted upward in the low-temperature region until the curves meet. At the high-temperature end no shifting should be done since the sample has healed by this time and the two runs are comparable. Therefore, a correction which is assumed to be linear with temperature should be applied. These calculations have not been made as yet, but when they are finished a $\frac{dS}{dT}$ curve will be plotted using equation (9), and the curve will be integrated graphically to determine the total stored energy healed out at 700°C.

FIGURE 13

SYKES CURVES FOR HEW IRRADIATED GRAPHITE (T-BAR)

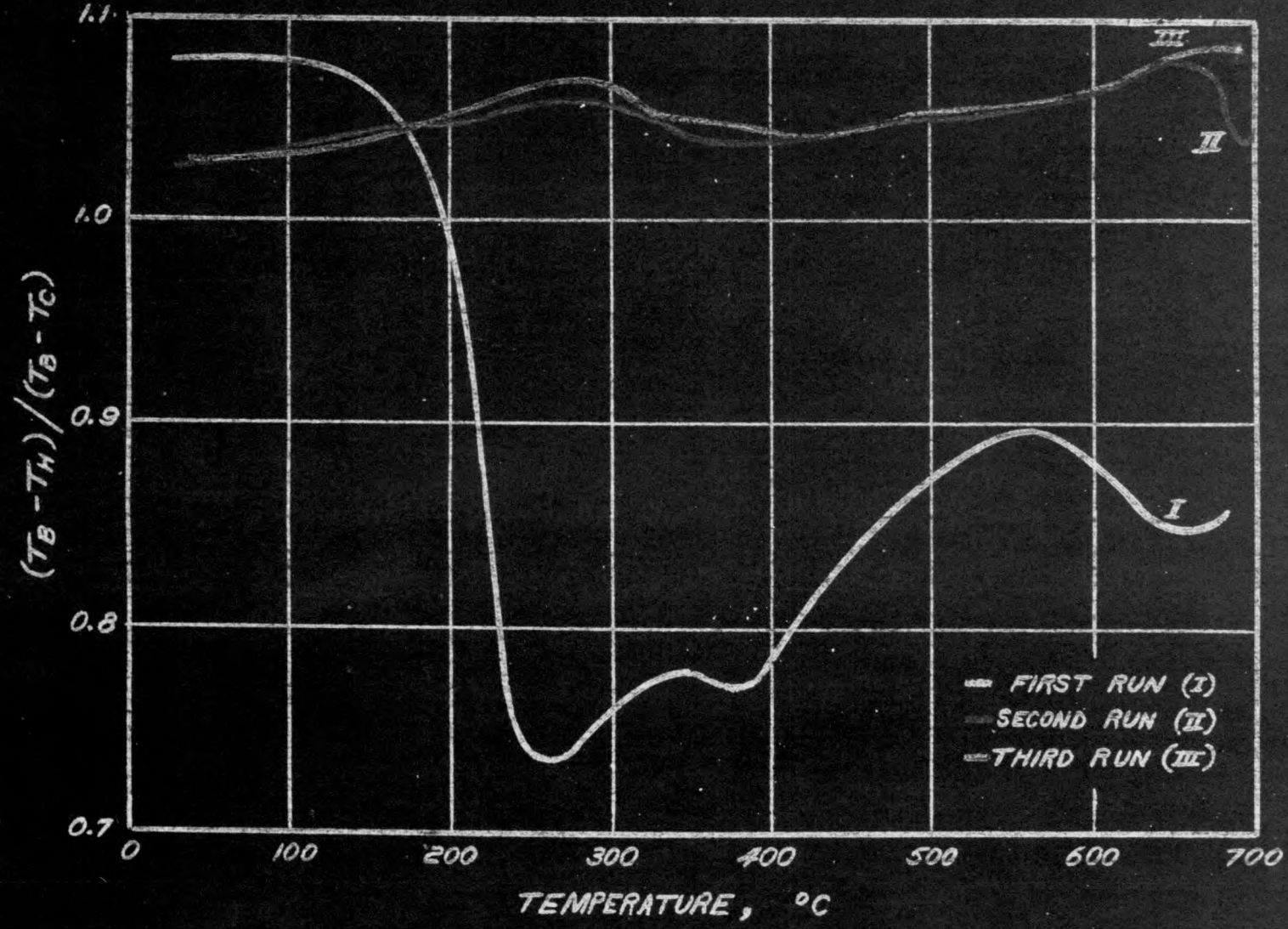

2.1.4 Isothermal Rate of Release of Stored Energy (E. C. Avery, C. M. Nelson)

It is known from the Sykes and other experiments [Wheeler and O'Connor, N-2191 (CS-NEW), 11/9/45] that the rate of release of stored energy in irradiated graphite is governed by a broad spectrum of activation energies. Since mathematical analysis of such a system is very difficult, it would be useful to heal samples in such a manner that only a narrow band of activation energies is affected. This can be done by heating the sample isothermally for short periods of time at successively higher temperatures, and determining the energy released by standard calorimetric methods. Thus advantage is taken of the fact that at constant temperature a small difference in activation energy makes a tremendous difference in the rate of reaction, so that disturbances having a particular activation energy can be characterized by the temperature at which they heal rapidly.

Apparatus The dunking apparatus consists of a vacuum calorimeter "S" (Figure 14) containing a bath of Rose metal (N) into which a sample of graphite can be quickly dropped or "dunked". The nickel cup containing the Rose metal is spaced from the calorimeter walls by the quartz peg (P) and the mica washers (O). A thermocouple (J) enters through a tubulation to permit the temperature of the Rose metal to be determined. The sample (T) with a thermocouple within it is mounted at the end of an alundum insulator (M). A brass bushing (L), which also serves as a stop and as a radiation shield, connects the alundum with a brass tube (G). The sample thermocouple (D) descends through this brass tube. The iron rod (A') is attached to the upper end of the brass tube. When the solenoid (A) is activated, it can be used to raise the whole sample-holding assembly until the guide (C) is above the iron rod and stop (B). The stop can be moved under the guide with a magnet, thus supporting the sample in the region of the water cooled joint (K). Other details of the apparatus are shown in Figure 14.

The calorimeter sits in an oil bath contained in a 2 gallon pyrex battery jar surrounded by firebrick insulation. The whole is set in a galvanized iron can. Current through an electrical winding on the outside of the battery jar is adjusted by means of a variac so that it can itself maintain the temperature of the oil bath about 5°C below the desired temperature. An auxiliary heater within the oil bath is used to regulate the bath to within $\pm$ 0.03°C of the desired temperature. The regulator consists of a photocell relay arrangement actuated by the light reflected from a Type R galvanometer connected to a portable Rubicon potentiometer which balances the EMF of a thermocouple immersed in the oil bath. This regulator permits the temperature of the oil bath to be changed easily and reproducibly. Three measuring thermocouples, that for the oil bath, that for the Rose metal, and that for the sample, can alternatively be connected to a Leeds & Northrup Type K-2 potentiometer by means of a battery of knife switches.

The procedure in carrying out an experiment is as follows: The sample is raised to the level of the water-cooled joint (K) where it is maintained well below the temperature at which stored energy is released. The oil bath is regulated to the desired temperature. Helium is admitted

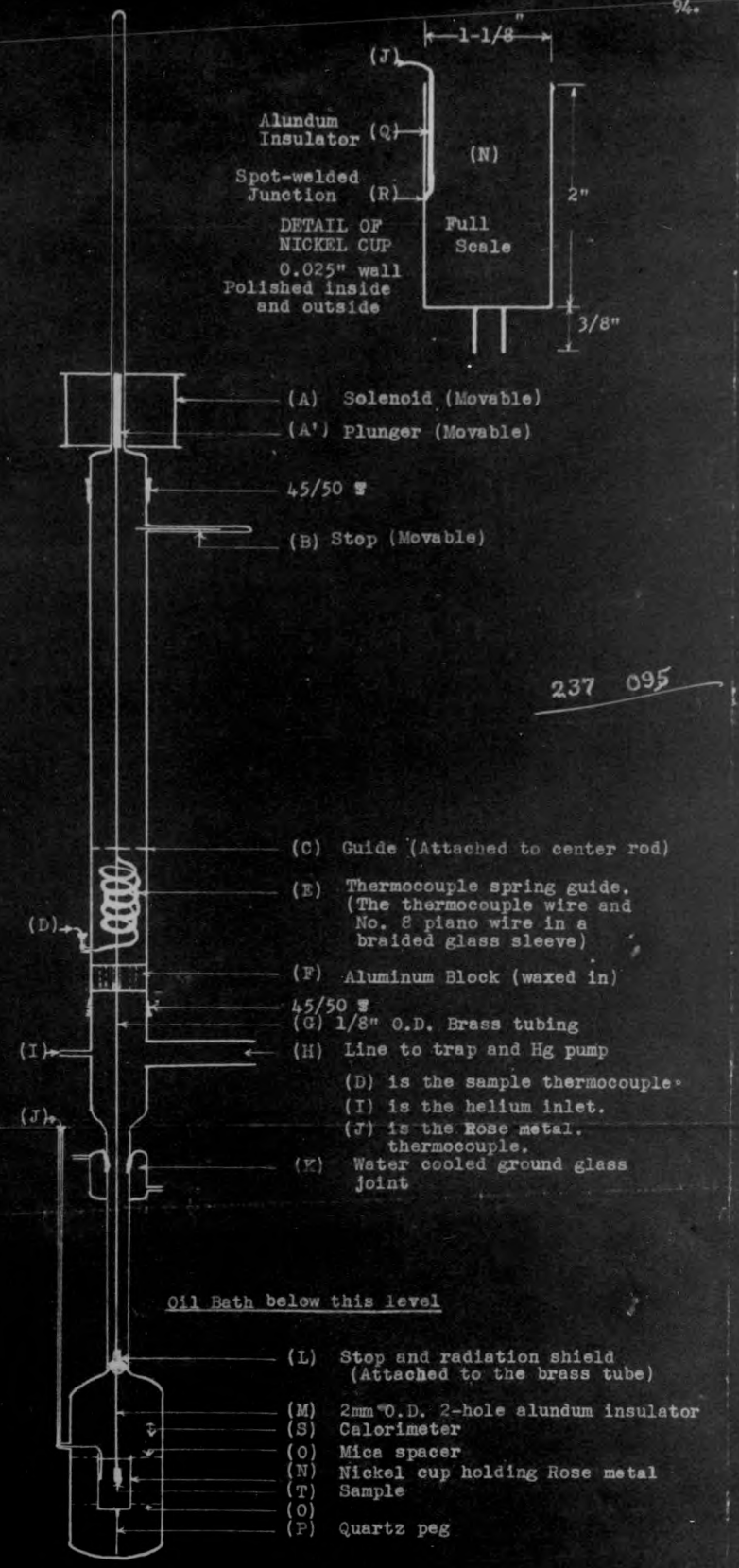

Figure 14 DUNKING APPARATUS
1/4 Natural Size
(Upper detail of nickel cup is natural size)

to the calorimeter to permit the calorimeter and its parts to come to the temperature of the oil bath. The calorimeter is evacuated to less then 5×10^{-5} mm, at which point the Rose metal is found to remain at a temperature slightly below that of the oil bath. The stop (B) is withdrawn, and the sample lowered into the Rose metal by lowering the solenoid (A). When the sample touches the Rose metal, an electrical timer is started by a relay which is connected between the thermocouple in the Rose metal and the thermocouple in the sample. The temperatures of the Rose metal and the sample are recorded periodically at 30 second intervals for the first five minutes, and then at longer intervals for 30 to 60 minutes. The temperature of the Rose metal drops so rapidly that the first reading is usually somewhat past the minimum. If no stored energy is released, the temperature slowly returns to the oil bath temperature. The release of stored energy hastens the return. Occasionally, when a great deal of stored energy is released, the temperature rises above that of the oil bath, and then slowly returns toward it.

Calculations When the sample is dropped into the metal bath, the bath and sample rapidly reach a mean temperature, T_i, defined by the equation

$$T_o C_M + T_S C_S = T_i (C_M + C_S) = C T_i \qquad (1)$$

where T_o is the oil bath temperature, C_M is the heat capacity of the metal bath, T_S and C_S are the initial temperature and the heat capacity of the sample, and $C = C_M + C_S$. If the sample has no stored energy, the temperature will then rise at a rate which is given sufficiently accurately for those purposes by Newton's law:

$$C \frac{dT}{dt} = K(T_o - T), \qquad (2)$$

or

$$\ln(T_o - T) = \ln (T_o - T_i) - \frac{K}{C} t , \qquad (3)$$

where K is a constant of the apparatus.

A preliminary experiment is performed using a copper sample of known heat capacity. By plotting the temperatures against time on semi-log paper, T_i and K are determined from the best straight line through the data. Then T_i is used in equation (1) to determine C_M.

When an irradiated sample of stored energy content S is dunked, the metal bath is heated by the release of stored energy as well as by radiation from the oil bath. The rate of rise of temperature is then

$$C \frac{dT}{dt} = K(T_o - T) - \frac{dS}{dt} , \qquad (4)$$

and

$$\Delta S = C(T_f - T_i) - K T_o t_f + \int_o^{t_f} T \, dt , \qquad (5)$$

where T_f and t_f are the temperature and time when the sample is removed from the bath and ΔS is the decrease in stored energy or the stored energy released.

T_i is determined as in the copper dunk by extrapolating the temperatures back to zero time on semi-log paper. C is calculated from equation (1) using this value of T_i, the known C_S of the sample, and the value of C_M determined in the copper dunk. Now the rate of stored energy release can be calculated according to equation (4) and the total stored energy released by equation (5), using a graphical integration of T.

Results The apparatus has been constructed and a few preliminary runs have been made, but no data have been obtained as yet.

2.1.5 Thermal Healing of Neutron-Induced Changes in Electrical Resistivity (C. Smith)

An apparatus has been constructed for determining the activation energy spectrum for thermal healing of dislocations in neutron-irradiated graphite. This is to be done by measuring the changes in electrical resistivity of an irradiated sample as it is heated at a uniform rate up to 1000°C. The data will be analyzed according to the method used by V. Vand [Proc. Phys. Soc. 55, 222 (1943)] in studying resistance changes in evaporated metal films.

A trial run has been made on two samples of unirradiated AGOT-Kendall graphite. The results of this run are plotted in Figure 15. The solid line is drawn from data reported by the National Carbon Company, and the plotted points represent experimentally determined resistances of the two samples. All resistances are plotted as fractions of the resistance of the sample at 48°C.

The maximum deviation from the National Carbon data is around 7%, but over most of the temperature range it is much less. It should also be noted that the agreement between our two samples is even better, and relative accuracy is all that is required in this method.

Some improvements will be made in the apparatus, as suggested by the trial run, and a complete description will be reported when the apparatus is in its final form.

4000 68

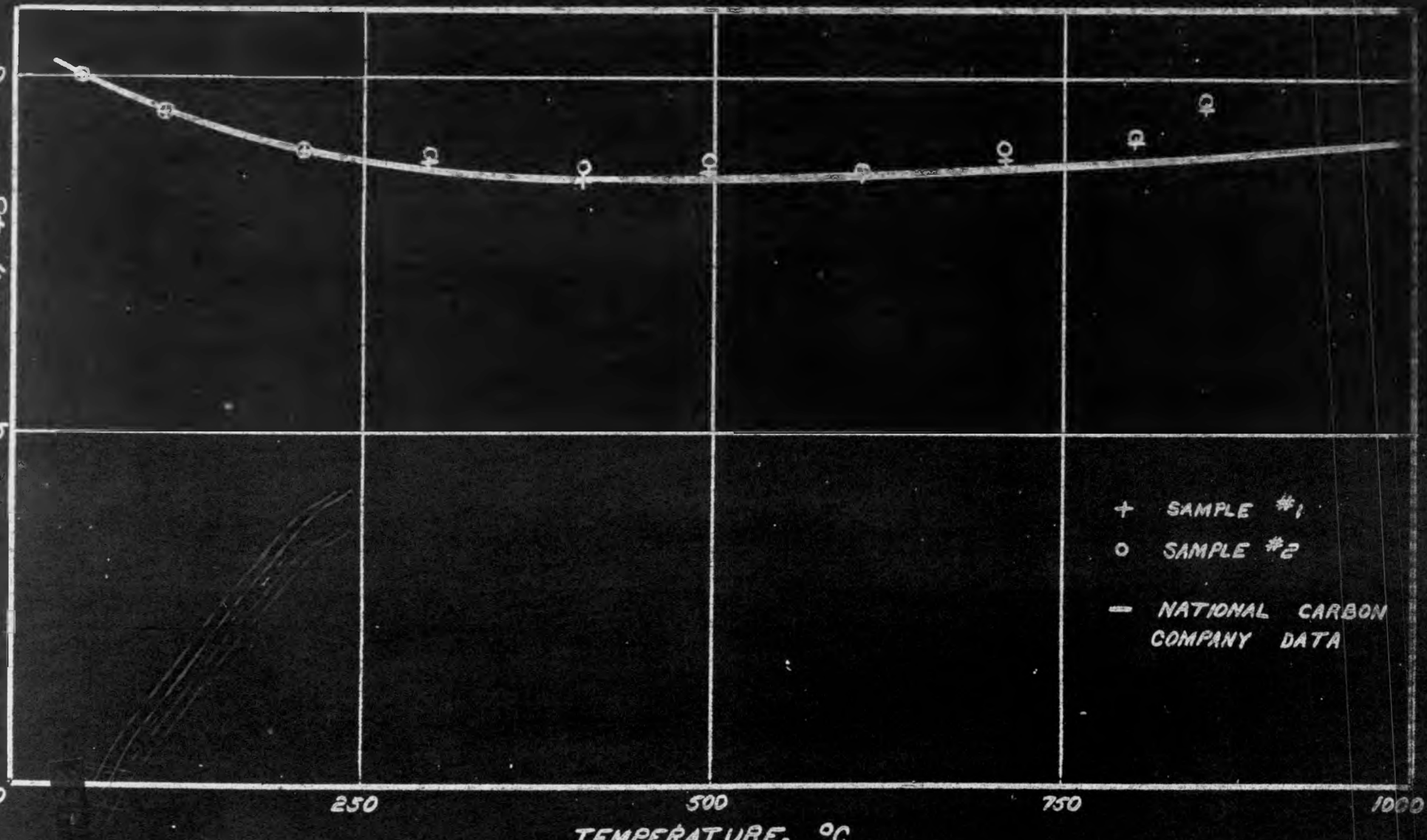

FIGURE 15. RESISTANCE OF GRAPHITE SAMPLES

2.2 Distribution of C^{14} in Graphite (W. H. Hamill)

The observations of J. R. Arnold in this laboratory demonstrate a selective oxidation of C^{14} in irradiated graphite by both high temperature combustion in oxygen and room-temperature oxidation in chromic-sulfuric acid. In both cases the C^{14} abundance decreases rapidly with continued oxidation and approaches a limiting value. This suggests the possibility of using C^{14} in irradiated graphite as a tracer for dislocated atoms.

A number of oxidation experiments have been carried out in the following manner: The graphite sample is thoroughly evacuated, and then small amounts of oxidizing agent are added. After each addition, the CO_2 formed is collected and counted, using a conventional end-window counter. Results are expressed as the ratio of the percent of the total count to the percent burned in an individual sample, which is a measure of the C^{14} enrichment in the gas fraction.

In Figures 17, 18, 19, and 20 this ratio is plotted as a function of the total percent of the carbon burned up to the time the sample was taken. The data refer to runs on samples of annealed and unannealed T-bar graphite.

If we make the reasonable assumption that oxidation starts at the surface of the crystallites and progresses inward, these curves give us a picture of the C^{14} distribution, and therefore the distribution of dislocated atoms, in the crystal. Figure 20 is particularly interesting since, with air at 770°C, it was possible to burn the whole sample. The last point at 96% burned indicates an enrichment ratio of 0.05 in the center of the crystal. Therefore, at most 5% of the displaced atoms have healed back to holes. This is a maximum figure since it is known that some interstitials remain unhealed at 770°C, and these would add to the count.

Since other experiments in this laboratory indicate that most of the dislocated atoms are healed at 770°C and since it has just been shown that they do not heal to holes, they must heal to edges. One might then expect that the crystallite would be enclosed in a sheath of healed dislocated atoms. Also, since the C^{14} concentration in these atoms is constant, one would expect a region of constant enrichment ratio in the initial portion of the curve. This appears to be the case in Figure 20.* From the value of this enrichment ratio, about 4.5, one can calculate an upper limit of between 20 and 25% for the fraction of displaced atoms. The length of the linear region sets a lower limit of about 3%. Of course this observation will have to be checked more carefully before we can have any confidence in these numbers. This will be done in the near future.

---

* The initial very high count is attributed to C^{14} deposited on the surface of the graphite from the (n,p) reaction with nitrogen in the atmosphere.

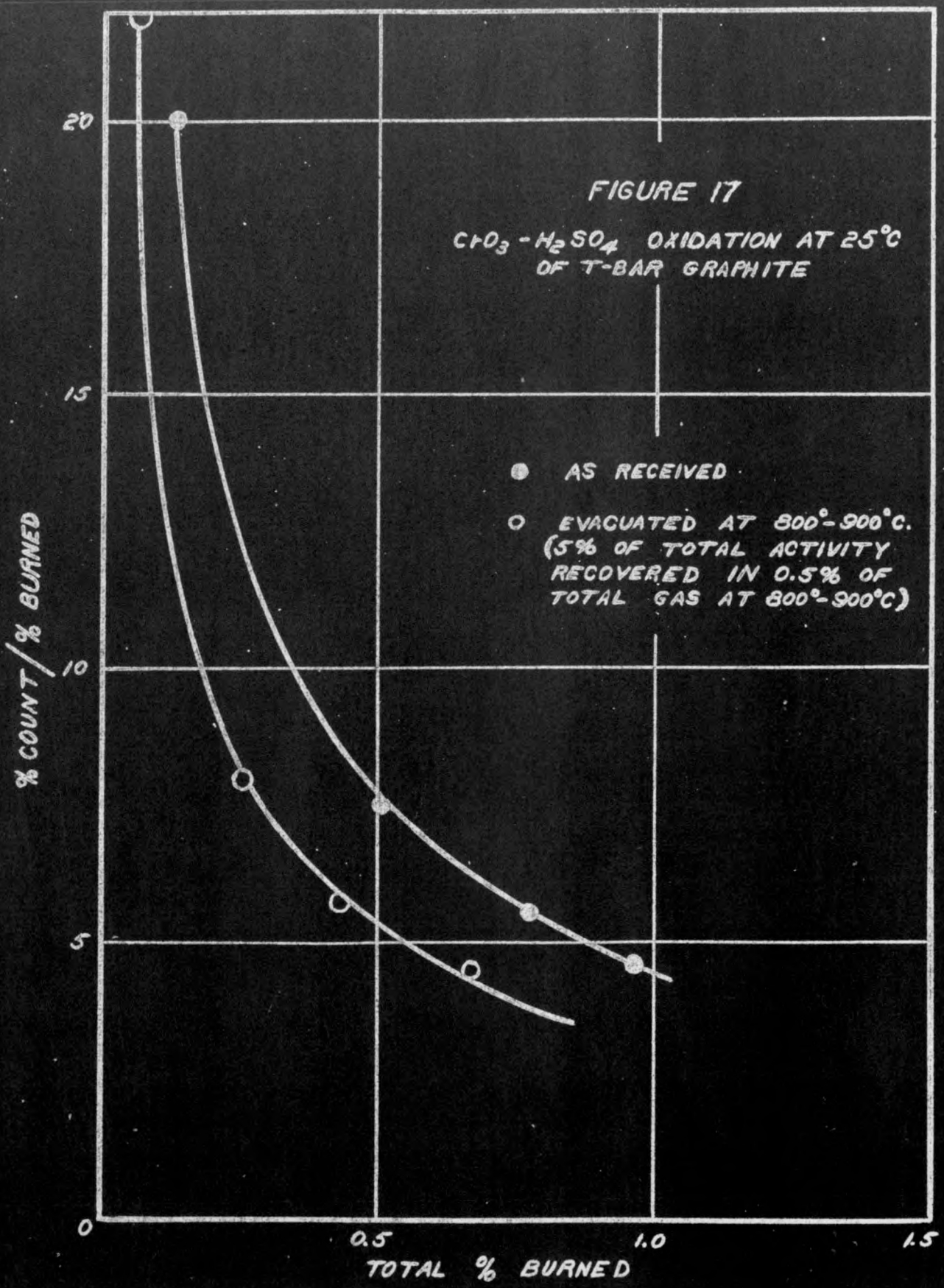

FIGURE 17

$ClO_3 - H_2SO_4$ OXIDATION AT 25°C OF T-BAR GRAPHITE

FIGURE 18

CrO_3-H_2SO_4 OXIDATION AT 25°C OF T-BAR GRAPHITE

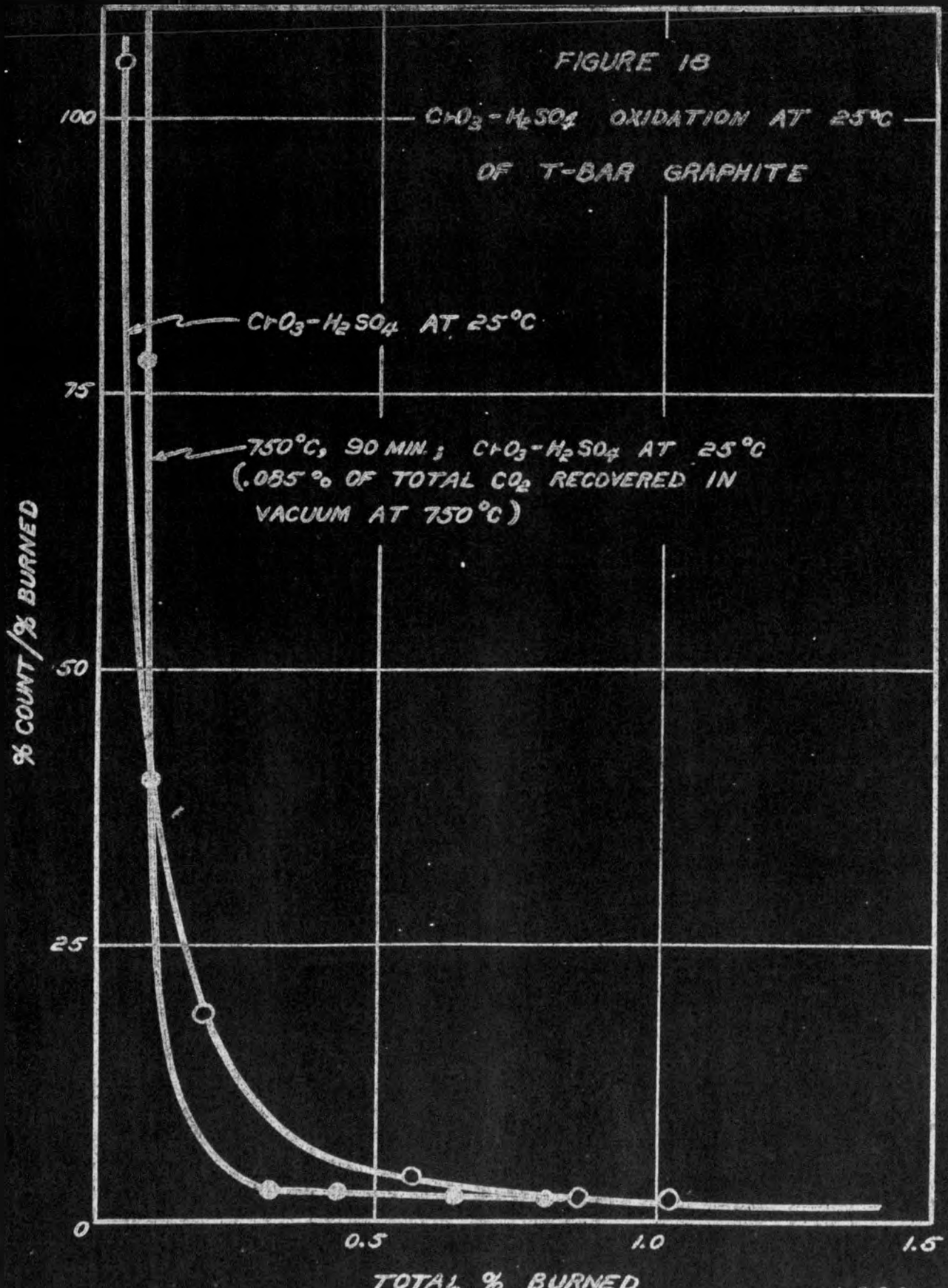

4000 71

FIGURE 19

CrO_3-H_2SO_4 OXIDATION AT 0°C OF T-BAR GRAPHITE

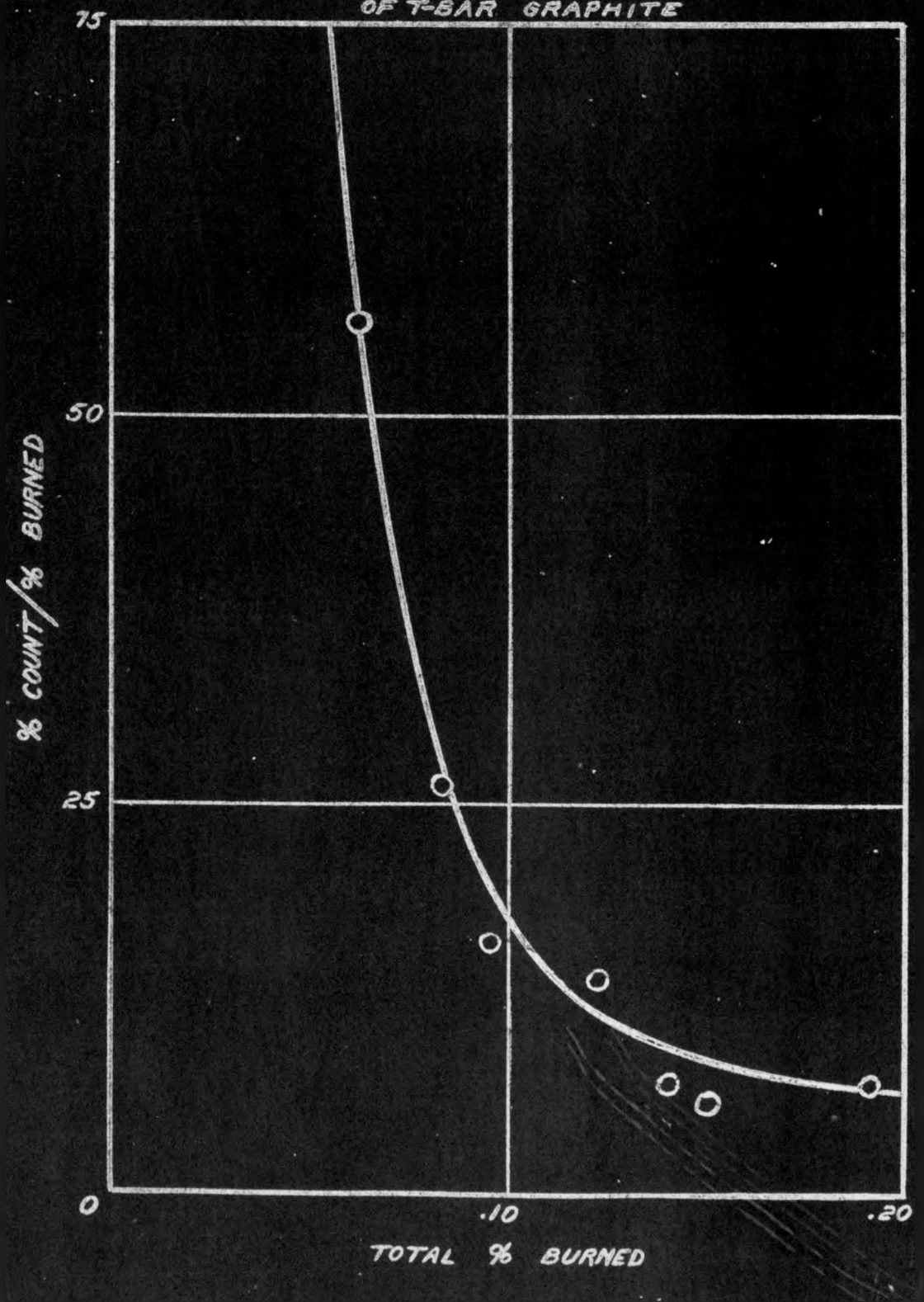

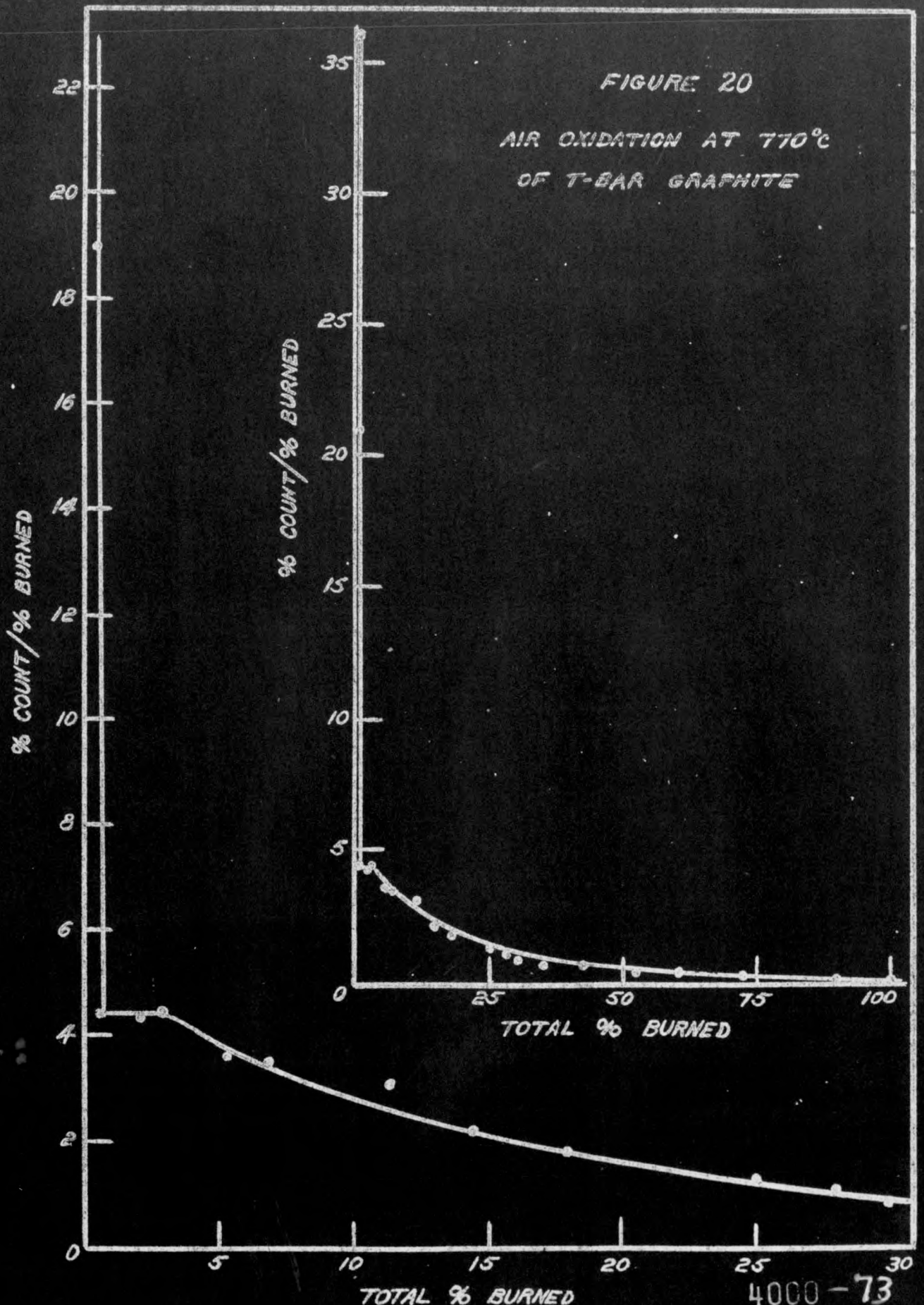

FIGURE 20

AIR OXIDATION AT 770°C

OF T-BAR GRAPHITE

2.3 Heat of Sublimation and Vapor Pressure of Graphite (R. J. Thorn)

Several attempts have been made to establish the heat of sublimation of graphite (i.e., the heat of sublimation to the monatomic form), but in spite of the attempts, the exact value remains doubtful. A summary of the investigations carried out before 1933 is given by Bichowsky and Rossini [1] who conclude that the value is between 110 and 170 kcal, the latter value being the more probable. These limits are based upon the uncertain dissociation energy of carbon monoxide; the extremes based upon vapor pressure measurements as given by Bichowsky and Rossini are 140 and 210 kcal. Since the period covered by these authors, Kelley [2] has calculated a value of 198 kcal at 25°C for the monatomic form using data obtained from the loss in weight of filaments by Wertenstein and Jedrzejewski. Aside from this recalculation the method which has been used most frequently during the past ten years is that based on a cycle involving the dissociation energies of carbon monoxide and oxygen and the heat of formation of carbon monoxide. Unfortunately, however, the dissociation energy of carbon monoxide has not been established conclusively. The values reported vary from 6.9 to 11.6 ev, corresponding respectively to values of 73 and 181 kcal for the heat of sublimation, or to 170 and 278 kcal if the hypothetical ^5S state of carbon is assumed. In the more recent publications Valatin [3] has supported the values of 6.9 ev and 170 kcal (the hypothetical ^5S state assumed); Long and Norrish [4] have supported Hertzberg's value [5] of 9.1 ev and 125 kcal; and Gaydon and Penney [6] have supported the values of 11.1 ev and 170 kcal. In view of these diverse values it has been impossible to state conclusively a value for the heat of sublimation to the monatomic form on the basis of the dissociation energy of carbon monoxide.

Other attempts have been made to calculate the desired property of graphite from the addition of bond energies, but these values also vary widely from 125 to 190 kcal. Most recently Syrkin [7] has obtained 125 kcal; Cherton [8] has calculated a value of 190 kcal (the ^5S state assumed); and Kynch and Penney [9] have found a value of 170 kcal by this method. Another possible method, which has received very little attention, is one based upon the dissociation energies of CN, nitrogen, and cyanogen, and the heat of formation of cyanogen. This method, however, presents one additional uncertainty; namely, the value for the heat of dissociation of cyanogen into CN. Although values calculated by this scheme vary from 121 to 200 kcal, White [10] favors the value of 169 kcal.

Since the spectroscopic method has received the most attention during the past decade and since the values obtained by this method do not agree very well with those found earlier by the vapor pressure measurements, it seemed desirable to redetermine the heat of sublimation by the latter method with the aid of recently developed techniques and equipment. This method of approach seemed particularly

---

[1] Bichowsky, F. R., and Rossini, F. D., The Thermochemistry of Chemical Substances, Reinhold Publishing Corp., New York, (1936).
[2] Kelley, K. K., U. S. Bur. Mines Bull. 383 (1935).
[3] Valatin, J. G., J. Chem. Phys. 14, 568 (1946).
[4] Long, L. H., and Norrish, R. G. W., Nature 157, 486 (1946).
[5] Hertzberg, G., Nature 137, 620 (1936).
[6] Gaydon, A. G., and Penney, W. G., Proc. Roy. Soc. A 183, 374 (1945).
[7] Syrkin, Ya K., J. Chem. Phys. (U.S.S.R.) 17, 347 (1943).
[8] Cherton, R. Bull. soc. roy. sci. Liege 11, 203 (1942).
[9] Kynch, G. J., and Penney, W. G., Proc. Roy. Soc. A 179, 214 (1941).
[10] White, J. U., J. Chem. Phys. 8, 459 (1940).

desirable because since the early publications on the vapor pressure method, the equilibrium constant for the dissociation of the diatomic carbon into the monatomic form has been recalculated. In addition to this reason for the redetermination, it was desirable to obtain also a vapor pressure equation for the "low" temperature region.

Essentially the method used to obtain the data reported in this paper is as follows: A known fraction of the carbon evaporating from the upper surface of a cylindrical crucible of graphite, heated inductively, was collected on a circular quartz target placed above and parallel to the surface. The rate of deposition of the carbon was determined by the rate of change of the transmissivity of the target. To determine the vapor pressure it was necessary to weigh the graphite deposited in a known time.

2.3.1 Theory

If the temperature of a hot body is measured by means of an optical pyrometer with a transparent material of thickness x interposed between the body and the pyrometer, the relation between the apparent temperature T_a, the true temperature T, and the thickness is found from Wien's radiation law and the absorption law to be

$$\frac{1}{T_a} = \frac{1}{T} + \frac{k\lambda}{c_2} x \,, \tag{1}$$

in which k is the absorption coefficient, λ is the wavelength of light passing through the pyrometer filter, and c_2 is the Wien's law constant. If the thickness of the deposit is increasing during the time of the measurements due to atoms and molecules condensing on the target, then the thickness is given by the expression

$$x = \frac{q_1 M_1 + q_2 M_2}{N_o D A} \tag{2}$$

in which q_1 and M_1 are respectively the number of atoms condensing and the atomic weight of the species of the first kind, q_2 and M_2 are the corresponding quantities for the species of the second kind (C_2 molecules in this particular case), N_o is Avogadro's number, D is the density of the solid phase, and A is the area of the deposit. If one assumes that every atom and molecule striking the target condenses, then one can write from the kinetic theory the equations

$$q_1 = \frac{K p_1 t}{\sqrt{2\pi M_1 RT}} \; ; \; q_2 = \frac{K p_2 t}{\sqrt{2\pi M_2 RT}} \,. \tag{3) and (4}$$

In these equations K is a constant for a given experimental arrangement; R is the molal gas constant; and p_1 and p_2 are the partial pressures of the two species. If the values of q_1 and q_2 given by equations (3) and (4) are substituted in equation (2) using $M_2 = 2M_1$ and the value of x so obtained is substituted then into equation (1), one obtains

$$\frac{1}{T_a} = \frac{1}{T} + C\left(\frac{p_1 + \sqrt{2}\, p_2}{\sqrt{T}}\right) t \,. \tag{5}$$

This equation is linear in $1/T_a$ vs t with a slope

$$a = C \left(\frac{p_1 + \sqrt{2}\, p_2}{\sqrt{T}} \right) . \qquad (6)$$

Taking logarithms and differentiating with respect to $1/T$, one obtains from equation (6),

$$\frac{d \ln a\sqrt{T}}{d\left(\frac{1}{T}\right)} = \frac{d \ln (p_1 + \sqrt{2}\, p_2)}{d\left(\frac{1}{T}\right)} \qquad (7)$$

If α is the degree of dissociation of the diatomic form,

$$\frac{d \ln a\sqrt{T}}{d\left(\frac{1}{T}\right)} = \frac{d \ln \left[\frac{\sqrt{2} + (2 - \sqrt{2})\alpha}{1 + \alpha}\, p \right]}{d\left(\frac{1}{T}\right)} , \qquad (8)$$

where p is the total pressure of both species. If α is constant over a given temperature range (see Table XXXII), then in view of the approximate Clausius-Clapeyron equation one obtains

$$\frac{d \ln a\sqrt{T}}{d\left(\frac{1}{T}\right)} = \frac{d \ln p}{d\left(\frac{1}{T}\right)} = - \frac{\Delta H_S}{R} . \qquad (9)$$

The quantity ΔH_S can be defined as the experimental heat of sublimation per "mole", since it is the value one would obtain from any experiment giving the vapor pressure as a function of temperature. Without a knowledge of the molecular and atomic species existing in the vapor and their relative concentrations, however, one cannot define a "mole". If one assumes that the reaction taking place during the process of the sublimation is

$$2C_S = 2\alpha C + (1 - \alpha) C_2,$$

then one can write for the heat absorbed

$$L = 2\alpha \Delta H_1 + (1 - \alpha) \Delta H_2$$

in which ΔH_1 is the heat of sublimation to one mole of the monatomic form and ΔH_2 is the heat of sublimation to one mole of the diatomic form. For the volume change associated with this reaction one writes

$$V = (1 + \alpha) RT/p .$$

Using these values for L and V in the Clausius-Clapeyron equation and the relation between the heats of sublimation and the heat of dissociation of the diatomic form, ΔH_D, one obtains from equation (9) the result

$$\Delta H_S = \frac{2\Delta H_1 - (1 - \alpha)\Delta H_D}{(1 + \alpha)} \qquad (10) .$$

To calculate the vapor pressure from the known weight of a deposit, one must know first the fraction of the total number of atoms and molecules

evaporating from the upper surface which are collected. In other words, one must know the geometry factor G in the equation

$$p = \frac{\sqrt{2\pi RT}}{G\sqrt{M'}} \frac{W}{t} \qquad (11)$$

in which M' is an average molecular weight, and W is the weight of the deposit formed in time t. This factor G can be calculated from the cosine distribution law which gives the relation

$$dN = \frac{pN_o}{\sqrt{2\pi M'RT}} \frac{\cos\theta_1 \cos\theta_2}{\ell^2} \, d\sigma \, ds ,$$

in which dN is the number of atoms and molecules arriving at an area $d\sigma$ from an area ds, the planes of $d\sigma$ and ds having angles θ_1 and θ_2 between their respective normals and a line of length ℓ joining them. In the present case the two areas are parallel and the circular area of the target is coaxial with that of the upper surface of the graphite, so that one writes the following conditions:

$$\theta_1 = \theta_2 = \theta$$

$$\cos\theta = d/\ell$$

$$\ell = \sqrt{\rho^2 + r^2 + d^2 - 2r\rho\cos(\alpha - \beta)} .$$

In these equations ρ and β are the polar coordinates in the plane of the target, and r and α those in the plane of the graphite surface and d is the perpendicular distance between these planes. When these conditions are substituted in the cosine law relation, one obtains for the geometry factor the expression

$$G = \frac{d^2}{\pi} \int_0^{R_2} \int_0^{R_1} \int_0^{2\pi} \int_0^{2\pi} \frac{r\rho}{(a - b\cos\gamma)^2} \, d\alpha \, d\beta \, dr \, d\rho ,$$

in which $a = r^2 + \rho^2 + d^2$; $b = 2r\rho$; $\gamma = \alpha - \beta$; R_1 = radius of the graphite cylinder; and R_2 = radius of the target. If the denominator of the integrand is expanded to obtain

$$\frac{1}{(a - b\cos\gamma)^2} \approx \frac{1}{a^2} + \frac{2b\cos\gamma}{a^3} + \frac{3b^2\cos^2\gamma}{a^4} + \frac{4b^3\cos^3\gamma}{a^5} ,$$

then the four integrations can be performed readily for the first and third terms, three can be performed for the second, and two for the fourth. The second and fourth terms can then be evaluated to a sufficient degree of accuracy by graphical integration and by Simpson's rule. The final result with $R_1 = 0.4901''$, $R_2 = 0.4103''$, and $d = 1.442''$ is

$$G = (0.0767_0 + 0.008_0 + 0.007_2 + 0.0014) \text{ inch}^2$$

$$G = 0.365_5 \text{ cm}^2 .$$

Using this value for G and taking the average molecular weight for 2α moles of C and $(1-\alpha)$ moles of C_2, one obtains from equation (9) the final expression by which the vapor pressure is calculated in the present case.

$$p\ (\text{mm}) = 13.539 \left[\frac{1+\alpha}{2\alpha + \sqrt{2}(1-\alpha)}\right] \frac{W}{t}\sqrt{T} \qquad (12)$$

2.3.2 Apparatus

The essential parts of the apparatus are shown in Figure 21. The enclosure for the graphite consisted of a water-cooled quartz jacket J having a water-cooled shelf upon which the combined quartz collimator and target holder M rested. The upper extension of the jacket was joined at C through a graded seal to a pyrex tube the upper end of which terminated with an optical pyrex window P. This section of pyrex tubing enabled one to open the system by cracking off the tube with the aid of a hot wire and to remove the collimator (inside diameter = 0.8206 inches) and the target L from the system via the top without removing the jacket from the assembly. At the lower end of the jacket a 34/45 standard taper joint N was sealed with Apiezon cement to a pyrex evacuation tube. On the bottom of this tube there was sealed an optical pyrex window P which was protected from the carbon vapors by a circular piece of sheet nickel. This piece of nickel could be lifted from the window and placed against the side of the tube by a magnet when one desired to sight through the window. A reentrant tube extended upwards inside the evacuation tube and through the ground joint to serve as a support for the graphite. The upper half of this tube was a quartz tube joined at O by a graded seal. To the upper end of the quartz tube there was sealed a quartz disc having a hole at its center.

The support for the graphite cylinder consisted of a circular disc of hot-pressed beryllia (diameter = 26.1 mm, thickness = 6 mm) with a circular hole (diameter = 6.7 mm) at its center. Grooves (1 mm deep) at 60° intervals extending across three separate diameters of the disc served to make the disc an approximately kinematic table. A counter bore (diameter = 19.4 mm, depth = 2 mm) in the bottom of the disc held it in place when it was set on the quartz disc at the upper end of the reentrant tube.

The targets L upon which the graphite was collected were optical quartz discs (diameter = 26 mm, thickness = 2 mm). These were thoroughly cleaned before use with boiling nitric acid and after proper rinsing in water and acetone finally washed with a condensing vapor from boiling xylene. Those used to determine the rate of deposition received no further treatment, but those used for the vapor pressure determination were heated for one-half hour in an open beaker over a Meeker burner. For the latter measurements two targets were placed in the collimator, one on top of the other, so that the top one could be used as a tare to determine the weight of the graphite deposited by difference.

The graphite cylinder (diameter = 0.9812 inch, height = 0.5842 inch) was turned out on a lathe from a piece of Kendall graphite. A hole (diameter = 2 mm, depth = 10 mm) drilled along the cylinder axis in the bottom surface served as a black body so that the temperature of the graphite could be measured by means of an optical pyrometer. Three tungsten

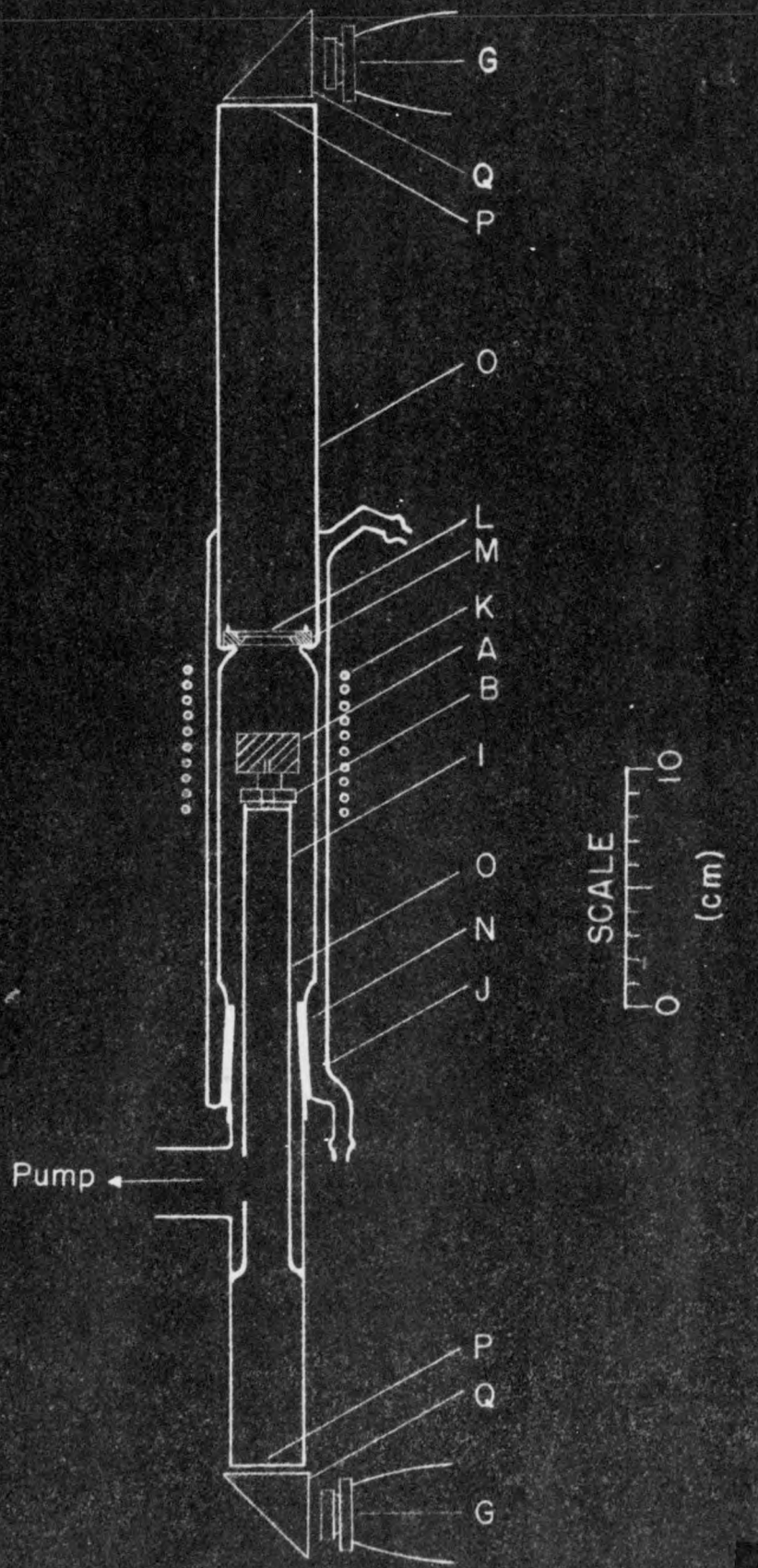

FIGURE 21

APPARATUS EMPLOYED TO DETERMINE THE HEAT OF SUBLIMATION AND VAPOR PRESSURE OF GRAPHITE

legs (diameter = 0.05 inch, length = 5/8 inch) forced into holes 1/4 inch deep drilled on the circumference of a circle of radius 21/64 inch and at an angular separation of 120° supported the cylinder above the beryllia table; the bottom ends of the legs were pointed so that they rested in the grooves of the table. Before the graphite was used for any experimental measurements it was baked out in a vacuum for seven hours at 2185°C. The distance between the upper surface of the graphite and the target (1.442 inches) was measured with a tungsten rod having a sliding cylindrical collar. The rod was lowered into the jacket from the top after the collimator had been placed on the shelf, the cylinder placed on the beryllia table, and the ground joint sealed; the collar rested on the recessed part of the collimator and the rod was slid on through the collar until its end touched the upper surface of the graphite. The distance was measured along the rod with a micrometer caliper.

The evacuating system consisted of a two-stage mercury diffusion pump supported by a Cenco Megavac pump, and the conventional liquid nitrogen traps. An ionization gauge (Distillation Products Type VG-1A) located between the first trap and the quartz condenser J furnished a means of determining the background pressure in the system. For all the runs reported in this paper this pressure was never greater than 10^{-6} mm at the start of a run.

A Leeds and Northrup disappearing filament type optical pyrometer (No. 8622) which had been recalibrated in this laboratory, was used to measure the temperature of the graphite; a similar pyrometer, mounted at the top of the condenser, was used to measure the rate of deposition of the graphite on the target. The other pieces of equipment used were reflecting prisms, an Ainsworth Type VM semi-microbalance (sensitivity $\cong$ 35 ug per division), an induction heating unit (Induction Heating Corporation Model 520), and a copper coil K surrounding the quartz jacket. The induction heating unit was supplied with a constant voltage from a Sola 10 KVA transformer thus stabilizing the output of the unit and maintaining the graphite at a reasonably constant temperature throughout a given run.

2.3.3 Results

A plot of the reciprocal apparent absolute temperatures, measured through the deposits, as a function of time gives linear curves in accordance with equation (5) except in the initial region. The length of this region depends upon the temperature of the run, increasing with decreasing temperature. In order to eliminate the error introduced by this non-linear region the highest temperature curve (Run 13) which shows no noticeable deviation for times greater than 4 minutes and less than 50 minutes was accepted as a standard. The slopes of the other curves were calculated then for corresponding regions, these being determined by the relation

$$\frac{T_1}{T_2} = \sqrt{\frac{\tau_1}{\tau_2}}\, e^{\frac{\Delta H_S}{R}\left(\frac{1}{T_1} - \frac{1}{T_2}\right)} \qquad (13)$$

in which τ_1 (4 minutes) is the time required to build up a deposit of a certain thickness at T_1 (2469°K) and τ_2 is the time required to build up another deposit of the same thickness at T_2. This method of limiting

the regions of the $1/T_a$ vs t curves enables one to calculate all of the slopes in the same thickness region. Since the minimum times calculated by equation (13) for Runs 3 and 7 are less than the maximum times of these runs, they have not been included in the final calculations. The numerical values of the slopes were calculated by the use of the least squares method.

A graph giving the logarithms of the product of the slope and the square root of the absolute temperature, $\log_{10} a\sqrt{T}$, as a function of the reciprocal absolute temperature [see equation (8)] is given in Figure 22. In general, as expressed by equation (8), one would not expect this curve to be linear. However, since the data do give a linear plot within the experimental error, one is justified in assuming that the degree of dissociation of C_2 does not change over the temperature range covered. Hence one can employ equation (9) to obtain the experimental heat of sublimation. The least squares slope of $\log_{10} a\sqrt{T}$ vs t curve is $4.35\ (\pm 0.08) \times 10^4$; this corresponds to a value of 199 ± 4 kcal for ΔH_S. On the basis of the weights of the deposits (see points represented by concentric circles in Figure 22), one obtains for ΔH_S a value of 183 kcal. Since this value is based upon only four experimental points, it has a large probable error.

Before this value of 199 kcal can be used in equation (10) to calculate the heat of sublimation of the monatomic form, ΔH_1, and also before the vapor pressure can be calculated from the weights of the deposits with equation (12), an expression must be found for the equilibrium constant for the reaction, $C_2 = 2C$. Several expressions, calculated from statistical mechanical relations and spectroscopic data, are available in the literature, the primary difference among the various relations being the value used for the dissociation energy of C_2. For reasons to be given later the writer at present accepts the values for the constant at various temperatures given by Zeise (11) which give by the least squares method,

$$\log_{10} K = -\frac{3.776 \times 10^4}{T} + 6.736 \quad . \qquad (14)$$

Zeise's values agree reasonably well with those given in one case by Vaughan and Kistiakowsky (12).

Even having an expression for K, however, one cannot calculate a value of α to use in equation (10) unless the vapor pressure is known, since α is calculated from the expression

$$\alpha = \sqrt{\frac{K}{K + 4p}} \quad . \qquad (15)$$

To obtain an expression for the vapor pressure one can assume for the first approximation that the vapor contains only the diatomic form. (A preliminary estimation of α gives about 0.1.) From the weight of the deposit an approximate vapor pressure then can be found by substitution in equation (12) with $\alpha = 0$. From this value of p an approximate value

(11) Zeise, H. Z., Elektrochem. 46, 38 (1940).
(12) Vaughan, W. E., and Kiatiakowsky, G. B., Phys. Rev. 40, 457 (1932).

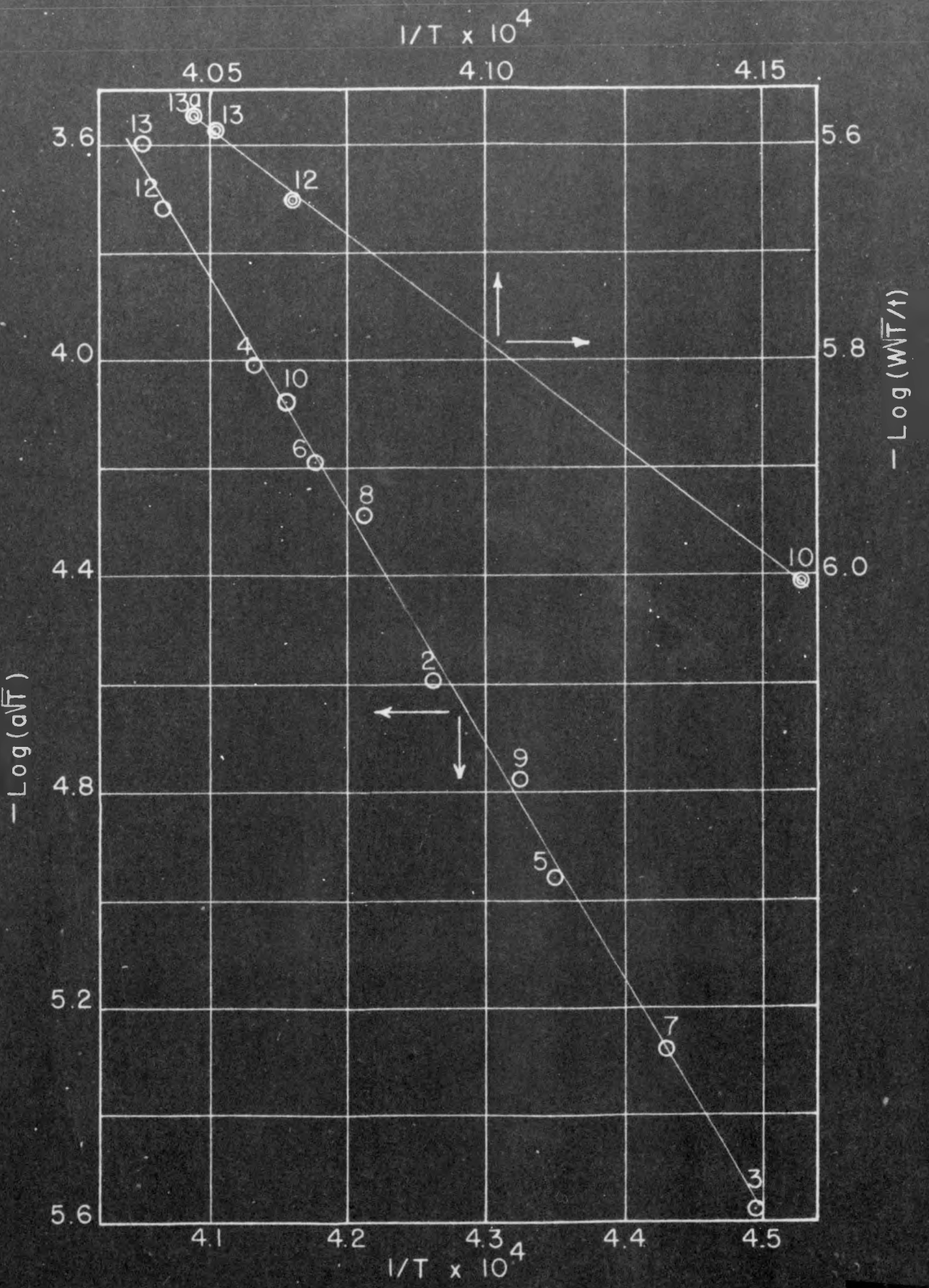

FIGURE 22

PLOT OF LOGARITHM OF RELATIVE VAPOR PRESSURE OF GRAPHITE AS A FUNCTION OF RECIPROCAL ABSOLUTE TEMPERATURE

of α can be found with equations (14) and (15). Successive approximations give sufficiently accurate values for α and p after three trials. The results are tabulated in Table XXXII. Using these values of p and the least squares method, one obtains for the vapor pressure the expression

$$\log_{10} p \text{ (mm)} = -\frac{43466}{T} + 13.044, \qquad (16)$$

for the temperature interval 1900°C to 2200°C. In view of the calculated values for α listed in Table XXXII, one obtains further evidence for the

TABLE XXXII

Vapor Pressure of Graphite and Degree of Dissociation of Vapor at Various Temperatures

Temperature (°K)	Weight of Deposit (μg per sec)	Degree of Dissociation	Vapor Pressure (mm)
2471	0.0538	0.139	2.76×10^{-5}
2469	0.0524	0.139	2.69
2461	0.0450	0.141	2.31
2406	0.0200	0.145	1.01

justification for the assumption of the constancy of the degree of dissociation in this interval.

Using the value of the vapor pressure calculated from equation (16) at 2384°K (the midpoint of the temperature interval covered), one obtains a degree of dissociation of 0.15 at this temperature. This value together with the value for the heat of dissociation of C_2 of 172.8 kcal per mol obtained from equation (14) gives for the heat of sublimation of the monatomic form, ΔH_1, 187.8 kcal per mol at 2384°K. If this is corrected to 298°K by the ΔC_p equation given by Kelley (13), the result is 189.7 kcal per mol.

(13) op.cit. (2)

2.3.4 Reflectivities of Graphite

During the course of this work the reflectivities of a number of the graphite deposits were measured at 0.665 μ. This was accomplished by measuring the intensity of light, both direct and reflected, from a fluorescent lamp with the aid of an optical pyrometer. The results are given in Table XXXIII.

TABLE XXXIII

Reflectivity and Transmissivity of Graphite Deposits on Quartz

Run	Relative Thickness	Reflectivity	Transmissivity	Absorptivity
5	0.37	0.22	0.29	0.49
8	0.38	0.21	0.11	0.68
9	0.91	0.20	0.06	0.74
6	1.02	0.23	0.06	0.71
2	1.68	0.25	0.02	0.73
12	7.67	0.26	0.00	0.74
13a	7.69	0.25	0.00	0.75

The transmissivities given in this table were obtained by measuring the apparent temperature of the graphite cylinder through the deposit at the end of each run. The relative thicknesses were calculated by the use of equation (13).

3 RADIOCHEMISTRY

3.1 Half Life Studies (J. A. Seiler)

As part of a general program to obtain more accurate decay constants for the fission products, samples of 40h La^{140}, 12.8d Ba^{140}, 66h Mo^{99} and 13.7d Pr^{143} formed in the fission of U and Pu have been isolated and their decay has been followed on an ionization chamber with an FP-54 amplifier, and on a standard mica window GM tube. Portions of the decay curves plotted on greatly expanded scales are given in Figures 23 - 28. The best values for the half lives of the isotopes, as determined most reliably on the FP-54 apparatus, are tabulated in Table XXXIV together with their estimated deviations as determined graphically.

3.1.1 Half Life of Ba^{140}

The Ba samples were isolated from Pu fission products and from U fission products using the standard method of isolation. The Ba was repeatedly precipitated as the chloride and as the nitrate from concentrated HCl and HNO_3 solutions in the presence of ca. 15 mg of Ba carrier, and employing Sr as a hold-back carrier. The Ba was finally mounted as $BaCrO_4$ on aluminum cards and was covered with scotch tape, the mounted sample weighing about 15 mg over a 2 cm^2 area. A few tiny crystals of the $BaCrO_4$ were similarly mounted on aluminum cards to follow the activity with a GM tube. The decay curve of the Ba from Pu fission was followed for seven half lives on the FP-54 chamber, at which time it became too weak to follow further. A half life of 308 $\pm$ 1h was obtained graphically with the data being plotted on an expanded scale (Figure 23a). The ionization chamber was sealed from the atmosphere so as to maintain constant gas density and hence constant efficiency. In addition, RaE standards ($T\frac{1}{2}$ = 22y) were read at each sample reading. The ratios of the unknown activity to the RaE standard are the values which are plotted for the graphical determination of the half life of all the isotopes in these experiments.

After the FP-54 measurements were completed, the sample was followed in a continuous fashion on the GM tube for six more half lives. Although the scatter of the points was now much greater, the sample showed no evidence of tailing off to a longer lived residue. The half life as obtained with the GM tube was 312 $\pm$ 6h (Figure 23b). The counting rate of the sample for the GM tube began at about 10,000 c/m, and no correction for the resolution losses in the GM tube was made. This correction would be in the proper direction and is estimated to be of the proper order of magnitude to bring the half life as determined on the GM tube into close agreement with that obtained on the FP-54 chamber.

Very similar results were obtained with the Ba isolated from U fission, the FP-54 sample giving a half life of 307 $\pm$ 1h over eleven half lives (Figure 24a) and the GM tube sample a half life of 312 $\pm$ 6h over three half lives (Figure 24b). Here again application of the correction for resolution losses in the GM tube would bring its value into close agreement with the FP-54 value. A value of 308h was obtained by D. W. Engelkemeir on the FP-54. The best value is therefore taken to be 308h or 12.8d.

3.1.2 Half Life of La^{140}

The La^{140} samples were prepared from 12.8d Ba^{140} isolated from U and Pu fission, by precipitating $La(OH_3)$ five times in the presence of 15 mg of La carrier. The La was finally mounted as the oxalate and its activity was followed on the FP-54 and the GM tube (Figures 25, 26a, 26b). The half life of La^{140} isolated from Pu fission was found to be 40.4 $\pm$ 0.1h (followed over eight half lives) and the half life from U fission was found to be 40.5 $\pm$ 0.1h (followed over eight half lives). Each of these samples was followed for eight more half lives on the GM tube with no evidence of tailing off. The La from U fission followed on the GM tube (beginning at about 7,000 c/m) gave a half life of 41 $\pm$ 1h. The best value of the half life of La^{140} is taken to be 40.4h.

3.1.3 Half Life of Mo^{99}

66h Mo^{99} was isolated from U fission products by the standard chemical procedures employing eight cycles of α-benzoin-oxime precipitations and $La(OH)_3$ precipitations. The Mo was finally precipitated as $PbMoO_4$ and several 20 mg aliquots of this precipitate were mounted on aluminum cards; in addition, a small aliquot was mounted separately for GM survey. The samples counted on the FP-54 chamber gave a half life of 66.0 $\pm$ 0.1h (Figure 27a) followed over eight half lives with eight succeeding half lives taken on a GM tube giving no evidence of tailing off. The sample was followed with 15.4 mg Al/cm^2 added absorber to cut out the soft radiations due to the 6h element 43 daughter. A sample followed in parallel on the GM tube gave a half life of 68 $\pm$ 1h (Figure 27b) over 10 half lives. The initial activity of this sample was ca. 18,000 c/m, giving a rather large resolution loss in the GM tube. The FP-54 value, 66.0h is taken as the best value of the half life of Mo^{99}.

3.1.4 Half Life of Pr^{143}

The Pr sample from Pu fission was prepared from the 33h Ce^{143} parent, which was isolated by the use of six cycles of iodate precipitations using La as a holdback carrier. The cerium iodate was allowed to stand for thirty days following which Pr was isolated by five cycles of oxalate precipitations followed by $Ce(IO_3)_4$ clean ups to remove the Ce parent. A 20 mg aliquot of the oxalate was mounted on an aluminum card and covered with scotch tape for following on the FP-54 chamber. A small aliquot was similarly mounted for GM tube survey. The half life observed on the FP-54 sample was 13.7 $\pm$ 0.05d (Figure 28a) followed through four half lives. The sample was then followed on the GM tube for nine half lives giving no evidence of tailing off. The GM tube sample gave a half life of 13.8 $\pm$ 0.2d (Figure 28b) followed through just two half lives. The initial count on the GM tube sample was 1,800 c/m so that the resolution loss probably did not exceed $\frac{1}{2}$% and this is substantiated by the agreement of the half lives from the GM tube and from the FP-54.

3.1.5 Interpretation of Results

From the experiments on the La and Ba isotopes there is no indication of any variation in the half lives of the isotopes originating in U or in

Pu fission which exceeds experimental error. Although there is no reason to anticipate any such differences, at the time these studies were started it appeared that there were significant differences in the aluminum absorption curves of 12.8d Ba^{140} from U and from Pu fission (see section 3.2 of this report). The agreement in the half lives is in correspondence with the observed agreement in the absorption curves. Further studies on half lives of isotopes of interest to the project continue.

TABLE XXXIV

Best Values for the Half Lives of La^{140}, Ba^{140}, Mo^{99} and Pr^{143}

Isotope	Half Life
La^{140}	40.4 ± 0.1h
Ba^{140}	308h (12.8d) ± 1h
Mo^{99}	66.0h ± 0.1h
Pr^{143}	13.7d ± 0.5d

Figure 23a
Ba^{140} Decay Curve from Plutonium Fission
Taken on FP-54

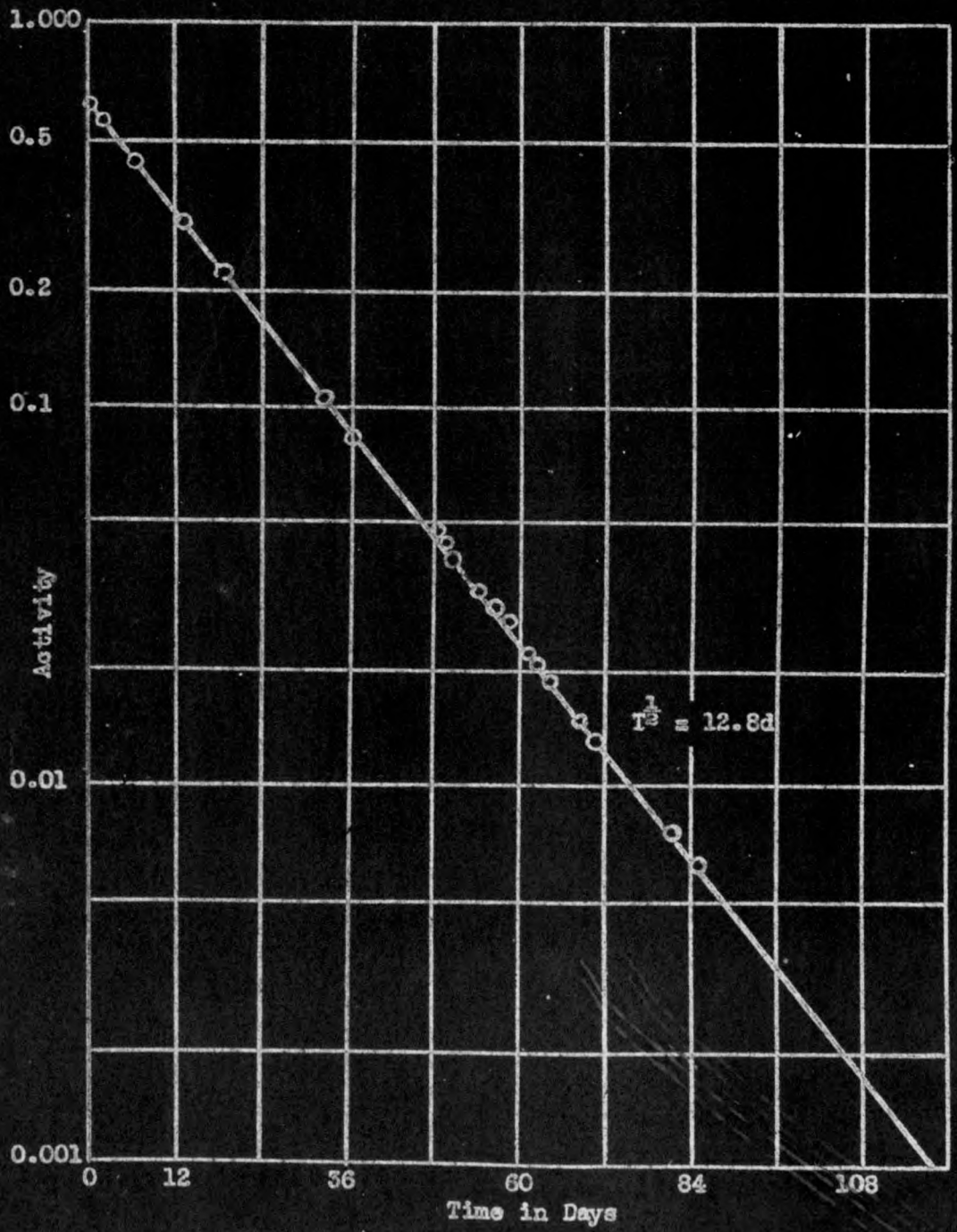

Figure 23b
Ba^{140} Decay Curve from Plutonium Fission
Taken on GM Counter

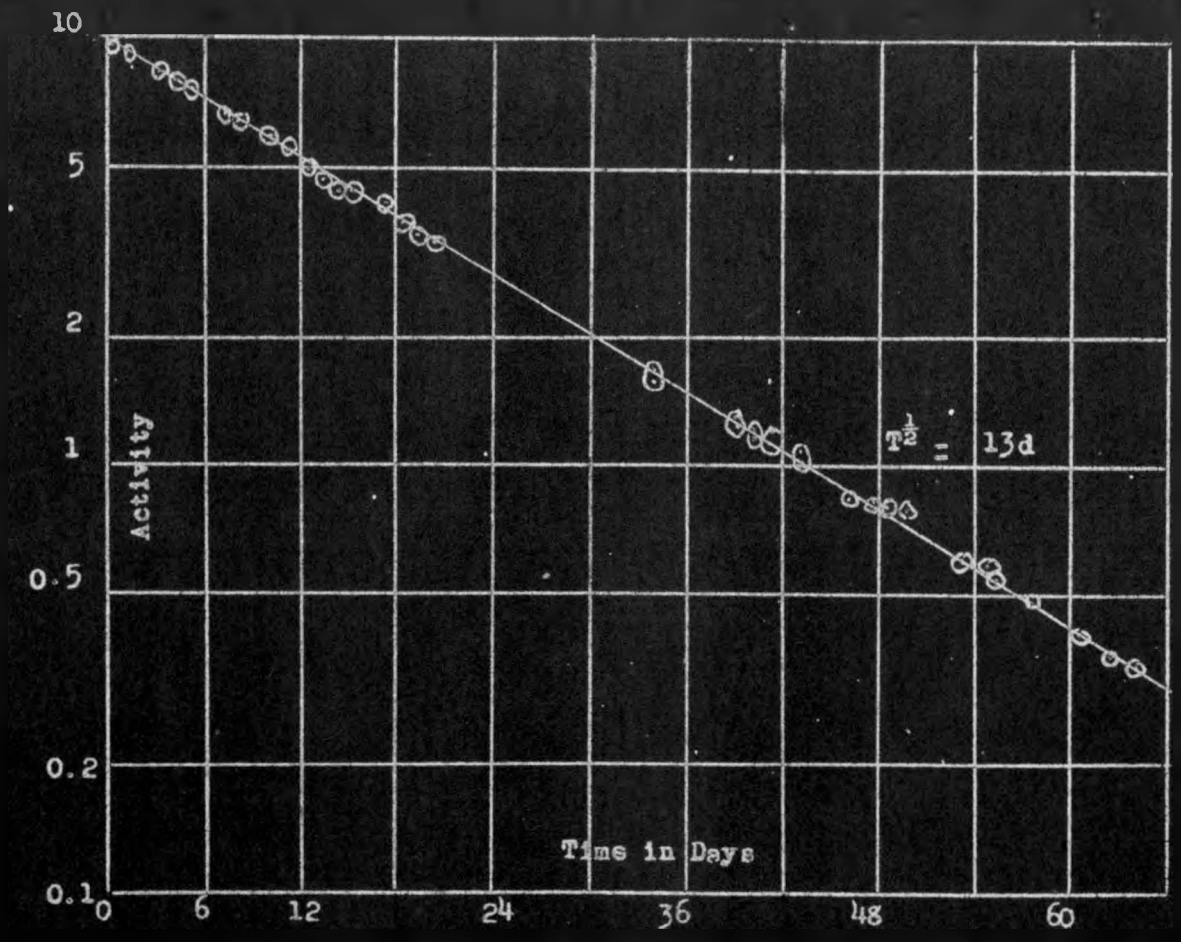

Figure 24a
Ba^{140} Decay Curve from Uranium Fission
Taken on FP-54

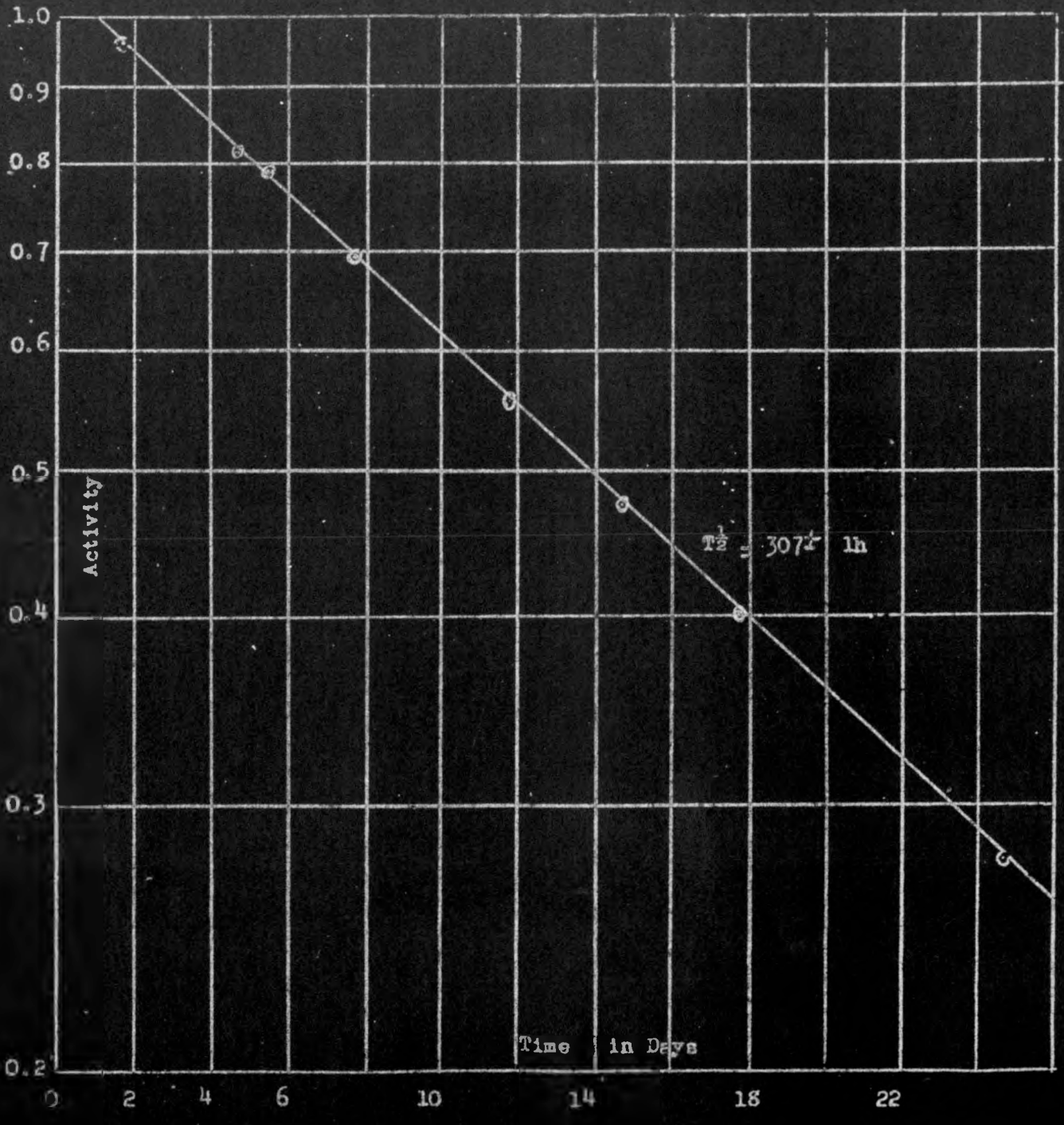

Figure 24b
Ba^{140} Decay Curve from Uranium Fission
Taken on GM Counter

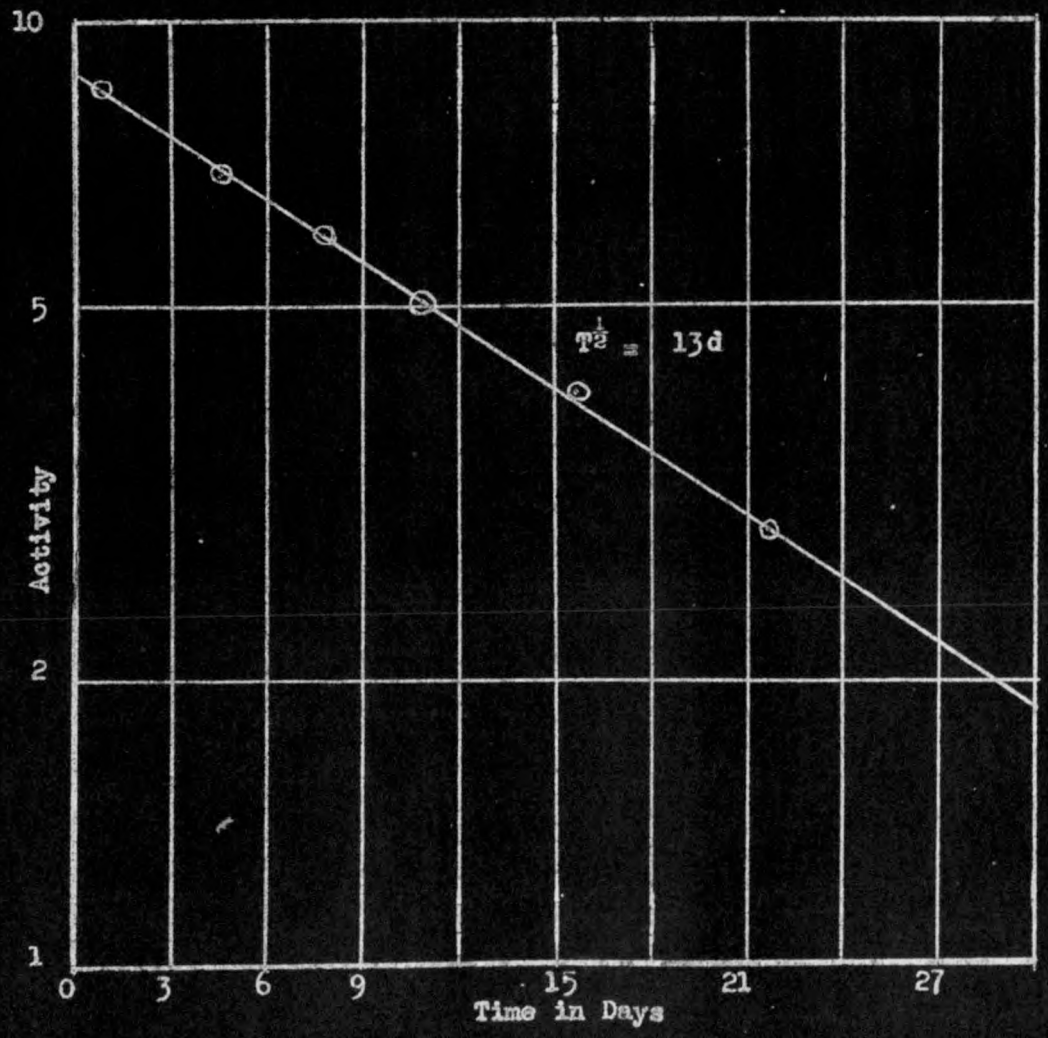

Figure 25
La^{140} Decay Curve from Plutonium Fission
Taken on FP=54

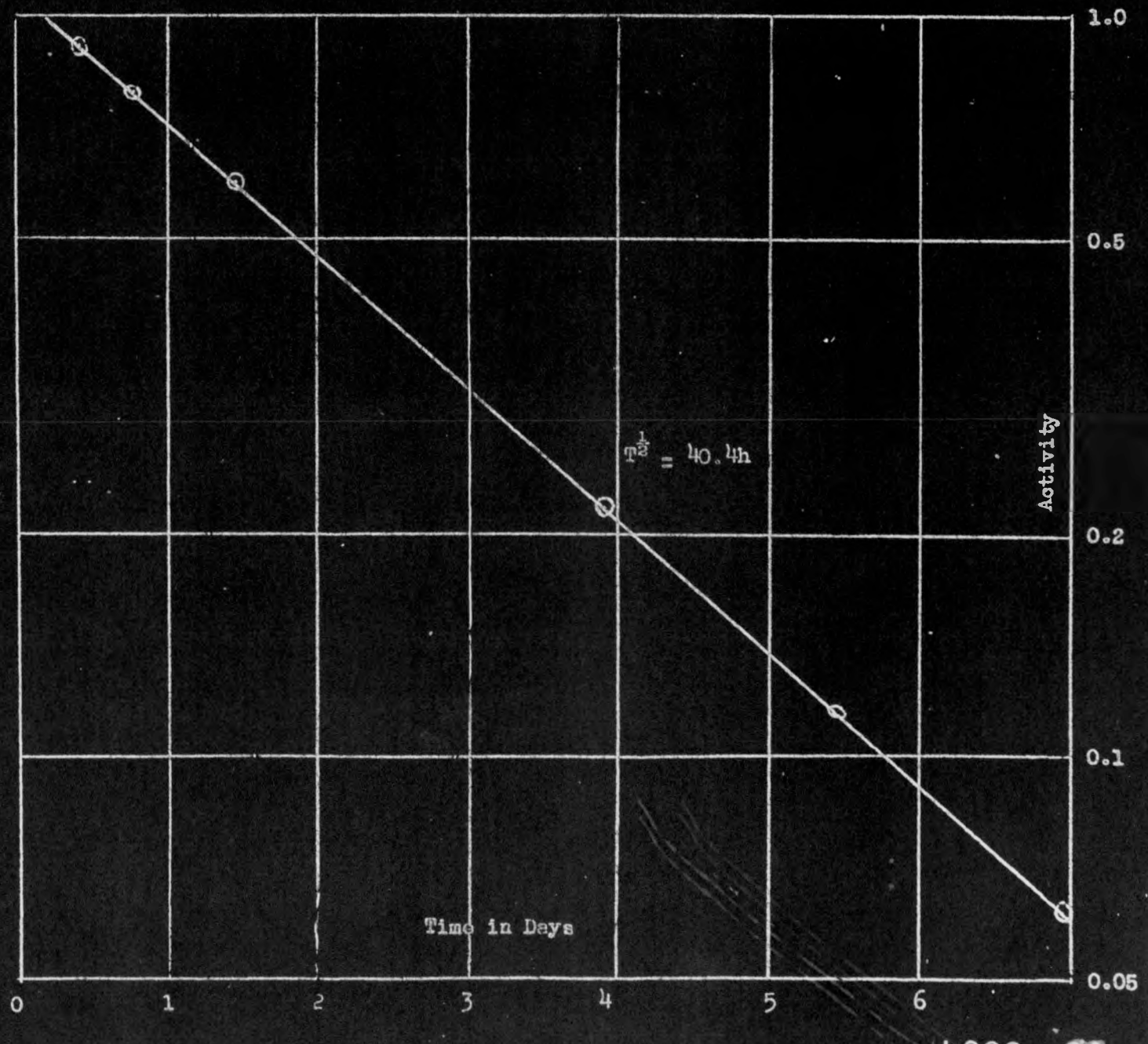

4000 92

Figure 26a
La^{140} Decay Curve from Uranium Fission
Taken on FP-54

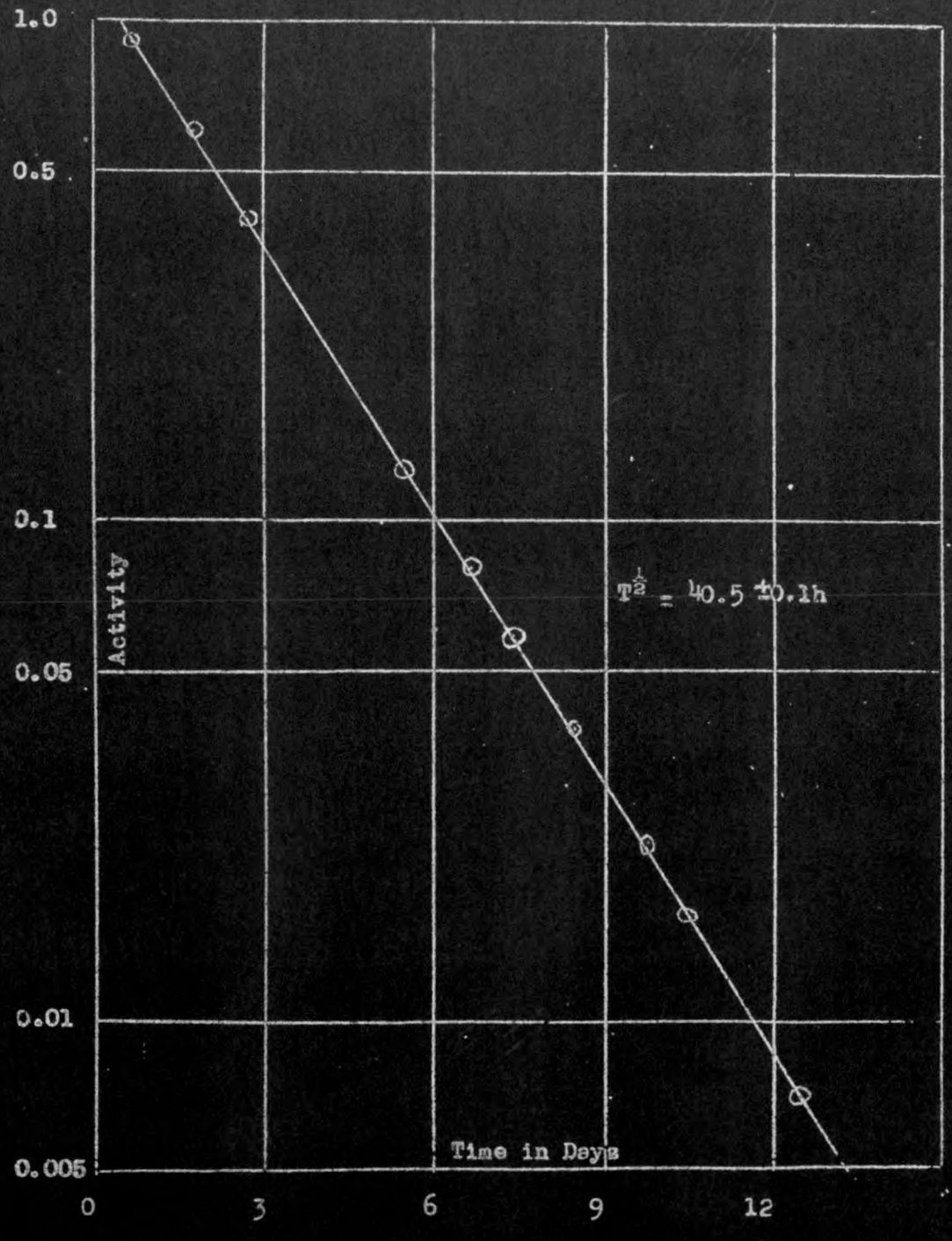

Figure 26b
La^{140} Decay Curve from Uranium Fission
Taken on GM Counter

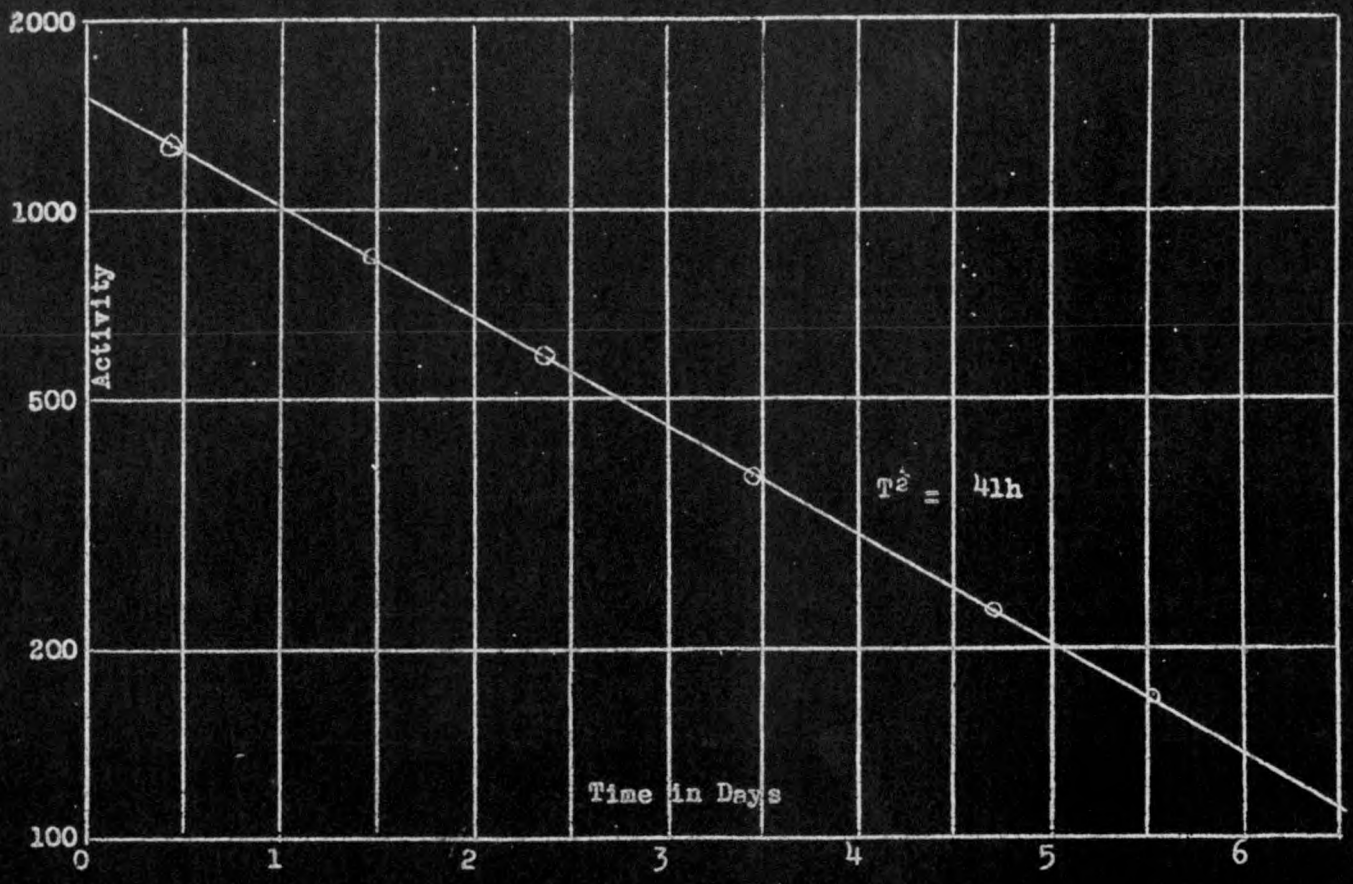

Figure 27a

^{140} Decay Curve from Uranium Fission
Taken on FP-56

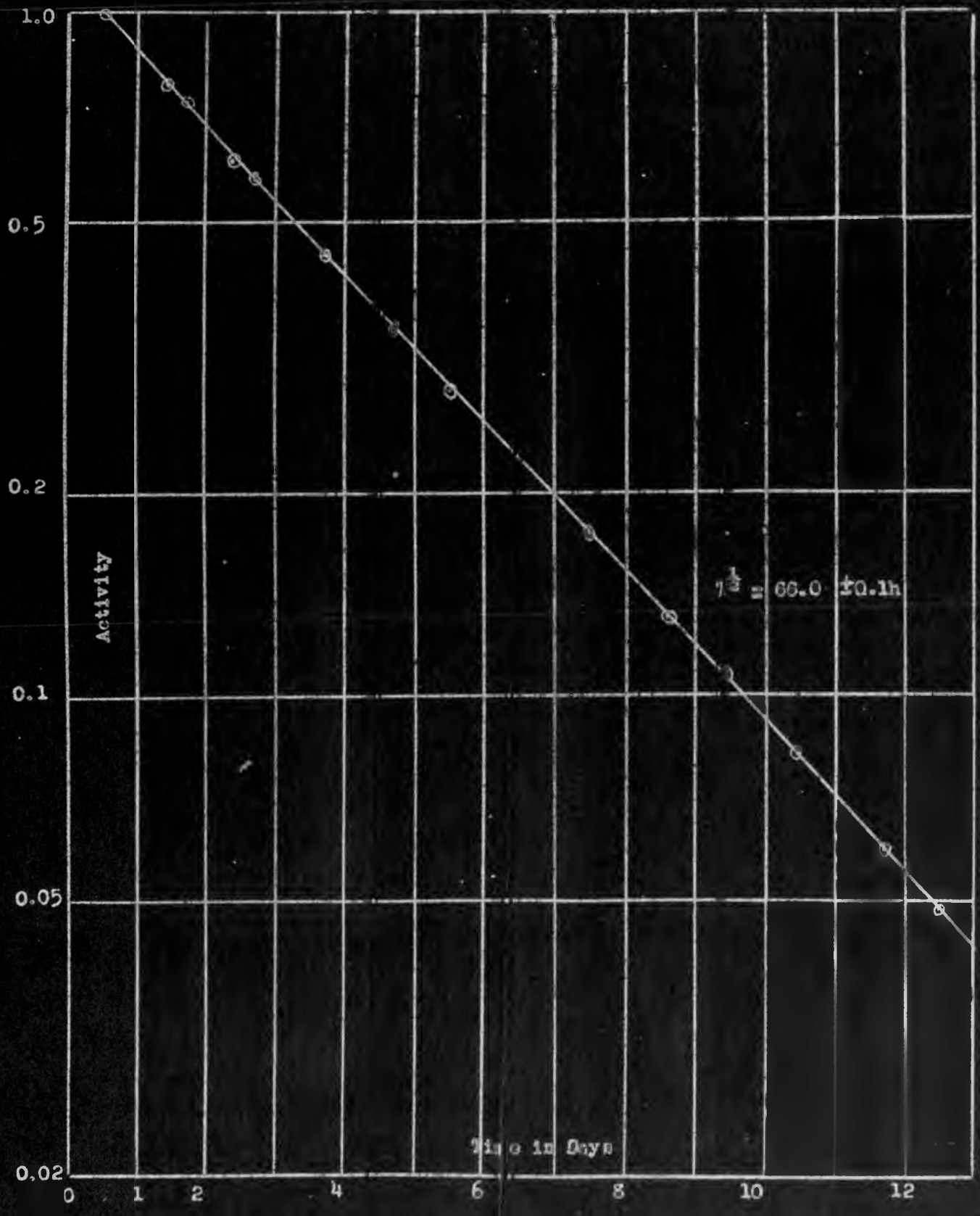

Figure 27b
Mo^{99} Decay Curve from Uranium Fission
Taken on GM Counter

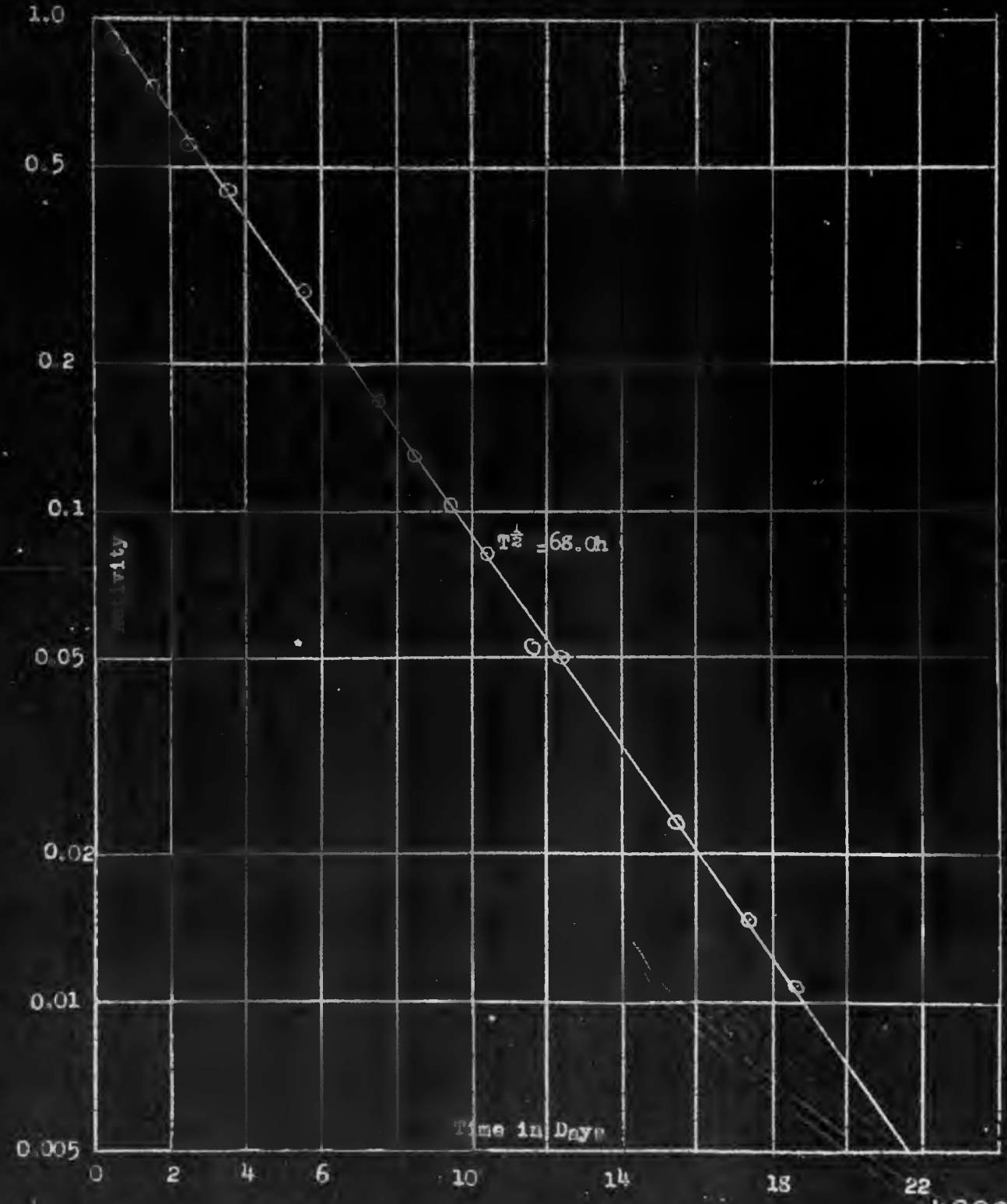

Figure 28a
Pr^{143} Decay Curve from Plutonium Fission
Taken on FP-54

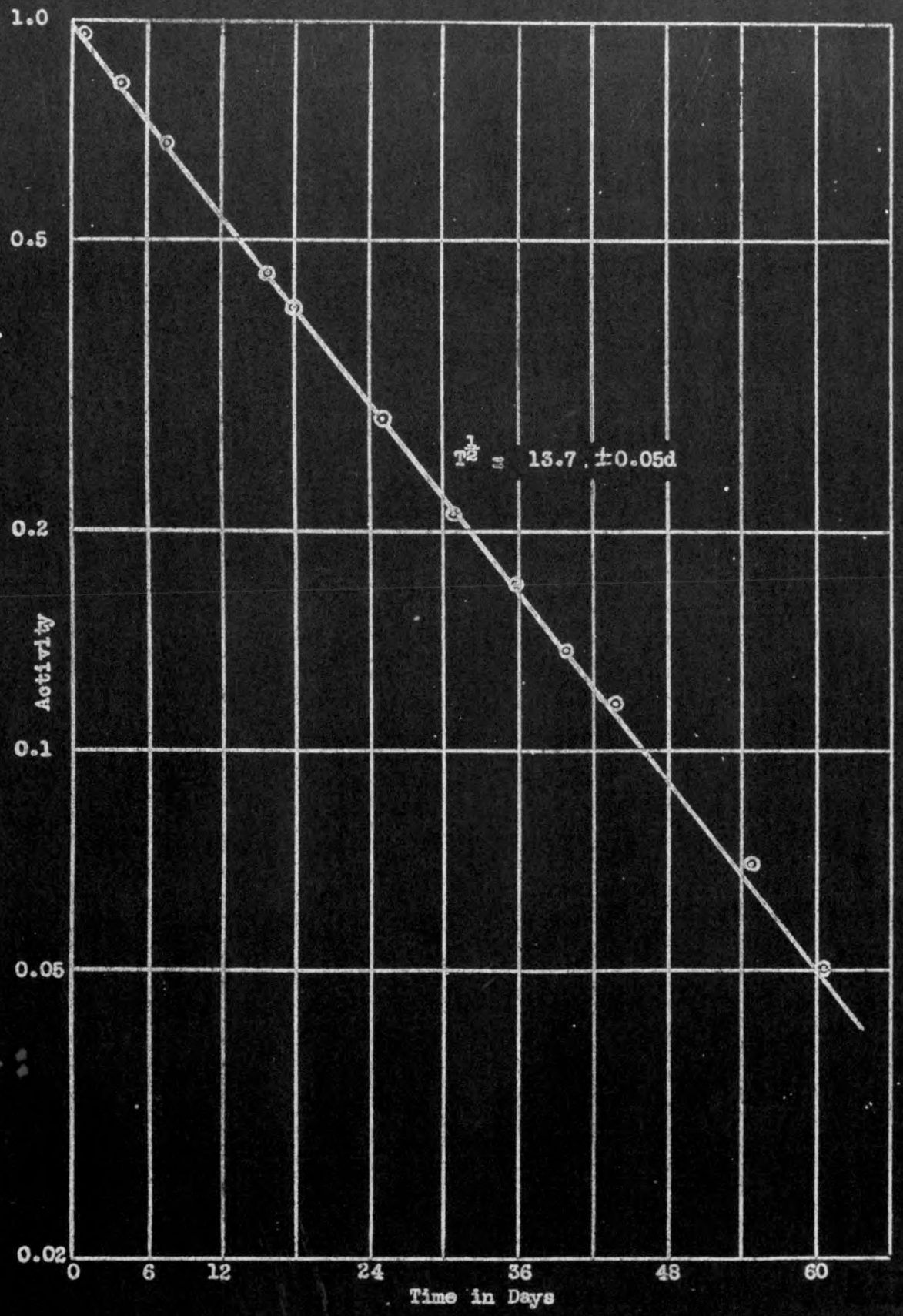

Figure 28b
Pr^{143} Decay Curve from Plutonium Fission
Taken on GM Counter

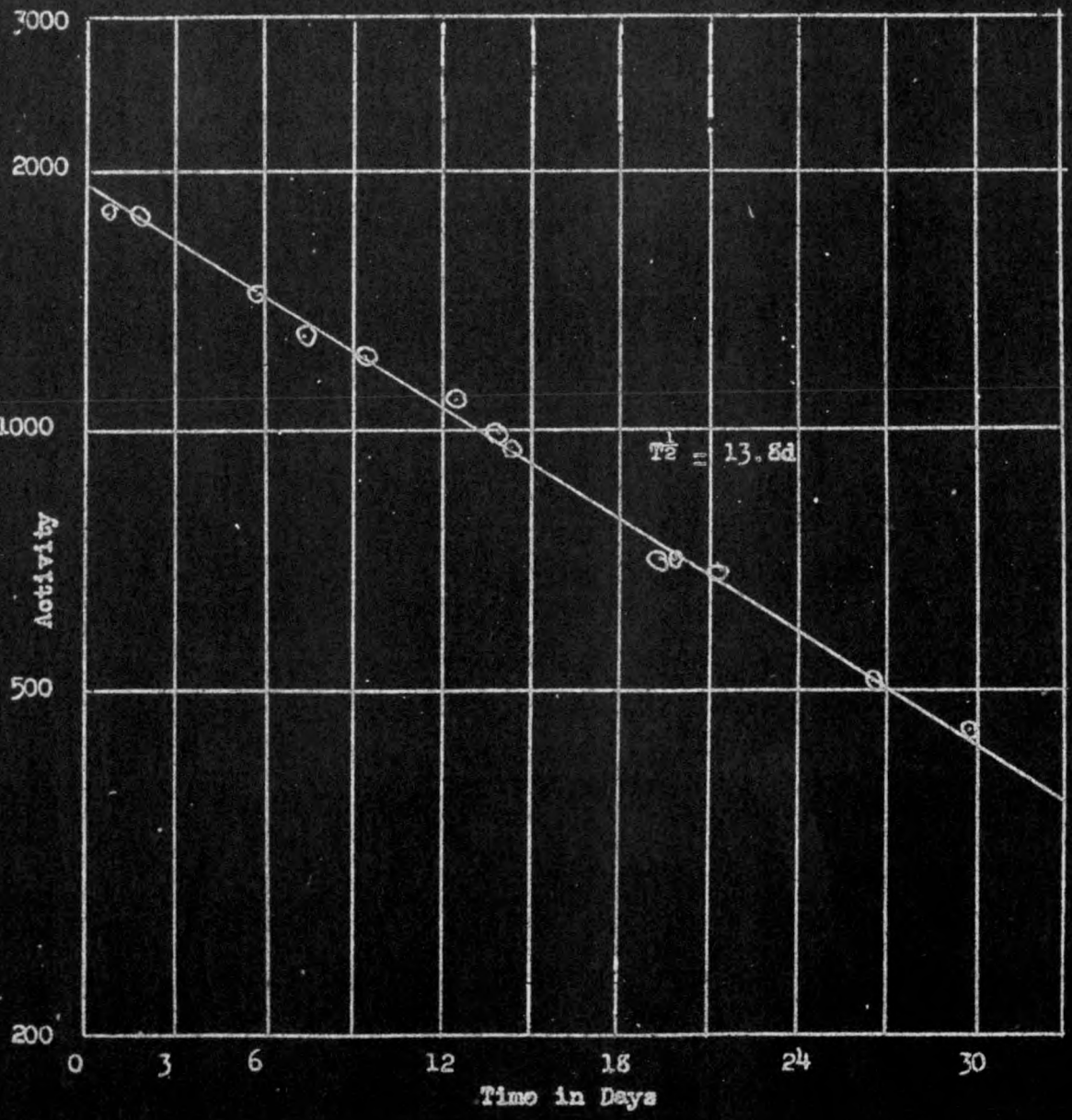

3.2 An Inconsistency in the Aluminum Absorption Curves of 12.8d Ba^{140} (J. A. Seiler)

The absolute fission yield of 12.8d Ba^{140} has served as a standard for the determination of the fission yields of other fission products in the fission of both U^{235} and Pu^{239}. Errors in the calculation of the beta disintegration rate of the Ba samples from their observed counting rates enter into the calculated values for all the relative fission yields.

A major correction in the calculation of the disintegration rate is concerned with the absorption of betas within the sample itself, in the cellophane used to cover the sample, in the mica window of the Geiger-Muller tube and in the intervening air path. In the standard radiochemical procedure the Ba is mounted as $BaCrO_4$ over a 2 cm^2 area, the precipitate weighing from 15 to 30 milligrams. The sample is covered with cellophane about 3.5 mg/cm^2 thick and is mounted on a cardboard counting card, and counted on the top shelf. The air path from sample to tube amounts to 0.5 mg/cm^2 absorber and the mica window thickness is generally about 3.5 mg/cm^2. The observed counting rate must therefore be corrected for the absorption taking place in a total of about 14 mg/cm^2 of materials, allowing about one half of the sample weight/cm^2 as added absorber. The correction is made by extrapolating back along an Al absorption curve to zero absorber. The initial observed slope of this Al absorption curve (if the curve is purely exponential in this region), or the precise shape of a non-exponential curve is thus the determining factor in the extrapolation. In the present case of interest, for example, aluminum absorption curves on 12.8d Ba^{140} from U^{235} or Pu^{239} fission, have shown apparent initial half thicknesses varying from 26.5 mg/cm^2 to 35 mg/cm^2, leading to a possible error in the extrapolation of ca. 8%.

The original standard Al absorption curve on Ba^{140} from U^{235} fission was taken by D. W. Engelkemeier. The value chosen for a standard half-thickness correction was 26.5 mg/cm^2 but this was obtained with a weightless sample of Ba^{140} [Figure 29, curve (a)]; although the (weightless) sample-curve was used on the project as the standard, other D. W. Engelkemeier curves for samples with approximately 20 mg Ba carrier showed a 28 mg/cm^2 half-thickness [Figure 29, curve (b)].

In 1945, when the absolute fission yields on Pu were being determined, Al absorption curves of Ba^{140} from Pu fission were taken on samples which had about 20 mg of Ba carrier. The curves were very nearly exponential all the way back to zero added absorber. An initial half-thickness of 34 - 35 mg/cm^2 was obtained (Figure 30), and this value was used in all Pu fission yield work.

In an effort to straighten out these discrepancies some very careful work was carried out and although not entirely completed some features were clarified. First, the data on Ba^{140} from Pu fission yield was replotted on a greatly expanded scale, and a very slight break in the curve was found at about 18 mg/cm^2 absorber [Figure 29, curve (c)]. Although only a few points were available in the region of 0 - 18 mg/cm^2 the half-thickness in this region was close to 28 mg/cm^2, but the exact turning point of the curve was still in doubt.

A series of experiments were then performed to see if any of the following conditions influenced the initial half-thickness of Ba^{140}:

(1) Presence of backing material beneath the mica mounted sample.

(2) Cover free as compared with thin nylon or cellophane covering on the sample.

(3) Carrier free samples as compared with samples with approximately 20 mg of Ba carrier.

(4) Growth of the 40h La during normal counting times (maximum 3 hours).

The curves obtained under any of the above set of conditions show no great deviation from the curves taken under the normal conditions of approximately 20 mg Ba carrier mounted on cardboard and covered with cellophane and counted one to two hours after the last La separation [Figure 29, curve (d)]. Again a half-thickness of 28 mg/cm^2 was obtained.

To insure accuracy in these experiments, precautions were taken to minimize the statistical counting errors, to ascertain reliable counting operations, and to use pure Ba^{140}. All samples had 7,000 to 10,000 counts per minute and were counted for three to four minutes for each point; this reduced probable statistical error to less than 1%. Standards were carefully counted before, during, and after the time that the curves were taken, and the entire curve was then retaken a second time. The agreement was always quite good. At least 10 points were taken between 0 - 70 mg/cm^2, most of them in the interval from zero to 20 mg/cm^2.

Although Ba^{140} is easily obtained radiochemically pure the half-life of the Ba^{140} samples was followed as a check on the purity. Measurements gave 307 $\pm$ 2 hours for the half life which was evidence that the Ba^{140} was very pure.

The curves of Figure 29 [(b), (c) and (d)] all taken with samples containing approximately 20 mg of Ba carrier, showed that the best value of the initial half thickness of Ba^{140} was 28 mg/cm^2.

However, the initial slope of 26.5 mg/cm^2 which D. W. Engelkemeier obtained with the weightless sample of Ba^{140} [Figure 29, curve (a)] was supported by evidence in an old experiment with the low absorption counter which showed a very pronounced upswing of the curve in the region 0 - 15 mg/cm^2. This work will be repeated in an attempt to clarify this discrepancy further.

Figure 29

Al Absorption Curves for 12.8d Ba from Plutonium and Uranium Fission

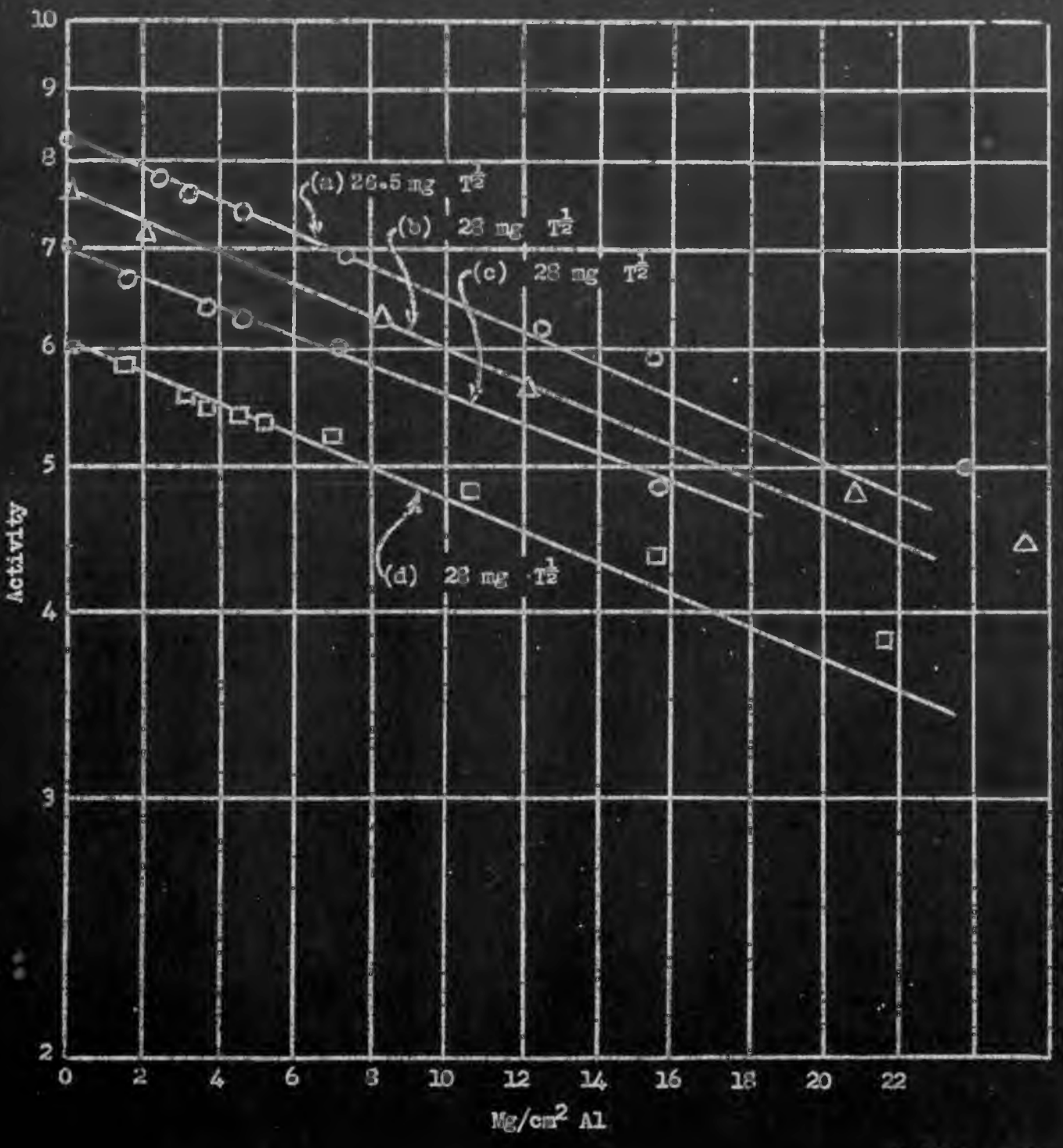

Figure 30

Al Absorption Curve for 12.8d Ba from Plutonium Fission
6/23/45

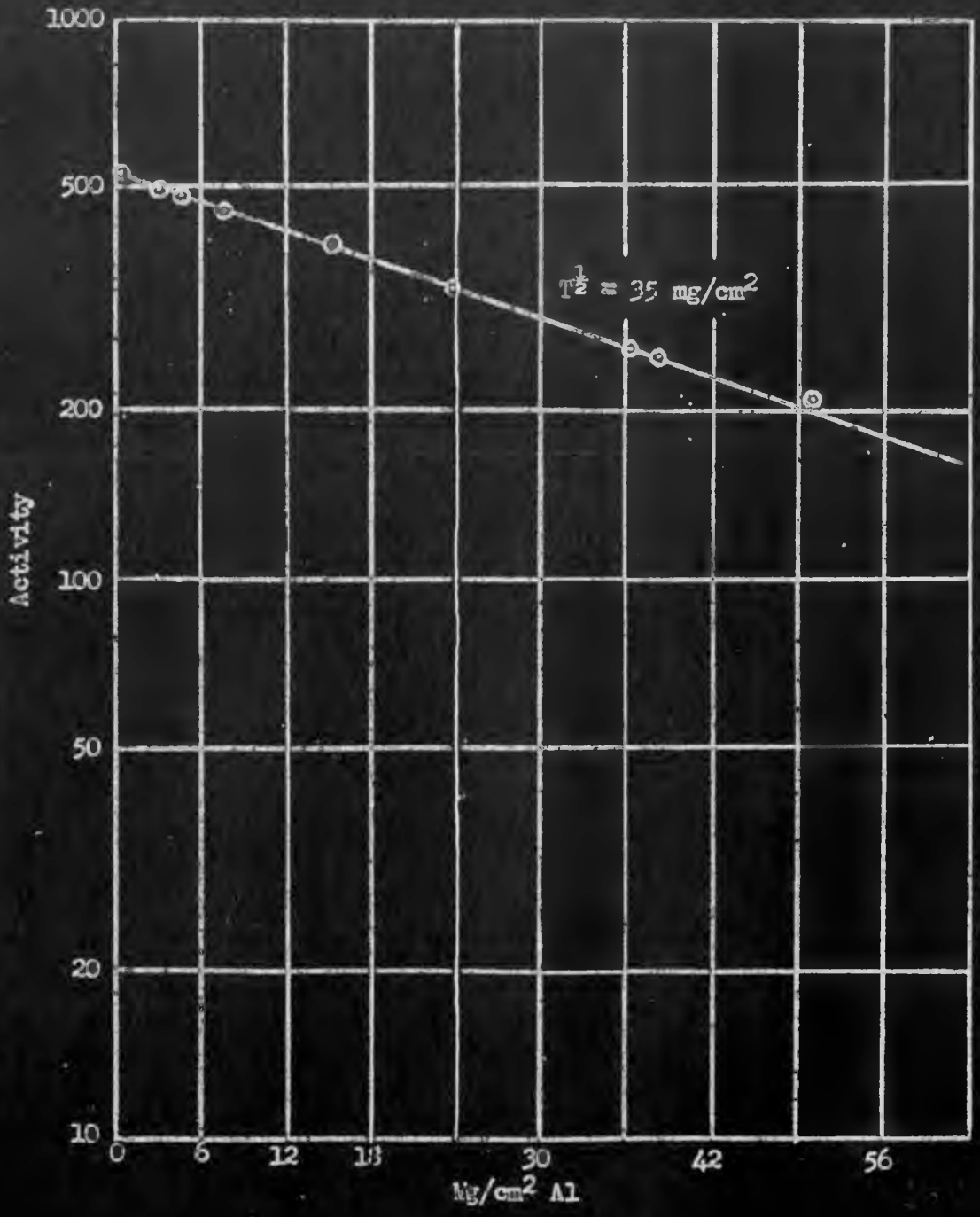

3.3 Geiger-Muller Tubes

3.3.1 Tube Development (M. S. Freedman)

Most of the measurements of beta and gamma ray activity made in the Chemistry Division have employed a thin mica window Geiger-Muller tube. The design and construction features of these tubes have largely been inherited from pre-Project work, and have been fairly well standardized by extensive use throughout the Chemistry Divisions, both at Chicago and at Clinton Laboratories (Figure 31).

It has long been recognized that the making of a satisfactory tube, one with a sufficiently long and flat "plateau" characteristic which remained constant for a reasonably long time, was an art of a very refined type. People learned in the art are ever ready to advise on the particular ritual to be followed to produce such good tubes; the novice trying to learn to make them suffers not from lack of a ready prescription but rather from an embarrassment of riches, and knows not how to choose among them. However, a detailed comparison of the performance records of thin window Geiger-Muller tubes made in different sections on the Project according to slightly varied procedures shows that the average results obtained are not as good as might reasonably be expected, and that all the tubes suffer from the same faults inherent in the design. The average tube life is seldom greater than a few percent of the theoretical lifetime, and the lifetime under laboratory conditions is generally a certain elapsed period of time, say three months, nearly independent of how many counts the tube has received, rather than being dependent almost solely on the total number of counts, as is the case with properly prepared silvered glass (Eck and Krebs) tubes.

With an eye to eliminating these faults, or perhaps only substituting other less annoying shortcomings for them, an attempt is in progress to alter the design and manufacture of these tubes. However, a great deal of very valuable information, in the form of absorption curves, incompleted decay curves, relative fission yields, neutron flux standardizations, etc., has been obtained using the standard thin window tube in a standard mount and shield. Most of this data cannot be accurately applied to tubes with different sizes, shapes, geometries, window thicknesses, or sensitivities. Consequently, consideration was given to maintaining these factors unchanged in any redesign so as to preserve the applicability of the accumulated data.

In assembling the standard mica window tube, the sheet mica is cemented to the brass flange with DeKhotinsky, Apiezon wax or a thermoplastic such as Gelva V-7 cement. All such organic cements suffer a slow deformation under stress when cold, and much more rapidly as the temperature rises to over 85°F. Consequently, the window, which is greatly stressed by the atmospheric pressure it bears, gradually develops radial wrinkles and folds which eventually open to the edge of the flange and leak air, or else the window implodes. On warm summer days in a room without air conditioning, the tubes may be spoiled in a few hours.

The major feature of the attempted redesign is the replacement of the wax cement by a low melting lead borosilicate glass which bonds the mica to the metal surface giving a leak-proof joint. The technique of sealing

CONVENTIONAL THIN WINDOW GM TUBE

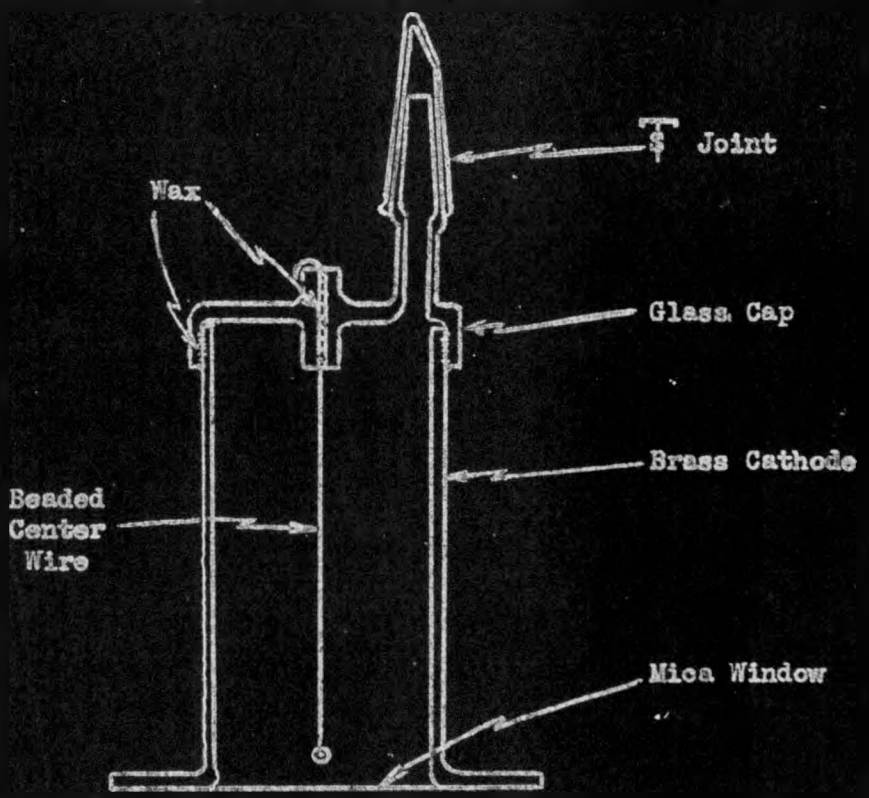

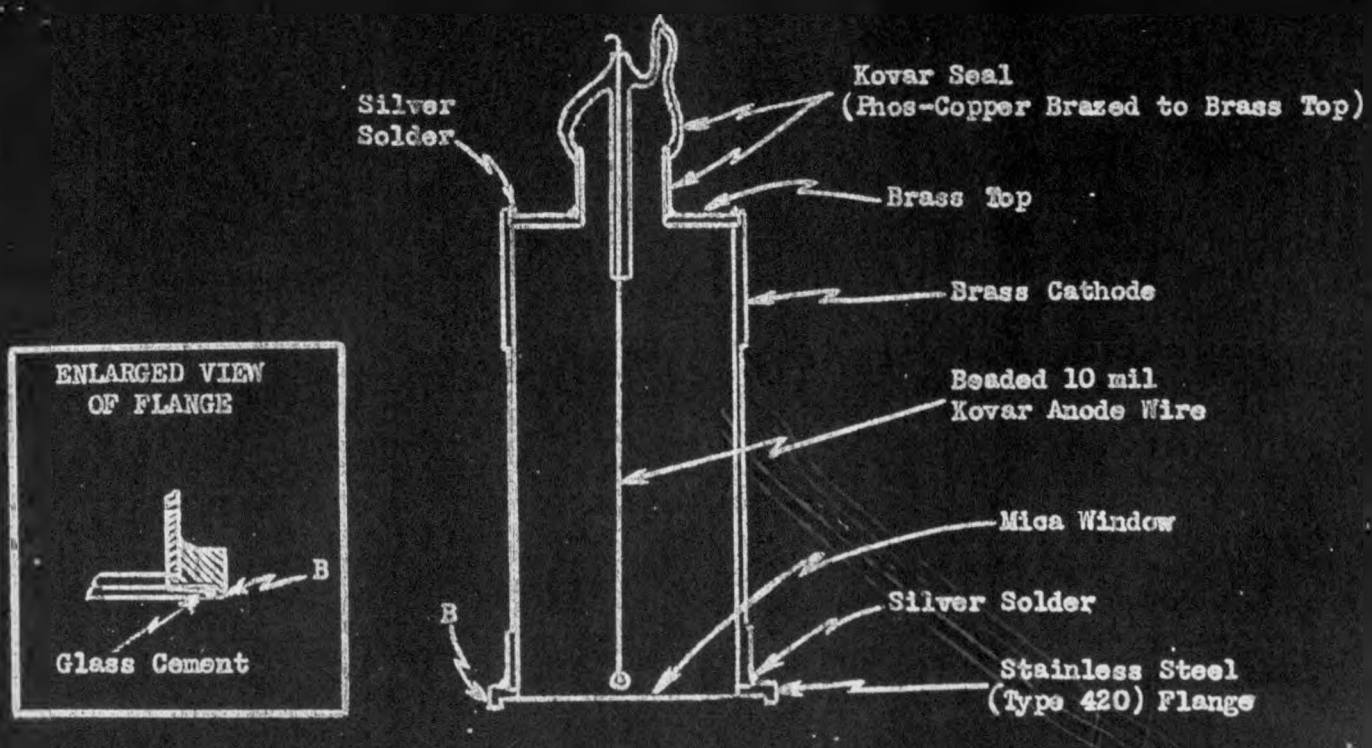

Figure 32

TENTATIVE DESIGN FOR THIN WINDOW GM TUBE

mica to soft glass envelopes (J. S. Donal, Jr., Sealing Mica to Glass or Metal to Form a Vacuum Tight Joint, R.S.I. 13, 266 (1942))developed at RCA Laboratories has been used by C. S. Wu (Report A-3207, Columbia) and C. L. Meaker to make GM tubes with the metal cathode cylinders contained within a soft glass envelope. The geometry of the conventional project tubes cannot be duplicated with such a tube, however, and the wire lead seals through the glass and the necessary graded seals are undesirable. A direct seal of the mica to the metal flange of the tube shell has been developed, using the low melting glass as a cement.

Since the softening point of the glass is 450°C, the window should not develop leaks or wrinkles at room temperature. Further, one should be able to heat the tube to perhaps 300°C while pumping it out and thus greatly accelerate outgassing of the cathode surface, which has not been possible with the older tubes. Tube shells with mica windows sealed on according to the method described below have been heated to over 200°C in a small cylindrical heating coil for several hours while being evacuated without spoiling the window. The greater outgassing of the tube should certainly contribute to better performance and longer tube life, as is found to be the case with Eck and Krebs tubes.

The elimination of the organic cement used for sealing the window suggested the elimination of other organic waxes and greases used in the conventional tubes for sealing the glass cap to the shell, the wire in its glass capillary, and in the taper joint. This is desirable in that it would permit degassing at high temperatures, would possibly avoid sources of troublesome leaks and, most important, would remove all organic matter exposed to the organic vapors in the gas filling mixture in the conventional tubes. This last has always been a cause for worry, because of the possibility that the alcohol in the gas phase would slowly dissolve into or combine with the solid organic material, or perhaps the organic material would slowly vaporize some undesirable component into the gas mixture, either possibly shortening the useful life of the tube. The cement at the glass cap has been eliminated by using a Kovar metal to glass seal, and at the central wire by sealing a Kovar wire directly to the glass. The taper joint has been dispensed with, and the glass is sealed off directly from the pumping lead with a torch.

The preparation of the cathode surface is all important for obtaining satisfactorily flat and long plateaus in Geiger-Muller tubes. A disadvantage of the conventional methods of assembly of thin window tubes is that the operations of assembly, putting on the window, glass cap and wire, etc. follow the cleaning and preparation of the surface. In these procedures it is difficult to avoid touching the prepared cathode surface with the fingers or with instruments; the surface is exposed to the air for some time, permitting dust and lint to settle on it, which are not easily seen or removed. With the proposed redesign one may introduce acids to dissolve surface oxides, or other solutions to sulfide or oxidize or rinse the surface, or one may heat the tube in oxygen to oxidize the surface, after the window and cap of the tube are assembled. This is not feasible with the older design because of the presence of waxes, etc. Since the tube can be evacuated immediately after cleaning the metal surfaces, the chance of their becoming dirty or changed is smaller.

At this date (September 30) no complete tubes have been fabricated but several of the procedures have been worked out and are at least in a usable state of development although they are not yet completely satisfactory. A proposed tube design is indicated in Figure 32. It was decided to retain the brass cathode of the conventional tubes. To this is silver soldered a flange of stainless steel (Carpenter #2, type 410) which is chosen because its coefficient of thermal expansion, 10.6×10^{-6}/°C, closely matches that of the lead borosilicate glass, 9.8×10^{-6}/°C, used for sealing on the mica window. The glass, when melted onto a clean machined surface of the steel, forms a bond that is so adherent that it can only be machined off by a steel tool. The silver solder used must not melt below 725°C, so the ordinary low melting variety available in most shops is not suitable.

The procedure for sealing on the window closely follows that recommended by J. S. Donal. A thin paste made of the powdered glass and water is spread on the flange surface and melted on at about 700°C in a furnace or by using an induction heater. A mica circle 3 to 4 mg/cm^2 thick, which just fits inside the projecting ridge at the edge of the flange (B, Figure 32 and 33), is placed on the glass film, and a small amount of the glass paste is put on the upper edge of the mica next to the ridge. The tube is then heated in a furnace to 675°C for 10 to 15 minutes and allowed to cool slowly over about one-half hour. A temperature of 600°C as specified by Donal gives poor results, the glass being unevenly fused with many bubbles, and poorly bonded to the mica. The mica does not deteriorate at 675°C for 20 to 30 minutes, though at 700°C bubbles (probably water of crystallization from the mica) begin to form between the layers and the mica is weakened. A very smooth, thin, almost bubble free bond is obtained in almost all cases, and the mica never breaks loose from the cement, but rather tears at the edge of the cement first if overly stressed. The glass forms a smooth meniscus inside the ridge, which aids in the formation of a continuous glass seal around the edge of the mica, and which serves to protect the sealed edge against mechanical damage. Too long heating at 675°C or too long a cooling period (> 1 hour) spoils the mica, the glass dissolving holes right through the mica sheet. This indicates that the mica to glass bond is probably more intimate than mere mechanical contact, and may involve formation of a mica-glass solution phase at the interface.

About one-half of the windows made this way "pop" upon evacuation, though nearly all are leak-free under low pressure differential. The mica is evidently cut on the sharp inner edge of the glass meniscus formed at the corner of the flange. A modification which will be tried is shown in Figure 33; the groove allows excess glass to collect without reaching the inner cathode surface, and the rounded inner edge of the metal A supports the mica, so that it is in lateral tension where it contacts the sharp glass edge, and so presumably would not be cut at this point.

A disadvantage of furnace heating is the large amount of oxidation and corrosion of the cathode surface which takes place, which necessitates extensive cleaning with the window in place. A controlled atmosphere furnace, filled with hydrogen, nitrogen or helium will be tried. Some indications of success in attempts to seal the window on using induction heating have been realized. The advantages of this technique are that the steel flange is heated while the brass cathode remains relatively cold, and that the center portion of the mica is also kept cool. Another solu-

Figure 33

ENLARGED VIEW OF TUBE FLANGE

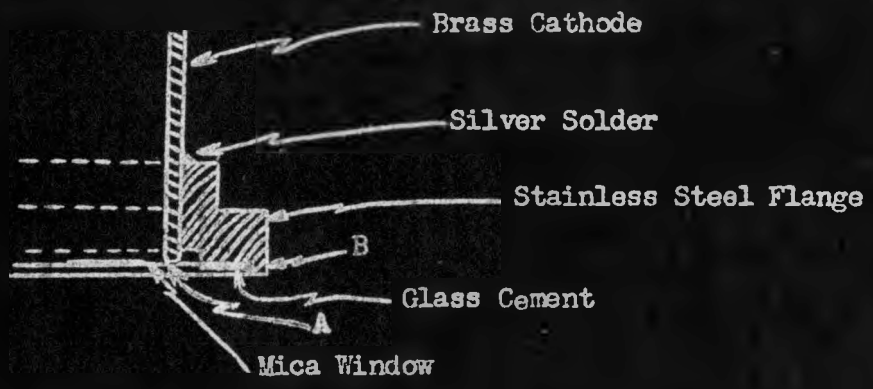

Figure 34

ENLARGED VIEW OF DOUBLE ANODE

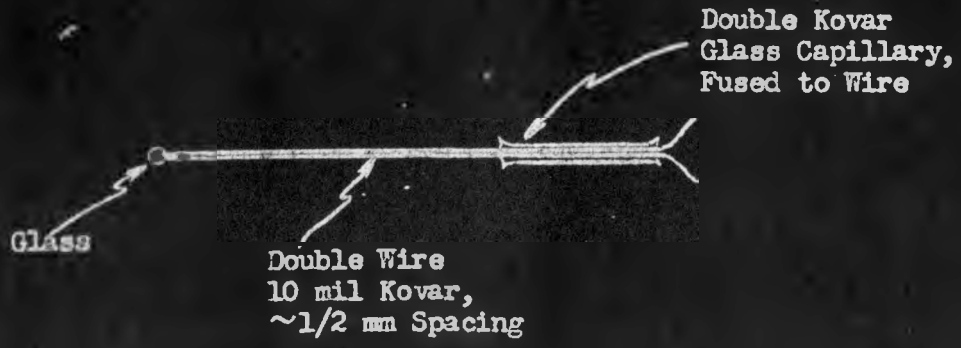

tion is to use a one piece construction with a stainless steel cathode surface, and this will be tried. An advantage here is the elimination of troublesome silver solder joints.

After the window is mounted on the tube, the shell is placed, window down, in a shallow dish of water ($\frac{1}{4}$" deep) and the assembled metal to glass Kovar seal is brazed in place using phos-copper brazing rod and a torch. Silver solder should not be used as it results in intergranular corrosion, embrittlement and possible cracking of the Kovar metal. Flux (Handiflux) should be used sparingly as it tends to spread to the Kovar glass (Corning 705-AJ) and to melt onto it, giving a badly crazed surface. The cathode shell is turned to 1/64" wall thickness to lower the amount of heat conducted to the window, and the water layer keeps the window cold enough to prevent it from being spoiled. Other methods of protecting the window such as cooling coils or fins placed around the shell absorb too much heat from the surface being brazed, thus requiring the use of too hot a flame with resulting cracking of the Kovar-to-glass seal.

Cleaning and preparing the cathode surface may be done at this stage, if necessary. Solutions may be introduced with a pipette through the opening in the glass insulator, taking care to avoid straining the window, although they seem to be remarkably sturdy. A handy device is a long glass tube connected to a water aspirator, which is used to drain solutions from the tube.

The last operation of assembly is the sealing in of the anode wire. Kovar wire (10 mil diameter) is straightened in a Bunsen flame and a 1 mm Kovar glass bead is carefully centered on the end. A sleeve of 2 mm Kovar glass tubing is slipped on the wire and sealed to it in the middle inch of its length. This sleeve is then sealed to the neck of the Kovar glass insulator, and as the glass cools the wire is centered in the tube with the glass bead about 2 mm from the mica window.

It is common practice in making GM tubes to flash the anode wire, if the ends are accessible, by passing a current through it. This outgasses the wire, burns off sharp points and dirt on the wire, and refines the crystal structure at the wire surface. In end window tubes this could not be done. A scheme for accomplishing this which will be tried is to use a double anode (Figure 34), made by doubling back a single 10 mil Kovar wire on itself, such that the two halves are parallel and $\frac{1}{2}$ mm apart. A glass bead fused over the end and a double glass capillary sleeve fused onto the two leads where they emerge through the Kovar glass insulator hold the wires firmly parallel, even when they are flashed at red heat. It remains to be seen what effect such a double wire arrangement will have on tube performance. In self-quenching Geiger Muller tubes it has been shown that the discharge is capable of jumping over a glass bead of $\frac{1}{2}$ mm radius in spreading out along the wire. Consequently, it appears that the discharge will spread along both wires, resulting in a larger pulse than from a single wire. It is unlikely that any important axial assymetries in the distribution of the sensitive region will be introduced by this double wire.

3.3.2 Sensitivity Distributions in End Window Tubes (M. S. Freedman, R. Pairs)

Some of the intensive properties of the standard thin end window Geiger-Muller tubes used in the Chemistry Divisions on the project are of special interest. Quantitative knowledge of some of these properties such as the absolute efficiency of the tubes for various kinds of radiations and the distribution and geometrical extent of the sensitive volume of the tube would enable one to resolve several discordant measurements of the counting "geometry" and counting yield of the standard counting setups. Many of the fundamental quantities of interest to the project, such as absolute fission yields and neutron fluxes, depend on precise knowledge of the counting geometries and yields of these GM tubes.

An experiment which gives information concerning both the absolute efficiency of the standard end window GM tubes and the distribution of the sensitive region has been performed. A standard flanged brass tube shell fitted with the usual glass cap and beaded center wire was used, with the bead about 2 mm from the plane of the window. The thin mica window was replaced by a plate of Pyrex, 2 mm thick, cemented to the flange. On the ground outside surface of this plate were scribed a series of concentric rings at ca. 2 mm radial intervals.

Before the glass cap and wire were fitted to the tube a small (ca. 4 mm diameter) round thin mica disc was introduced. The disc carried the α ray source used in the experiment. To form the source one drop of a pure polonium solution was evaporated on the center of the mica disc, the deposited film covering only the central 2 mm circle on the disc. The source is free of β's and practically free of δ's.

The tube was evacuated and filled with the conventional counting gas mixture, 9 cm argon and 1 cm ethyl alcohol. The tube had a plateau length of 100 volts, sloping ca. 2%/100 volts. Counts were taken with the Po source at various positions along the window face of the tube, the positions being measured by sighting through the window with the aid of the scribed circles. The source was shifted around by tilting the tube and lightly tapping.

Figure 35 illustrates the results of one experiment. The ordinate gives counts per minute, plotted against the radial position of the center of the mica disc. The dotted line gives the count determined in a "50%" α counter. The maxima of the curve correspond to a maximum counting efficiency, for α's, of 97.5%.

The sensitivity drops uniformly to ca. 60% of maximum at the sides of the tube. The shallow dip in the middle appeared in several experiments with the same tube, but did not appear in similar experiments on another tube. Measurements made along different radii in the same tube gave similar results. In one case in which the anode wire was off center by ca. 2 mm, the sensitivity curve remained symmetrical about the geometrical axis of the cathode.

The sample was also moved to positions along the cathode wall of the tube by tipping the tube on its side and tapping. The tube performance was more erratic with the sample in this position, but counts could be taken. For various positions along the side the counting rate fluctuated around

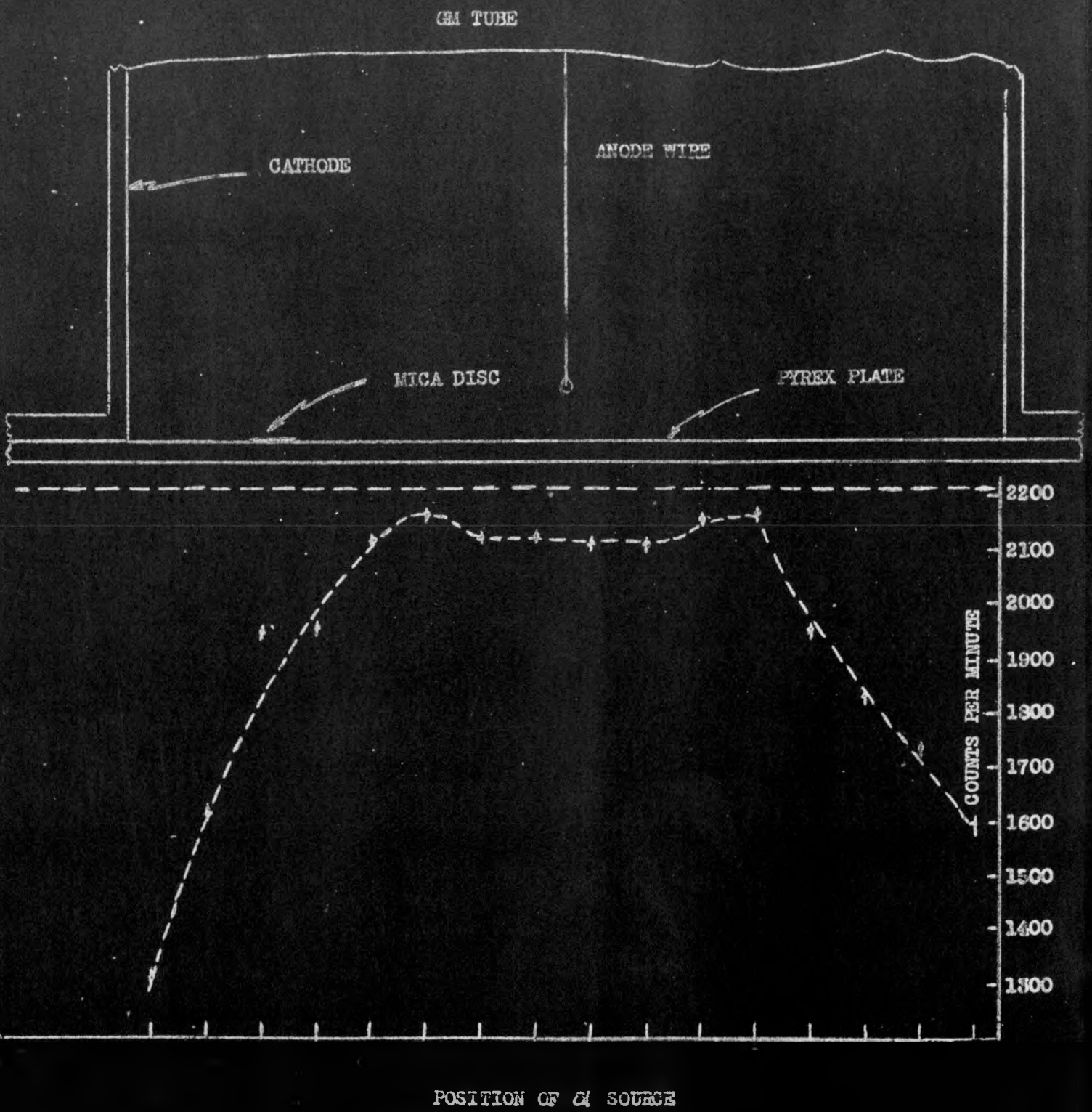

FIGURE 35. DISTRIBUTION OF THE SENSITIVE REGION IN A GM TUBE

the value 2150 c/m, which was obtained near the middle of the face, except near the window where it fell off. The source could be viewed only with difficulty so no quantitative data are given.

The above results are certainly surprising, and it is difficult to understand them. The specific ionization of Po α's in the counter gas should be of the order of 400 ion pairs per mm, and the minimum path length in the gas is at least one mm, even for α's ejected tangentially from the thin sample toward the wall when the mica sample holder touches the wall. Thus it appears that a large fraction (up to 40%) of the α's fail to count although each produces several hundred ions. Moreover, the radiation is presumably nearly isotropically distributed around the sample, so that even when the sample is far off center, only a very small fraction of the α's travel directly toward the wall, and most move toward the middle of the tube or upwards into the region of cylindrical field distribution. Geiger-Muller tubes filled to these pressures should have efficiencies of ca. 99.8% for every beta ray entering the sensitive region, and this value has been checked by coincidence counting experiments. For α's the value should be even closer to one, so it appears that the sensitive region is of much smaller extent and is located further from the window of the tube than had been supposed. Also, the ions produced in the insensitive region would have to be completely removed by recombination, which is hardly possible from present knowledge. The field distributions in such a cylindrical system, even near the window, give ion collection times of the order of 10^{-3} seconds, for which recombination should be negligible.

The whole situation is so muddy that further experiments alone can hope to clear things up. One experiment which is planned is to build into the GM tube a beam α source which can be moved from the outside through a spherical ground joint so as to point a thin pencil of α's at a small region to investigate its sensitivity independently of the volume sensitivity of the neighborhood. A simple source of this kind has been made by plating out Po on the end of a 1 mm diameter silver wire set flush in a plastic disc, and then mounting a plastic cylinder coaxial to the disc with a 1 mm collimating axial hole. The 1 mm diameter pencil of α's will be swept across the face of the GM tube to explore the local sensitivity.

3.4 Construction of Magnetic Lens β-Ray Spectrometer (M. S. Freedman, B. Smaller)

Plans for the construction of a magnetic lens β-ray spectrometer were initiated in July 1946. Preliminary calculations in design considerations were promulgated in August and additional information and verification was achieved by a visit to the various institutions having magnetic lens β-ray spectrometers in operation.

3.4.1 Requirements

Specifications for the instrument were as follows:

(1) High Transmission — A minimum of 5% T was required and if possible it was desirable to go as high as 10%. This feature was stressed because of need of obtaining accurate β and δ-ray energy analyses where the total activity of the sample was very low.

(2) High Resolution — It was desirable to achieve resolution of the order of 3% half width in order to obtain accurate data on line spectra and to separate out components of complex spectra. As expected, high resolution is incompatible with high transmission characteristics because, analagous with optical lens design, aberrations increase with transmission and tend to reduce the system's resolution. In order to correct these aberrations, radical changes in design and requirements must be introduced.

3.4.2 Types of Magnetic Focusing Systems

(1) 180° Focusing System — In this system, electrons confined to the region between pole pieces of a high-field electromagnet are curved through a semi-circle whose radius depends on the momentum of the electron. This system can be made to yield high resolution but because of intrinsic design factors is limited to transmission of about 0.1% and hence was eliminated as a possible design.

(2) Solenoidal Lens — If electrons are projected into a solenoidal field they will describe helical paths where the "pitch" of the helix is dependent on the momentum of the electron and hence possess focusing properties. Such a system will exhibit fair resolution and transmission properties but at the expense of very high field requirements.

(3) Simple Thin Magnetic Lens — Because of its intrinsic field pattern a thin coil has considerably higher refractive power (for the same power input) than the solenoidal type lens. However, for equal transmission, resolution is reduced and becomes too objectionable under high transmission requirements.

(4) Compound Thin Lens — For high transmission, use must be made of two or more lens coils in cascade. Such a system can be adjusted to yield satisfactory resolution provided one is willing to provide for very high fields and hence large power requirements. However, in contrast to optical systems where divergent and convergent lens can be compounded to neutralize aberrations, magnetic

lens having axial symmetry are intrinsically convergent and hence any design must be in the direction of minimizing rather than neutralizing the aberrations.

3.4.3 Installations at Other Institutions Having these various considerations as a basis for future design, an inspection trip was made to the various centers having magnetic lens beta-ray spectrometers. At Columbia University an instrument designed by Dr. Witcher was inspected. The lens was a long solenoidal coil, and in operation used about 18 kw of power in order to focus 4.4 Mev betas with a transmission of 1% and resolution of 5%. A thin lens type instrument was also inspected at MIT, designed by Drs. Deutsch and Elliott. This single lens could focus 3 Mev betas using about 3 kw power with a transmission of 0.8% and resolution of 6%. Lastly, a newer design of Dr. Elliott was inspected at Chalk River Laboratory which was built for high transmission purposes, but also of single lens design. The transmission given was 10% with a 10% resolution under a coil-energizing power of about 3 kw.

Study of these various instruments verified the original postulate that in order to achieve high transmission under high resolution conditions it would be necessary to go to a combination lens system using large input power. A new lens coil system was decided upon and coil design was initiated. In order to accomodate large power inputs with low dissipation it is advisable to use low resistance-high amperage coils, hence it was decided to use wire tape as conductor, winding the coil in Archimedean spirals which add together laterally to form each coil. For reasons of limited heat transfer the number of such spirals to a coil was limited to six, and cooling end plates containing circulating water were added to carry away the heat dissipated. The power unit to energize the field required careful consideration. Since it was thought advisable for convenience not to exceed 100 amps, and since 220 v would be desirable for standardization purposes, these conditions along with the heat dissipating ability of the systems decided in favor of a 220 v 25 kw motor generator unit.

Although power requirements were apparently large, they were dictated by the specifications required by the performance of the instrument. Hitherto no instrument has been designed which gives 10% transmission with 3 to 5% resolution, but it is believed that these characteristics can be approximated.

Calculations and design are continuing toward the completion of this

4 ANALYTICAL CHEMISTRY

A report from the Analytical Group covering a six month period will appear in the Quarterly Report of the Chemistry Division, Section C-II, for the fourth quarter of 1946.

5 SPECIAL PROBLEMS

5.1 Magnetic Moment of Plutonium (G. H. Winslow)

It is proposed to investigate the electronic configuration and, eventually, the nuclear magnetic moment of Pu by a molecular beam method. In spite of some doubts as to its feasibility, (the chief one being the complication which would arise in case thermal excitation to levels of higher J value than the ground level occurs) a start will be made by the method of Gerlach and Stern (Zeits. f. Phys. 8, (1921) 110).

Present plans call for a beam 40 cm long and 3 mm high defined by an oven slit of width 0.024 cm and a collimating slit 0.0075 cm wide. These two slits will be separated by 15 cms; the collimating slit will be at the entrance to an inhomogeneous magnetic field and on the oven side of the field. The field is to be 15 cm long. There will be an additional distance of 10 cm from the field to the detector. The inhomogeneity of the field will be about 1.5×10^4 gauss/cm. The oven temperature will be 1500°C at which temperature the vapor pressure of Pu is ca. 10^{-2} mm Hg.

One of the chief functions of these initial experiments will be to try out a quartz fiber condensation detector suggested by O. C. Simpson. The fibers are to be mounted parallel to each other and to the beam height. After a sufficiently long exposure the deposit on the separate fibers will be weighed by γ counting.

It has been suggested that actinium represents the beginning of another "rare earth" series and thus has the electron configuration of lanthanum. This second series is formed by the addition of 5f electrons. If this is so and if there is exact correspondence, then Pu corresponds with samarium which has the ground state $^7F_0$. Atoms in this ground state would not be deflected in the inhomogeneous field. The g value for all states $^7F_{0123456}$ is 3/2 and the apparatus design is such that any atoms with states having a projection of 3/2 Bohr magneton on the field direction would be deflected outside the limits of the undeflected beam. If the intensity of such atoms is great enough they can be detected directly, although if it is small their presence can only be detected by the weakening of the undeflected beam. It has been estimated that if 10% of the atoms are in other states than $^7F_0$ the resulting count will be measured without too much trouble with a reliable error of 1%.

The above discussion is on the basis of Russell-Saunders coupling, which is probably not correct. Further consideration of such problems can be done with the greatest profit after the first beams are measured.

5.2 Effect of Neutron Irradiation on the Thermocouple Power of the Chromel-Alumel Junction (E. C. Avery)

Four single junctions of chromel-alumel thermocouple wire were made at the same time by the same method using adjacent two foot lengths of wire from each spool. Three of the single junctions were placed in aluminum cans and subjected to

neutron irradiation at Hanford while the fourth junction was preserved for a reference standard.

After 24 days bombardment at Hanford one of these junctions was removed from the pile and checked against the standard by the following method. The standard and test couples were bucked against each other by connecting the two chromel wires. The two chromel-alumel junctions were kept in the same ice bath while the temperature of the chromel-chromel junction was varied. The thermoelectric force of the combination varied from 0.004 μv/°C to 0.26 μv/°C when the temperature of the chromel-chromel junction was changed from 28°C to 170°C.

These small changes are of the same order as those to be expected from variations in the wire or due to handling, and certainly indicate that no serious change in the calibration takes place due to neutron irradiation at Hanford fluxes for 25 days. It, of course, does not rule out the possibility of changes existing during bombardment which could conceivably anneal out at room temperature in a short time after bombardment had ceased.

5.3 Effects of Gamma Radiation on Insulating Materials (H. C. Andrews, F. L. Belletiere, S. Gordon, M. E. Rebonak)

Selected samples of insulation material under consideration for use in the electrical equipment of the Zinn fast pile were exposed to γ radiation from a tungsten target placed in the Van de Graaff electron beams in order to determine whether any harmful radiation effects might be anticipated.

The first sample tested was a sample of ceramic coated wire #1063 Ceroc #21 A.W.G. manufactured by Sprague Electric Company of North Adams, Mass. The experimental set-up is shown in Figure 36. Two short pieces (ca. 2½ cm long) of the wire were twisted together and an emf (120 v) applied to the two wires as shown in the Figure 36 in such a manner that the potential was applied across two thicknesses of insulation. The current was fed to and read on an inverted triode amplifier (Zeus) and the conductivity of the sample was measured after each bombardment interval. The γ source was a tungsten target bombarded with 1 Mev electrons with the sample placed at about 0.5 cm from the target. The resistance of the sample was greater than 3×10^{13} ohms (the limit of sensitivity of the detection instrument) and did not fall below this limit in an exposure which is estimated to have been somewhat greater than 2×10^{6} roentgens.* On further exposure, however, the sample shorted. The apparatus was disassembled and closely examined. It was found that cracks were present in the insulation and that in these cracks salts had been deposited. These salts probably resulted from the high humidity of that day. When another piece of wire, which had not been bombarded was twisted in the same manner as before, similar cracks were produced. The cracks, therefore, were not due to the effects of the radiation.

*The magnitude of the exposures to which these samples were subjected is not accurately known. The quoted exposure figures are probably low, perhaps by a factor of as much as ten. However, all figures will be off by approximately the same factor and consequently the relative magnitudes of the exposures are probably approximately correct. Efforts are now underway to secure more accurate exposure calibrations for the Van de Graaff generator.

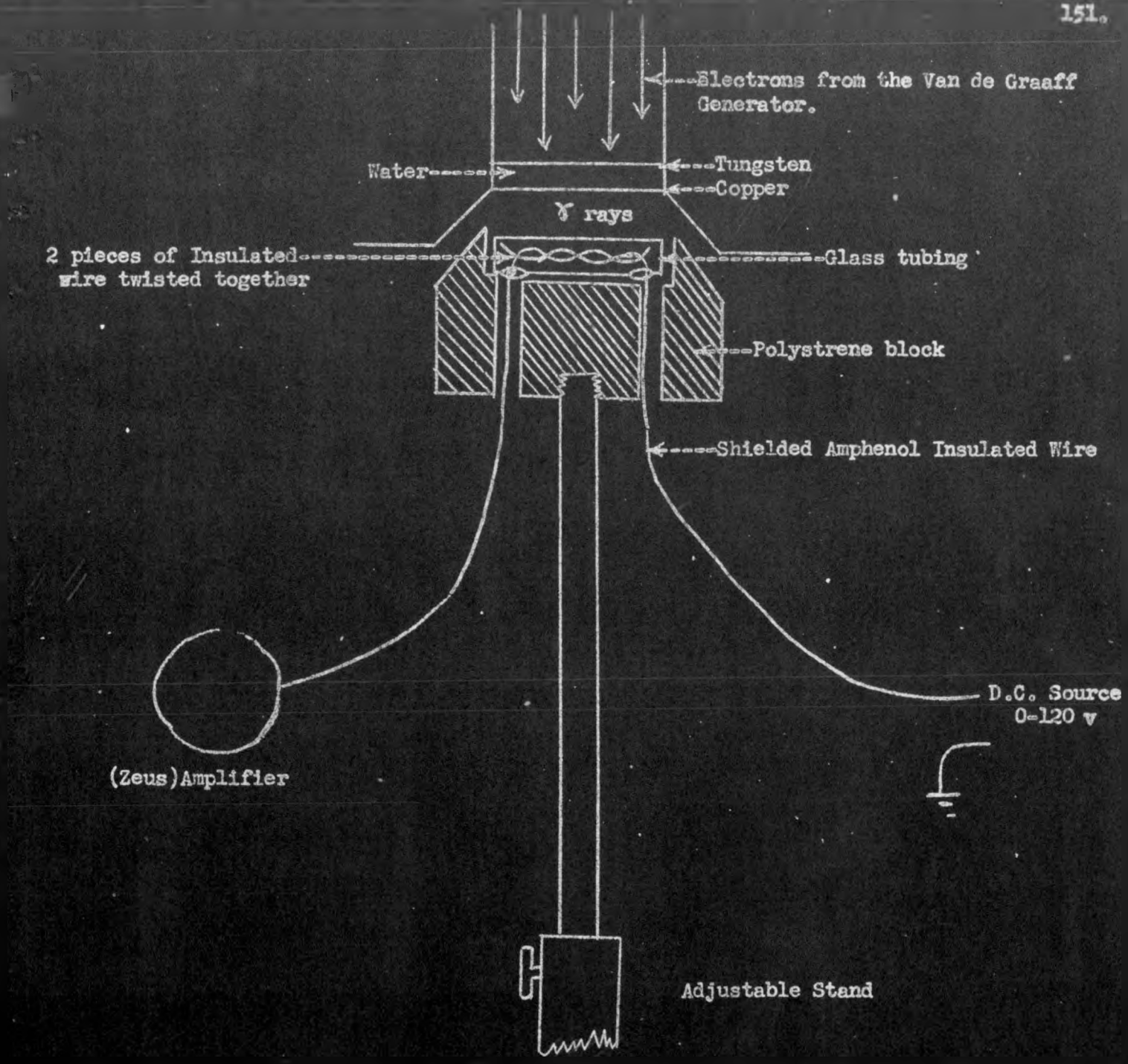

Figure 36

Apparatus For Testing

Wire Insulation

(Side View)

The second sample tested was #18 Anaconda WC, single vitrotex covered, silica bond wire. The experimental set-up was exactly as described for the ceramic coated wire. The sample received greater than 36 x 10^6 roentgens. Readings were taken at twelve approximately equal exposure intervals. At no time did the resistance of the sample fall below the limit of sensitivity of the measuring instrument, namely 3 x 10^{13} ohms. There was no visible physical change in the sample.

The third sample tested was a sample of Vartex, silicone resin coated, glass fiber cloth. The experimental set-up is shown in Figure 37a. It is similar to that described for the wire except that the sample was prepared in a different manner (Figure 37b). Two discs of copper 3.14 cm^2 area and 0.025 cm thick to which wire leads were soft soldered were each molded into a disc of lucite. Both lucite discs were sanded down to expose the faces of the copper discs opposite the soldered sides. These faces were then polished. The sample, 4.9 cm^2 in area and 0.0175 cm thick, was placed between the two copper discs and the two lucite molds clamped together tightly. Lucite dissolved in acetone was applied to the junction of the two pieces and allowed to dry. Approximately ten coats were applied. The mold was then set in the sample holder as shown in Figure 37 and exposed to the γ source as before.

The results are shown in Figure 38 where current (with 120 v applied) is plotted against bombardment in roentgens.* After the first bombardment period (ca. 8 hrs) the conductivity of the sample increased slightly to point A. On standing 14 hrs it rose slightly again to point B. In the next bombardment interval the conductivity rose to point C and after standing 14 hrs more rose further to point D. After the next bombardment period the conductivity exhibited an effect opposite to the first two. The conductivity decreased from point D to E and rose slightly on standing to point F. With further bombardment the sample showed for the most part an increase in conductivity on bombardment followed by a recovery on standing. One fact that should be mentioned is that the bombardment D - E was made on a very humid day and trouble was experienced with moisture condensing. This behavior of increasing conductivity with bombardment followed by a recovery on standing has been noticed previously in this laboratory (CC-1097 (A-1487) J. G. Burr and M. W. Garrison 12/6/43).

The fourth sample tested was 0.010" Macallin, Silicone Resin Bonded, Flexible Mica plates. The same apparatus was employed as that used in Sample 3.

The results are shown in the accompanying graph, Figure 39, where current (40 v applied) is again plotted against exposure in roentgens.* After the first bombardment period of ca. 3 x 10^6 r there was a slight increase in conductivity to point A. Upon standing 14 hours, the conductivity increased further from point A to point B. The second bombardment of ca. 7 x 10^6 r showed the conductivity to increase from point B to point C, and after standing 14 hours to decrease to point D. In the third bombardment of ca. 5 x 10^6 r the conductivity increased from point D to point E. After an interval of 40 hours there was a further increase from point E to point F. From point F to point G, and thereafter, the sample showed an increase in conductivity after bombardment followed by a recovery on standing.

---

*See footnote on previous page.

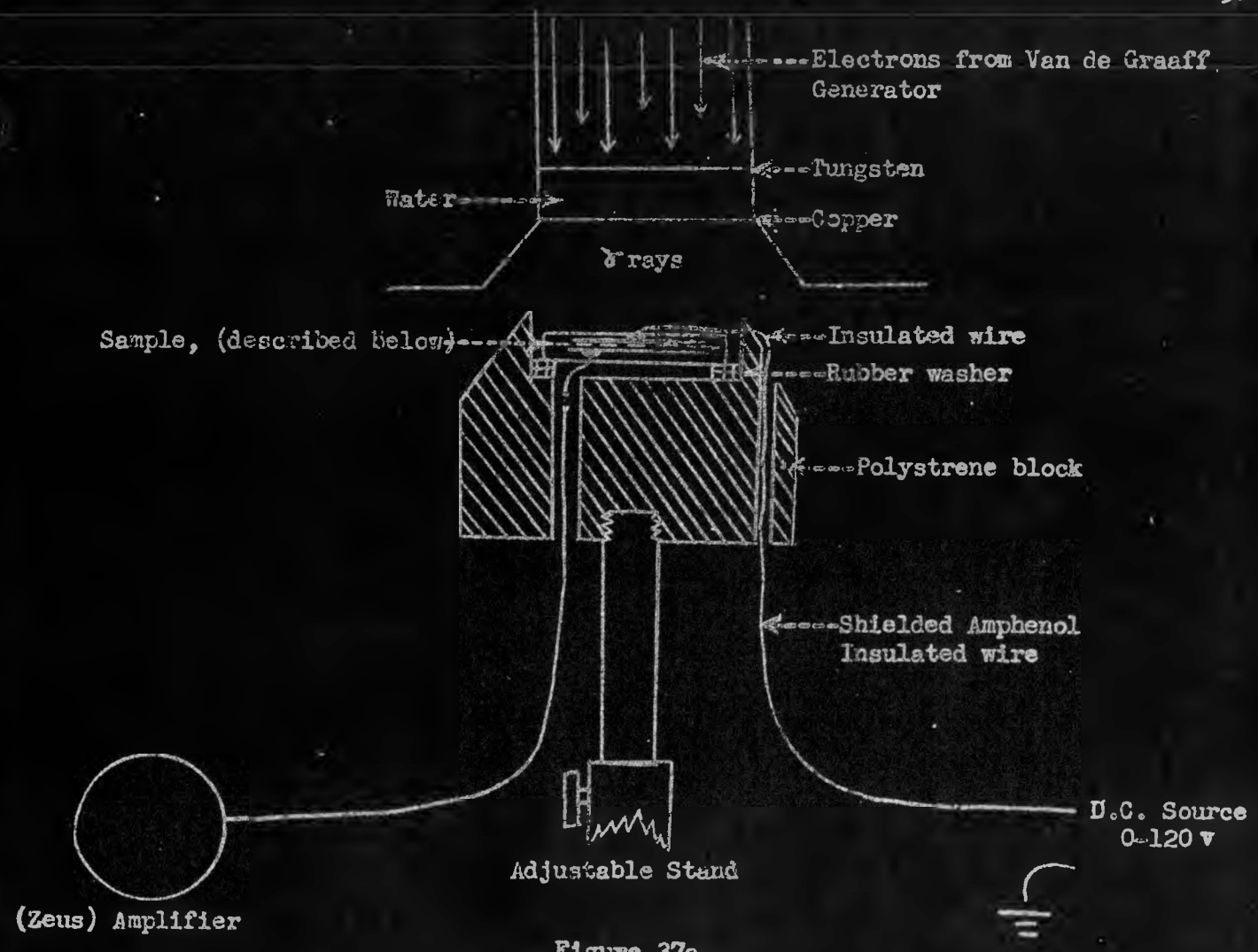

Figure 37a

Figure 37b

Apparatus for Testing Insulation Properties

of Treated Mica and Fiber Glass Cloth

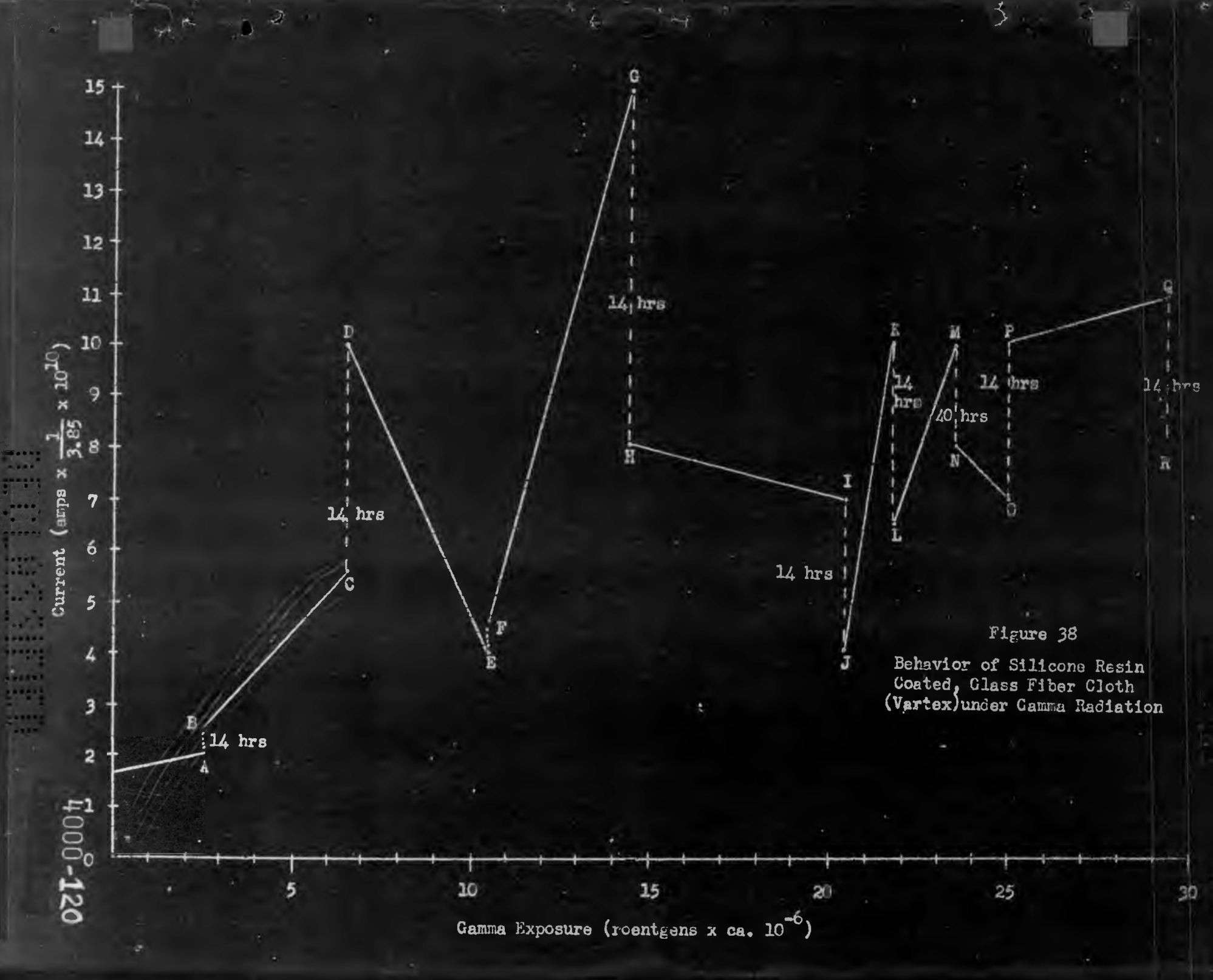

Figure 38

Behavior of Silicone Resin Coated, Glass Fiber Cloth (Vartex) under Gamma Radiation

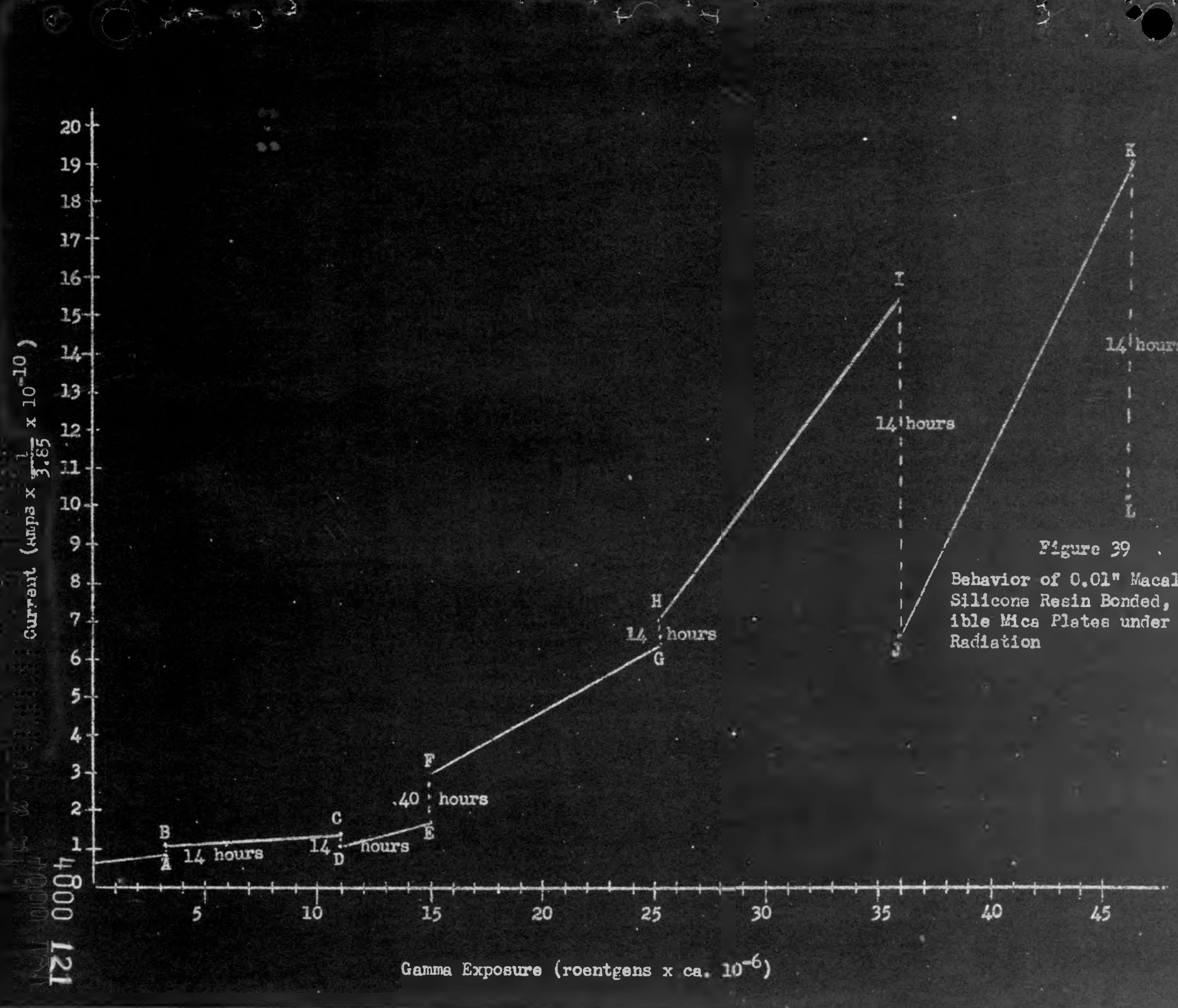

Figure 39

Behavior of 0.01" Macallin, Silicone Resin Bonded, Flexible Mica Plates under Gamma Radiation

As in samples 1, 2 and 3, the results show that there was no serious change in conductivity with bombardment of γ rays up to the order of at least 30×10^6 roentgens. Also, no physical changes were noticed in any of the samples.

5.4 Remote Control Development (H. C. Andrews, F. L. Belletiere, M. E. Rebenak)

5.4.1 Improvements in Present Hot Labs

The usefulness of the Room 12 hot lab has been seriously limited by the lack of sufficient storage space for hot materials. Consequently plans have been drawn up for a storage room adjacent to the Room 12 lab and construction of this auxiliary room is now underway. Plans are also being made to install a rail and hoist in this storage room to facilitate unloading trucks, etc. This room will be equipped with two large lead lined vaults containing a number of individual storage compartments. These vaults are now being renovated in the shops.

Considerable thought has been devoted to the renovation of the B-2 hot lab which was devised for solution work but has been considerably outmoded by the Room 12 hot lab. Plans are being made to install in this lab, where possible, the additional features which characterize the Room 12 hot lab. New lead doors, additional lead shielding, rear and front wall tracks and numerous other modifications will have to be provided.

5.4.2 Improvement of Remote Control Devices

With the cooperation of the New Chemistry, Site B and Ryerson shops and their drafting departments, intensive work has begun on the redesigning of some of the present instruments and the adaptation of commercially available instruments to remote control operation. Plans are being made to set up a mock wall behind which it is intended to test various pieces of equipment which have been adapted to remote control operation.

(1) Cave Periscope The design of the present model traveling periscope is being refined and improved. The two main improvements contemplated are: (a) Installation of a window that can be rotated through 180° rather than the present fixed forward viewer, and (b) provision for variable magnification.

(2) Hydraulic Tongs The design of the present model hydraulic tongs is being modified considerably. The new tongs will be equipped with interchangeable jaws of various shapes. The tongs will be connected to the remote control crane by a ball and socket joint to provide adjustment to any desired position. Since the present design is quite cumbersome, it is planned to streamline the housing, thereby materially reducing its size.

(3) Mirrors Two double reflection mirrors have been fabricated at the Site B machine shop and have been installed in the Room 12 hot lab.

(4) Remote Control Crane Rough sketches have been made and detailed drawings are being started on a new remote control crane. The three dimensional movement of the present crane carriage will be retained and an additional unit will be mounted on the crane shaft to provide the three rotational motions necessary in pouring beakers, turning stopcocks, etc.

(5) Milling Machine A milling machine has been procured from the Atlas Press Company and will be adapted for remote control use to facilitate the opening of cans after irradiation and to perform various other milling and cutting operations.

(6) Analytical Balance An Ainsworth analytical balance has been secured and plans are being made to adapt it to complete remote control operation.